

COMPOSTABLE AND RECYCLABLE PAPER PACKAGING USING MODIFIED  
SOYBEAN OIL COATING WITH EXCELLENT WATER- AND OIL-RESISTANT  
PROPERTIES

By

Vikash Kumar

A DISSERTATION

Submitted to  
Michigan State University  
in partial fulfillment of the requirements  
for the degree of

Chemistry – Doctor of Philosophy

2025

## ABSTRACT

Originating from plants as a natural, renewable resource, paper-based materials have garnered significant interest in recent years across packaging and non-packaging sectors. However, the utility of paper-based packaging remains limited due to its porous nature and the presence of hydroxyl (-OH) groups, which confer hydrophilic characteristics. This makes it susceptible to the permeation of liquids and gases through cellulose fibers, leading to rapid deterioration of its barrier and mechanical properties.

To address these shortcomings and promote broader adoption of paper-based packaging in daily life, various coating materials have been developed and applied to paper surfaces. For instance, PFAS (per- and polyfluoroalkyl substances, also known as "forever chemicals") and synthetic polyethylene (PE) and polypropylene (PP) have been widely used. However, these fluorinated chemicals are toxic, and plastic-based packaging presents additional challenges, such as low recycling rates (currently <9% in the U.S.), extremely slow degradation rates (>100 years), and microplastic contamination of landfills and water bodies.

This PhD thesis explores the potential of sustainable, plant-based soybean oil as a source for paper coatings, offering a greener alternative to develop recyclable, repulpable, and biodegradable paper packaging materials with enhanced water and oil resistance properties. The first section of the thesis highlights the use of acrylated epoxidized soybean oil (AESO) for paper coating applications. AESO coatings achieved exceptional oil and water resistance, as evidenced by a perfect kit rating (12/12) and a Cobb1800 value ( $\sim 2 \text{ g/m}^2$ ). The coating process involved applying AESO with 2wt% of a photoinitiator (2-hydroxy-2-methylpropiophenone) using a doctor blade, followed by UV curing to form a highly crosslinked polymeric surface.

The second section focuses on optimizing a waterborne coating system using an AESO blend with biocompatible polyvinyl alcohol (PVOH) as an emulsifying agent. PVOH, approved for direct food contact, provides a sustainable approach to emulsifying AESO. The AESO emulsion was applied to kraft paper, UV-cured, and achieved excellent oil and water repellency, with Cobb600 and Cobb1800 values of  $\sim 9$  and  $\sim 13$  g/m<sup>2</sup>, respectively, and a kit rating of 7/12. Optimization of AESO loading revealed that the best-performing sample had a loading range of  $\sim 15$ – $20$  g/m<sup>2</sup>. The coated paper retained over 90% of its mechanical properties and demonstrated more than 90% biodegradation within 90 days under industrial conditions.

The third section investigates the incorporation of magnesium hydroxide nanoparticles (Mg(OH)<sub>2</sub> NPs) into the waterborne AESO system to impart antimicrobial properties for potential applications in food and medical packaging. The Mg(OH)<sub>2</sub> dispersion in the AESO emulsion produced coatings with robust water and oil resistance. Tests revealed excellent moisture and oxygen barrier performance (in thin films of cured AESO) and a  $\sim 4$  log reduction in *E. coli* populations, achieving 99.99% bacterial elimination. These properties make the coated paper highly suitable for food and medical packaging applications.

The fourth section examines the integration of degradable crosslinkers into soybean oil to enhance the recyclability of coated paper. A photocurable AESO emulsion was blended with oligoacrylate lactide/glycolide to improve recyclability. In parallel, epoxidized soybean oil (ESO) was modified with glycolic and methacrylic groups. Hexagonal boron nitride (H-BN) nanosheets were employed as emulsifiers to stabilize these blends. The coated paper underwent extensive water and oil resistance tests, with its repulpability and recyclability successfully validated. Vermicomposting tests confirmed the compostability of the coated paper, presenting a sustainable alternative to conventional PFAS-coated packaging materials.

Dedicated to my mother Smt. Rekha Devi & my  
father Sri Pramod Kumar Gupta

## ACKNOWLEDGMENTS

The completion of this PhD thesis has been a journey filled with challenges, learning, and growth, and I am deeply grateful to everyone who has supported me along the way.

First and foremost, I must say I am very lucky to have amazing Ph.D. supervisor Prof. Muhammad Rabnawaz. His mentorship and unwavering support throughout my Ph.D. have been truly a game changer for me. He stands with all career decisions, and I am truly grateful to him for being a strong support. His insights, expertise, and encouragement have been instrumental in shaping this research. I am truly fortunate to have had the opportunity to learn under his mentorship.

I would like to express my appreciation to my thesis committee members Prof. Gary Blanchard, Prof. James Jackson, Prof. Mohammad Mohiuddin, Prof. Christopher Saffron, for their constructive feedback and thoughtful suggestions, which have greatly improved the quality of this work. Their time and efforts are sincerely appreciated. I would like to extend my thanks to my manager Salvador Crespo for giving me opportunities as an intern at Henkel. His mentorship and support helped me to learn a lot and to look at a given problem from an industrial perspective.

Special thanks to my colleagues (Dr. Ajmir Khan, Dr. Rishi Sharma, Dr. Muhammad Naveed, Dr. Saleh Alkarri, Dr. Syeda Shamila Hamdani, Dr. Mohamed Abdelwahab, Dr. Samin Aayanifard, Dr. Tanyaradzwa S. Muzata, Dr. Mohamed Shaker, Dr. Hazem, Subhaprad Ash, Gurjot Inder Singh, Rishabh Tiwari, Julia Anulare, May Dam, Anurag Ganapathi, Sarla Yadav, Sneha Naresh, Dhawal Sonar, Aparajith Venkataramanan, Ian Wyman) for their camaraderie, insightful discussions, and the many moments of encouragement that made this journey more enjoyable. The collaborations, shared experiences, and countless coffee breaks have been invaluable. I would like to particularly thank Dr. Ajmir Khan for all his input on my PhD projects

as well as being a great friend. I would thank to all my wonderful friends Dheerendra Rajput Singh, Gaurav Barnwal, Atul Chaudhary, Priyanshu Chandra, Vikrant Verma, Pushpender Yadav, Akhil Shajan, Shrirang Sabde for being in my life.

I am profoundly grateful to my family for their unconditional love, and belief in me. Their constant encouragement has been my pillar of strength throughout this journey. To my parents, Smt. Rekha Devi, Sri Pramod Kumar Gupta, my wife Komal Kumari for being very supportive, believing in me and encouraging, my elder brother Rajeev Kumar Gupta who always motivated me from a very young age to excel in life and do better, my sister-in-law Puja Gupta, my lovely niece Purva Gupta. I am also particularly excited about my newborn baby boy Om Gupta for making my life more joyful.

Finally, I would like to acknowledge the funding agencies and institutions that provided financial support for this research. Their contributions have made this work possible. This thesis is the culmination of years of hard work, but it would not have been possible without the incredible support system I have been fortunate to have. Thank you all. Thank you, GOD, for all the opportunity in my life.

## TABLE OF CONTENTS

CHAPTER 1: INTRODUCTION .....	1
CHAPTER 2: LITERATURE REVIEW .....	7
CHAPTER 3: A PLANT OIL-BASED ECO-FRIENDLY APPROACH FOR PAPER COATINGS AND THEIR PACKAGING APPLICATION .....	27
CHAPTER 4: SUSTAINABLE PACKAGING WITH WATERBORNE ACRYLATED EPOXIDIZED SOYBEAN OIL .....	49
CHAPTER 5: WATER, OIL AND MICROBE RESISTANT PAPER COATINGS VIA MgNP BLEND ACRYLATED EPOXIDIZED SOYBEAN OIL (AESO) EMULSION FOR PACKAGING APPLICATIONS .....	68
CHAPTER 6: DESIGN OF COMPOSTABLE AND RECYCLABLE MODIFIED SOYBEAN OIL COATED PAPER WITH ENHANCED WATER AND OIL RESISTANCE.....	88
CHAPTER 7: CONCLUSIONS AND FUTURE OUTLOOK .....	105
REFERENCES .....	108
APPENDIX A: SUPPLEMENTARY MATERIALS FOR CHAPTER - SUSTAINABLE PACKAGING WITH WATERBORNE ACRYLATED EPOXIDIZED SOYBEAN OIL .....	122
APPENDIX B: SUPPLEMENTARY MATERIALS FOR CHAPTER - DESIGN OF COMPOSTABLE AND RECYCLABLE MODIFIED SOYBEAN OIL COATED PAPER WITH ENHANCED WATER AND OIL RESISTANCE .....	144

## CHAPTER 1: INTRODUCTION

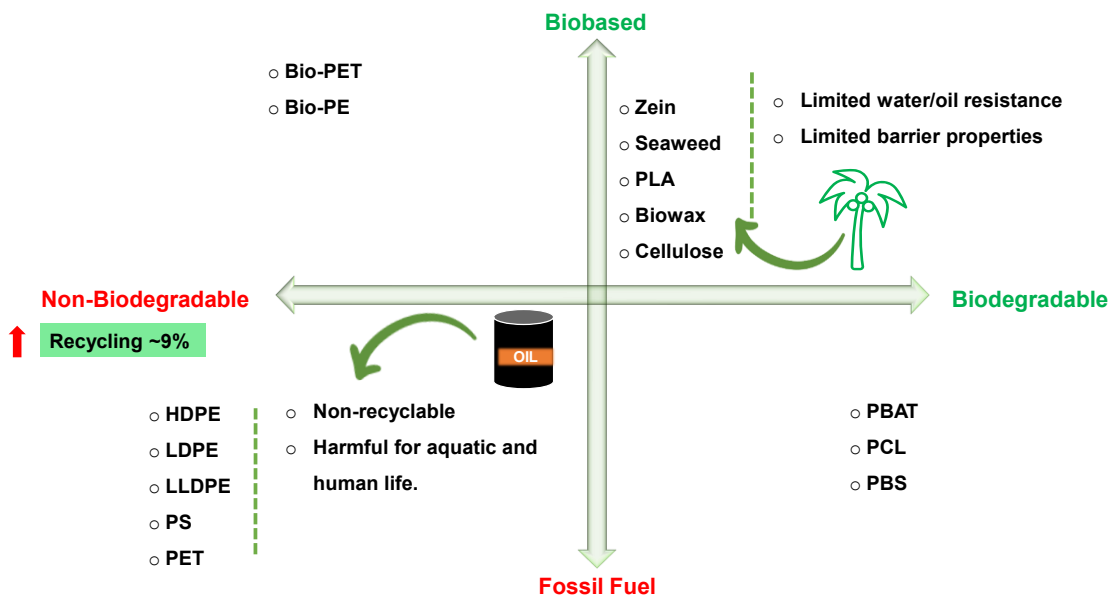
### 1.1 Background and Motivation

Paper packaging is an eco-friendly method for packaging goods as the main ingredient “pulp” is made up of cellulose fiber originating from plant material (wood).<sup>1,2</sup> Paper packaging is particularly valued for its recyclability, biodegradability, and renewability, making it a sustainable alternative to plastic-based packaging.<sup>3</sup> Growing environmental awareness and rapid climate change has led to a surge in demand for sustainable packaging, driving a shift toward paper-based solutions in industries like food, retail, and e-commerce.<sup>4,5</sup> However, the transition from plastic to paper packaging is not an easy path, there is a strong need for technological advancements in paper packaging to further improve its functionality and applicability as well as simultaneously considering the cost aspect.<sup>6,7</sup> The primary concern with paper packaging is absence of water/oil resistance as well as barrier properties; hence it is out of use for myriads of applications and plastic thus become primary choice.<sup>8,9</sup>

Paper usually lacks water/oil resistance and barrier properties mainly due to porosity as well as polar hydroxyl (-OH) unit responsible for hydrophilic nature of cellulose.<sup>10</sup> To address the water and oil resistance properties of paper there has been tremendous effort of research in recent years. All the approaches involved in modification of paper can be broadly categorized into two parts: internal and surface sizing (surface coating) methodology.<sup>11</sup> Internal sizing involves direct chemical modification/functionalization of cellulose structure of pulp to impart water resistance and it is beyond the scope of this work and focus has been on utilizing the surface coating methodology. The most commercial success for water- and oil-resistant paper has been mainly driven by coating/lamination of low-density polyethylene (LDPE), polystyrene, acrylic latex, and waxes.<sup>12</sup> Apart from deriving from petroleum-based products, there are numerous other concerns



raised from sustainability to safety aspect. For instance, paper coated with LDPE is difficult to recycle and hence there is a high chance of ending up in landfills instead of getting recycled.<sup>13</sup>



**Scheme 1.** Different categories of polymers are based on their source (fossils fuels or biobased) and their biodegradability features.

Additionally, petroleum derived polymers such as high/low density polyethylene (HDPE/LDPE), polystyrene (PS), polyethylene terephthalate (PET) are not biodegradable (**Figure 1**) and can take more than hundreds of years to degrade.<sup>12</sup> Microplastic generation is another alarming concern from these plastic waste generation as it could potentially alter the cellular processes in living organism and could be responsible for deadly disease such as Alzheimer.<sup>14</sup>

Another alternative such as per- and polyfluoroalkyl substances (PFAS) for creating water- and oil-resistant paper packaging has been widely adopted.<sup>15</sup> PFAS chemicals have historically been favored due to their low surface energy, which imparts strong resistance to liquids.<sup>16</sup> However, concerns over their persistence in the environment and associated health risks, including increased cancer risks and other toxic effects, have prompted efforts to phase them out.<sup>17</sup> Driven

by the mentioned concern of plastics and PFAS based coating for paper, there has been a strong surge for biobased alternative for paper coating applications. Biobased feedstock will not only take care of most of the above flaws, but it will also help to achieve carbon neutrality.

Biopolymers such as chitosan, zein, and starch have been utilized as coating materials.<sup>18,19</sup> These biopolymers offer advantages such as biocompatibility, non-toxicity, biodegradability, and renewability. Owing to these features biopolymer from biomass that is biodegradable as well (**Quadrant I, Figure 1**) could be potential solution for sustainable packaging.<sup>12</sup> Nonetheless, their practical application in packaging is difficult mainly due to limited resistance to water and oils and the innovation. Several other challenges remain as well for large-scale industrial adoption. Many of these methods involve complex processes, including multiple steps, the use of organic solvents, dual-layer coatings, or chemical grafting, which reduce cost-efficiency and environmental sustainability.

Another alternative, such as plant-based oils (e.g. soybean oil) offers an affordable and abundant alternative biobased feedstock.<sup>20</sup> These oils are biodegradable, non-toxic, and environmentally friendly. In 2021, soybean oil production exceeded 25.7 billion pounds, showcasing its vast availability.<sup>13</sup> The United States is a leading producer of soybean oil, which is widely utilized in both food and industrial applications. In the polymer industry, soybean oil serves as a renewable and sustainable feedstock. Its chemical structure supports modifications to create low molecular weight polymers for diverse applications, including plasticizers, paints, inks, biodiesel, lubricants, and coatings.<sup>21</sup> For instance, soybean oil conversion to epoxidized soybean oil (ESO) and further modification to acrylated epoxidized soybean oil (AESO), produced via a two-step process involving epoxidation and acrylation, which expands its utility in industrial applications.<sup>22</sup> These applications help replace petroleum-based materials, offering environmental

benefits while maintaining performance. There have been few studies that highlight the uses of modified soybean oil for paper packaging applications. For instance, silylated soybean oil has been used to coat kraft paper for water resistance, however, the improvement was only 35-45% reduction in water adsorption.<sup>23</sup> An alternate study utilizes 3-aminopropyltriethoxysilane (APTES) modified nanocrystalline cellulose (NCC) to disperse and stabilize the AESO emulsion in water.<sup>24</sup> The chemical modification involves multiple steps as well as using thermal driven polymerization process takes time ~2 h and 90 °C for curing. AESO emulsified using NCC-APTES coated paper has only been studied for water vapor barrier properties and the improvement is not significant as the barrier drops only from 1926.7 g/m<sup>2</sup>.day to 1286.3 g/m<sup>2</sup>.day (~33% reduction).

Detailed investigation into water and oil resistance properties of paper using modified soybean oil in their neat form as well as waterborne based emulsified form has not been explored in literature, especially UV curing methodology. Moreover, compostability, recyclability, repulpability, mechanical, antimicrobial properties of coated paper using modified soybean oil has not been explored substantially that will further strengthen the utility of modified paper packaging using plant oils. To tackle these challenges, this PhD thesis investigates strategies to achieve water and oil repellency on paper using modified soybean oil, eliminating the need for synthetic plastic/fluorinated chemicals.

## **1.2 Project Goals and Objectives**

The primary aim of this study is to establish a sustainable, plastic- and fluorine-free, closed-loop method for creating water- and grease-resistant paper. This will be achieved through specific objectives outlined in the research plan.

1. Neat commercially available AESO monomers were polymerized and tested on kraft paper

using UV light and a photoinitiator for the first time. The curing was confirmed using FTIR. Thermogravimetric analysis (TGA) was used to evaluate the thermal stability of the coatings. Further tests, including bending stiffness, ring crush, and internal tearing resistance, showed significant improvements in paper compared to uncoated paper. The tensile properties significantly reduce upon increasing loading of cured AESO. The coated kraft paper demonstrated excellent oil/grease and water resistance, with a kit value of 12/12 and a Cobb 1800 value of  $\sim 2 \text{ g/m}^2$ .

2. Develop a practical approach to create waterborne paper coatings using food-safe, biodegradable emulsifying agents. After screening various emulsifiers, polyvinyl alcohol (PVOH) emerged as the most effective for stabilizing AESO emulsions, while maintaining water and oil resistance. The AESO-emulsion coated paper was evaluated for its water and oil resistance, mechanical properties, printing performance, and biodegradability, ensuring it meets the requirements for environmentally friendly and functional packaging applications.

3. Developed and formulated the emulsion of AESO and magnesium hydroxide nanoparticles dispersed using polyvinyl alcohol (PVOH). This emulsion was applied to Kraft paper, enhancing its water and oil resistance. The coated paper was also tested for moisture barrier properties and demonstrated antimicrobial activity, with a  $\sim 4$  log reduction in *Escherichia coli* populations. Due to these properties, the coated paper shows significant potential for use in food and medical packaging applications.

4. We explored a novel approach to paper coating by incorporating a degradable linker into modified soybean oil using both extrinsic and intrinsic methods. In the extrinsic method, a photocurable AESO emulsion was blended with a degradable crosslinker, oligoacrylate lactide (AOLA) or oligoacrylate glycolide (AOGL), to improve degradability and recyclability. In the

intrinsic method, epoxidized soybean oil (ESO) was modified with glycolide and methacrylated. Hexagonal boron nitride (H-BN) nanosheets were used as emulsifiers to stabilize the blends. The coated paper exhibited excellent water/oil resistance, repulpability, recyclability, and compostability, offering a sustainable alternative to PFAS, acrylic, and polyethylene-coated papers.

## CHAPTER 2: LITERATURE REVIEW

### 2.1 Biopolymers from Biomass

One aspect of sustainable development for the packaging industry demands more integration of biomass-based biopolymer and swap partly/completely petroleum derived polymers. Biopolymers can be categorized into three categories: proteins, lipids, polysaccharide.<sup>12,25</sup> Each of them can be sub categorized further as shown in **Figure 2.1**.

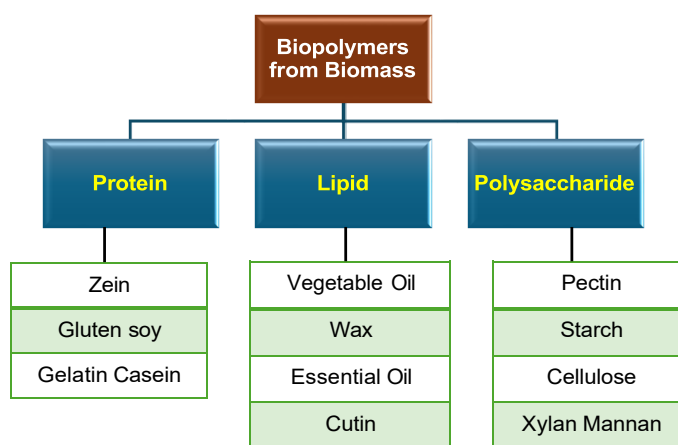


**Figure 2.1** Different categories of biopolymers derived from biomass. Lipid here only refers to naturally derived.

Out of all these categories our interest is mainly related to vegetable oils falling under lipid section. Lipids are insoluble in water but readily solubilize in organic solvents. There are three categories of lipids: simple lipids (fats/oils and waxes), compound lipids (glycolipids and phospholipids) and derived lipids (terpenes, carotenoids and steroids).

### 2.2 Structure, composition and properties of vegetables oils

Oil, in general, is naturally synthesized mainly via the esterification process of glycerol and fatty acids to form triglyceride.<sup>26</sup> The general structure of triglyceride that represents most of the oil can be described as shown in **Figure 2.2** where glycerol backbone and ester functional group have

been highlighted.<sup>25</sup> Soybean oil is a versatile vegetable oil extracted from the seeds of the soybean plant. It is one of the most widely produced and utilized edible oils worldwide, valued for its high content of unsaturated fatty acids, particularly linoleic and oleic acids.

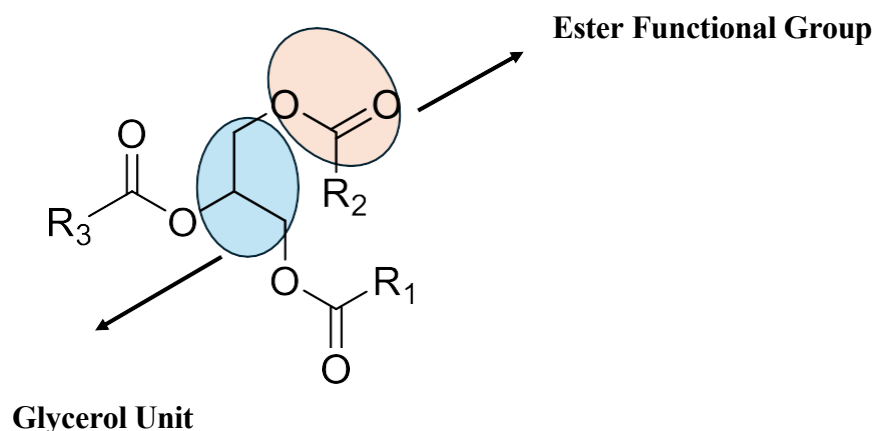


**Figure 2.2** Triglycerides (general structure) where R<sub>1</sub>, R<sub>2</sub>, R<sub>3</sub> represent different fatty acid chains.

Beyond its primary use in cooking, soybean oil is also a crucial feedstock for various industrial processes, including biodiesel production, the manufacture of lubricants, and as a precursor for chemical intermediates.<sup>21</sup> The chemical structure of soybean oil as well as most of the other vegetable oils can be described by the chemical structure provided in **Figure 2.3**. The structure has three segments mainly highlighted as oleic (one double bond), linoleic (two double bond) and linolenic (three double bond) fatty acid component.<sup>27</sup> There could be more variation in the chemical structure as oil is a mixture of triglycerides and detailed composition and classification of different vegetable oils has been provided in **Table 2.1**. All the vegetable oils generally have varying degrees of unsaturation. The name and chemical structure of different fatty acids possibly present in vegetable oils has been provided in **Table 2.2**.<sup>28</sup> Linseed oil has the highest linolenic component; however, linoleic and oleic components are higher in soybean oil (**Table 2.1**). Moreover, soybean oil is more abundant, and the US is the second largest producer of

soybean oil, hence, soybean oil is the preferred choice for this study.

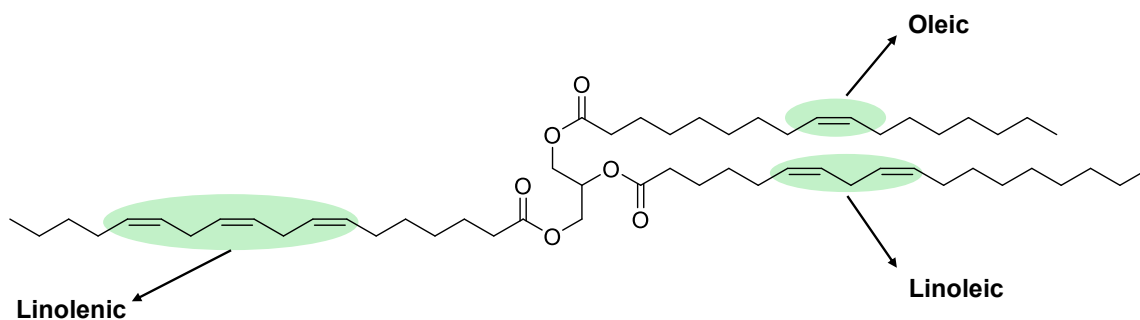


**Figure 2.3** Chemical Structure of plant oil with major components consist of oleic, linoleic and linolenic.

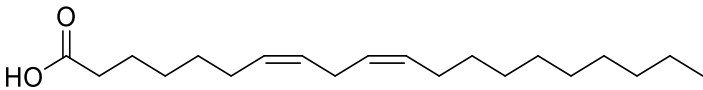
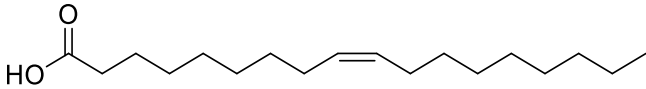
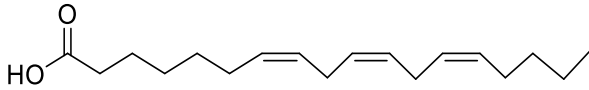
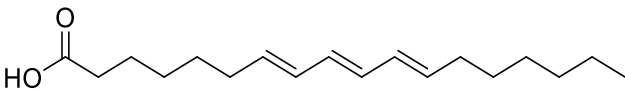
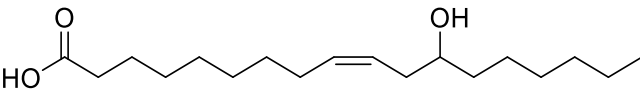
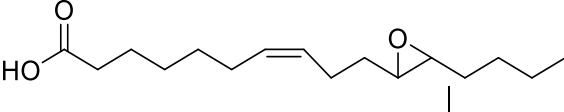
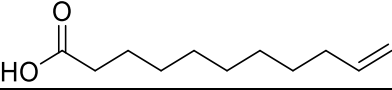
Since the vegetable oils have multiple double bonds present, it provides an opportunity for a chemist to utilize these unsaturated sites for further chemical modifications. For instance, double bonds can undergo hydrogenation, metathesis, ozonolysis, epoxidation, thiol-ene and so on. These different chemicals transformations have been highlighted in **Scheme2.1**.<sup>25</sup> such as acrylation. Epoxidized soybean oil is a chemically modified derivative of soybean oil, created through the epoxidation process. This process transforms the double bonds in the unsaturated fatty acid chains of soybean oil into epoxy groups using oxidizing agents such as peracids.<sup>29</sup> The presence of epoxy groups enhances ESO's chemical reactivity and improves its thermal and oxidative stability. ESO is widely applied as a plasticizer and stabilizer in the polymer and plastics industry, particularly for PVC-based products.<sup>30</sup> Due to its renewable, biodegradable, and environmentally friendly characteristics, ESO serves as an eco-conscious alternative to traditional petroleum-derived additives. Acrylated epoxidized soybean oil (AESO) is a further advancement of ESO, produced by reacting to its epoxy groups with acrylic acid. Detailed chemical modification steps of soybean oil to ESO and further conversion of ESO to AESO has been shown in **Scheme 2.2**.

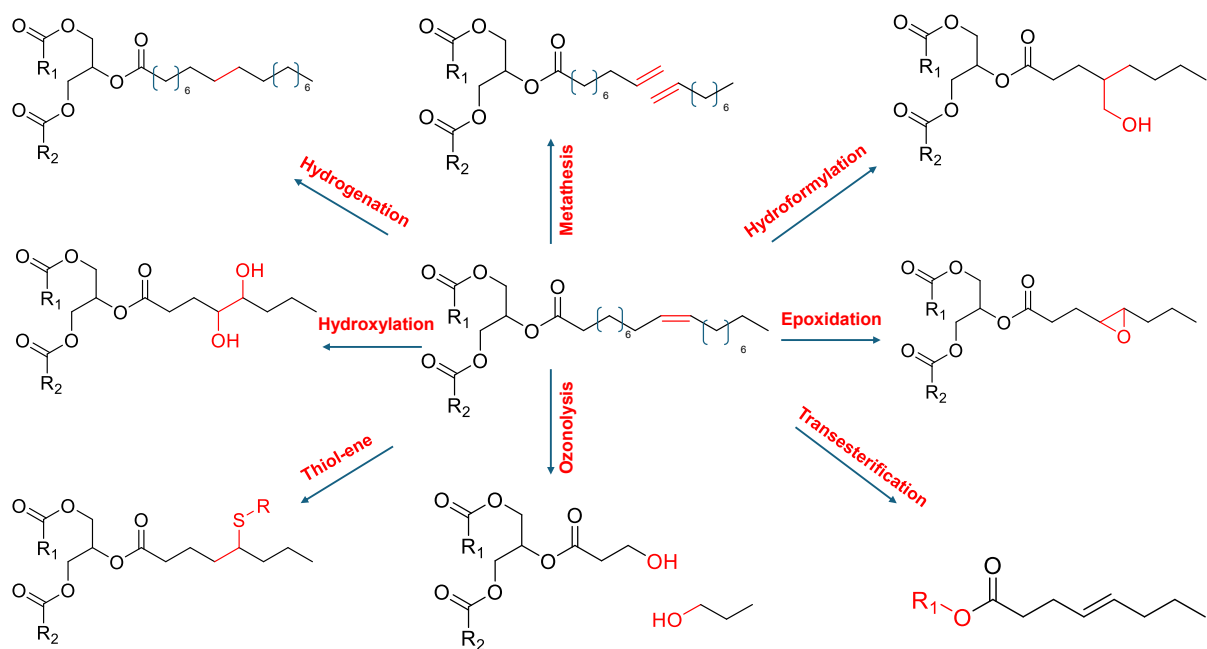


**Table 2.1** List of different vegetable oils with detail on the different fatty acid compositions.<sup>28</sup>

Oil	Fatty Acid Composition (X:Y, where X is the number of carbon atom and Y is the number of double bonds) %							
	Palmitic	Stearic	Oleic	Linoleic	Linolenic	Gadoleic	Erucic	Recinoleic
	16:0	18:0	18:1	18:2	18:3	20:1	22:1	18:1
Linseed	5.5	3.5	19.1	15.3	56.6	-	-	-
Soybean	11	4	23.4	53.2	7.8	-	-	-
Palm	44.4	4.1	39.3	10	0.4	-	-	-
Rapeseed	3	1	13.2	13.2	9	9	49.2	-
Castor	1.5	0.5	5	4	0.5	-	-	87.5
Sunflower	6	4	42	47	1	-	-	-

**Table 2.2** Name and chemical structure of different fatty acids possibly present in vegetable oils.

Name	Chemical Structure of common Fatty Acid Group
Linoleic acid	
Oleic acid	
Linolenic acid	
$\alpha$ -Eleosteaic acid	
Ricinoleic acid	
Vernolic acid	
10-undecanoic acid	



**Scheme 2.1** Various chemical pathways for conversion of triglyceride via reaction at unsaturated double bond sites.

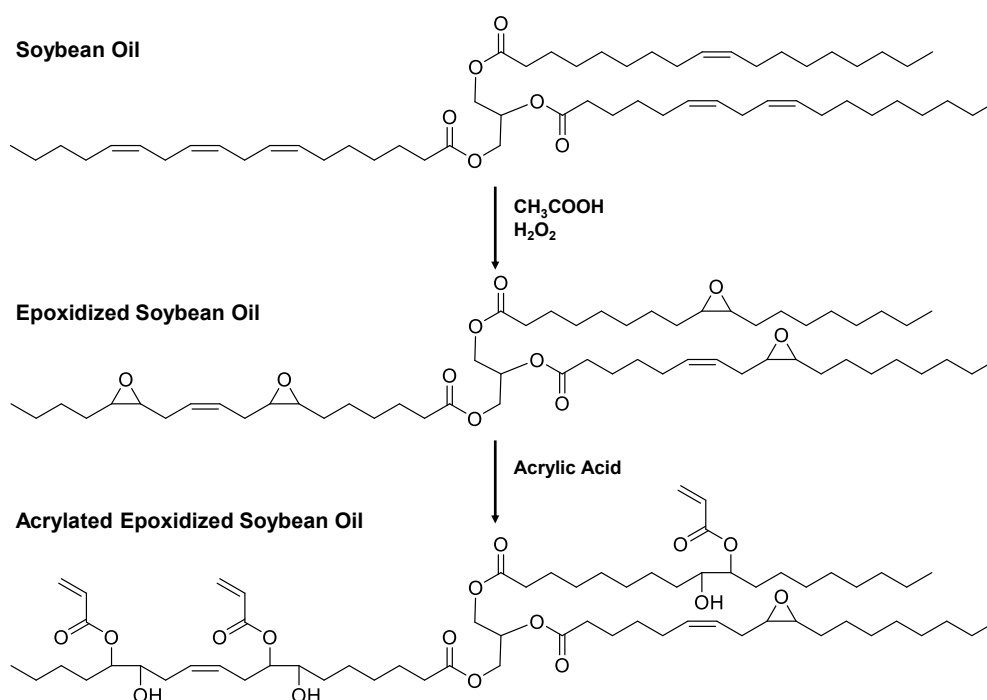
The triphenyl phosphine (PPh<sub>3</sub>) act as a nucleophile and abstract hydrogen from acrylic acid thus producing a carboxylate anion and thus attack on electron deficient carbon atom of epoxy ring. This results in ring opening and form ester and alcoholate anion which abstract proton from PPh<sub>3</sub>, thus acrylation is completed successfully.<sup>29</sup> Degree of epoxidation and acrylation can vary depending upon catalyst/reaction time/temperature and so on. Introduction of acrylate functional groups, making AESO highly reactive and ideal for free-radical polymerization. For instance, polymerized AESO can have varied glass-transition temperature ( $T_g$ ) as it increases linearly from -50 to 92°C with an increase in the number of acrylates unit from 0.6 to 5.8 acrylates per mole of triglyceride and hence a transition from soft to rigid polymers.<sup>21</sup>

AESO finds extensive use in UV-curable resins, coatings, adhesives, and inks, where its properties such as renewable sourcing, low toxicity, and excellent mechanical strength are highly valued.<sup>31</sup> These attributes make AESO a key material in sustainable and high-performance applications. The

development of soybean oil derivatives, such as ESO and AESO, highlights the potential of green chemistry to deliver eco-friendly and cost-effective solutions across diverse industries. By leveraging renewable resources like soybean oil, these innovations contribute to reducing dependence on fossil fuels while promoting sustainability.

### 2.3 Advancement in paper coating using Vegetable Oils

In recent years there has been a focus on using modified vegetable oils as coating ingredients for paper to impart water and oil resistance properties. To the best of my knowledge, up to date literature review has been summarized and provided in **Table 2.3** to highlight the paper packaging application using different vegetable oils.



**Scheme 2.2** Various chemical pathways for conversion of triglyceride via reaction at unsaturated double bond sites.

**Table 2.3** Summarized literature report on water/oil resistance properties using different vegetable oils via exploring different chemistry for functionalization. NA represents “Not Available”.

Sample, Year Published	Methodology	Cobb60 (gsm)	WVTR Reduction	KIT	Reference
<b>Palm Kernel Oil (PKO) (2020)</b>	Paper coating using PKO crosslinked with Furfuryl alcohol	NA	~22%	NA	32
<b>Acrylated epoxidized soybean oil (AESO) (2021)</b>	Paper coating using 3-aminopropyltriethoxysilane (APTES)-Nanocrystalline cellulose (NCC) stabilized AESO through Michael Addition Reaction	NA	~33%	NA	24
<b>Downstream Corn Oil (2019)</b>	Silane modified epoxidized downstream corn oil (SECO) coated paper	NA	~67%	NA	33
<b>Epoxidized Soybean Oil (ESO) (2017)</b>	Cured ESO with stearic acid as linker and ZnO nanoparticle coated on cellulosic fabrics	NA	NA	NA	34
<b>Tung Oil (2023)</b>	Paper coating using photopolymerizable tung oil and	17	NA	NA	35

Table 2.3 (cont'd)

<b>Vegetable Oils (2024)</b>	Plasma -enhanced chemical vapor deposition (PECVD) polymerization of chia/safflower/olive oils	NA	NA	NA	36
<b>Castor Oil (2019)</b>	Thiol-Castor Oil and 2, 4, 6, 8-Tetramethyl-2, 4, 6, 8-tetravinylcyclotetrasiloxane dissolved in THF	NA	NA	NA	37
<b>Epoxidized Soybean Oil (2016)</b>	Grafting cellulose with Polymeric Epoxidized Soybean Oil in n-hexane	NA	NA	NA	38
<b>Olive Oil (2022)</b>	UV-induced thiol-ene photocrosslinking of olive oil and 1,8-Octanedithiol	NA	NA	NA	39
<b>Epoxidized sunflower oil (2021)</b>	Chitosan-graft-sunflower oil	8	7.66/12	~40%	40
<b>Gelatine/palm/wax/lemongrass essential oil (2020)</b>	Mixed in water	87	NA	~7%	41
<b>Acrylated Epoxidized Linseed Oil (AELO) (2023)</b>	AELO-Beeswax formulation	NA	NA	~91%	29
<b>Castor Oil (2021)</b>	Chitosan-graft-castor oil	29.16	9/12	~50%	42
<b>Castor Oil (2024)</b>	Silanization of castor oil	NA	NA	~40.3	43

Table 2.3 (cont'd)

<b>Soybean Oil (2017)</b>	Silylation of unsaturated site of soybean oil	$\sim 22.24 \pm 0.45$	NA	$\sim 35\text{-}45\%$	23
<b>Waste cooking oil (2024)</b>	Water based emulsion using polyvinyl alcohol (PVA) of acrylated waste cooking oil coated on paper	NA	12/12	$\sim 40\%$	44
<b>Castor Oil/Methyl Ricinolate (2021)</b>	Epoxidized form of Castor Oil/Methyl Ricinolate are Silanized	NA	NA	$\sim 77.5\%$	45
<b>Rubber Seed Oil (RSO) (2024)</b>	Amidation, Esterification, Oxidation step on RSO and then stabilized using cellulose nanofibers (CNF) in water	NA	NA	$\sim 95\%$	46
<b>Camelina Oil (2024)</b>	Maleic anhydride grafted camelina oil (MCO) in DCM	NA	NA	$\sim 94\%$	47

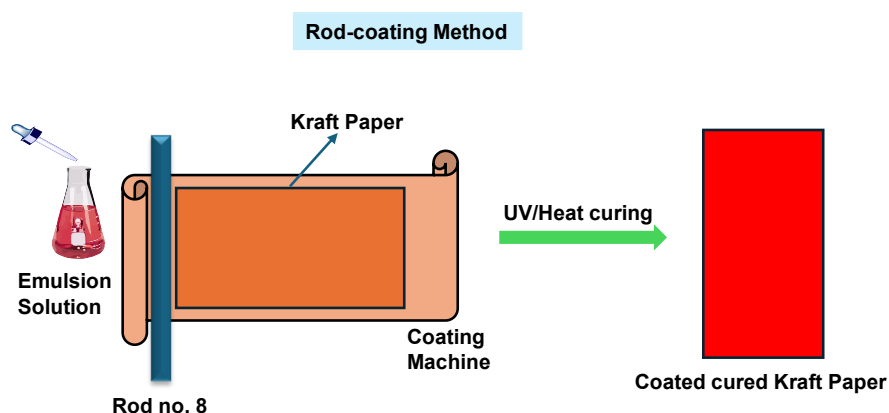
Different chemistry has been explored to functionalize these vegetable oils such as silylation of soybean oil and castor oil, grafting chitosan on sunflower and castor oil, acrylated soybean oil/linseed oil/waste oil and so on. Water resistance has been evaluated in most cases using water vapor transmittance rate (WVTR) studies but very few explored oil resistance properties. WVTR is good indication for water vapor resistant properties, but the Cobb test (water adsorption method) gives more confidence on direct water contact resistance. Along with water resistant properties, oil/grease resistance is crucial for food packaging applications. All the references in **Table 2.3** have focused on WVTR, and the Cobb test is missing in most cases. In a few cases the Cobb60 test has been performed, Cobb60 indicates the exposure of paper for 60 seconds. Although

Cobb60 is good method to judge the coated paper for very short period time (60 s), longer time (30 mins i.e. Cobb1800 testing) evaluation is critical for packaging application where coated paper can be in contact and exposed with water for prolonged time. Other factors such as biodegradation, repulpability, recyclability, mechanical properties, antimicrobial activities are equally important to investigate for modified coated paper to enhance the use case in packaging industry.

## 2.4 Fabrication of coating on paper-based materials

### 2.4.1 Rod Coating Method

The rod coating method uses a different type of rods having various groove depth that results in variation in coating thickness. First the paper has been pressed under the rod and the solution is poured underneath the rod and machine is turned on. The rods begin to move alongwith solution and uniformly coat the substrate (paper). This method helps with uniform coating with controlled thickness. The rod coating method has been illustrated in **Figure 3**. Usually for our experiment we used the rod coating method more often. However, there are several other coating methods discussed below.

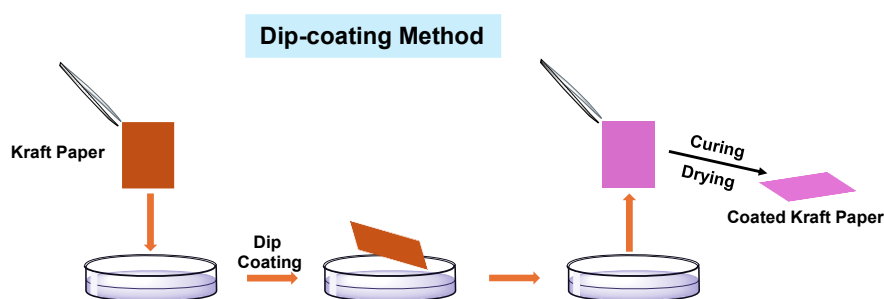


**Scheme 2.3** Rod coating method to coat kraft paper using emulsion solution followed by curing.

### 2.4.2 Dip Coating

The dip coating method is a simple and versatile technique used to apply thin films or coatings

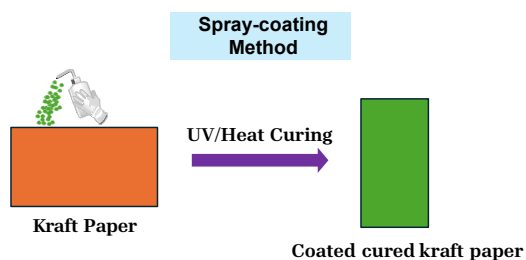
onto substrates. It involves immersing a substrate into a coating solution (slurry), withdrawing it at a controlled speed, and allowing the coating to dry and cure. The coating solution usually consists of a solvent or a mixture of solvents with dissolved or dispersed materials such as polymers, nanoparticles, or other functional compounds. Precision in controlling the coating thickness and uniformity can be challenging, especially with viscous coating solutions. The process is sensitive to environmental factors such as humidity and temperature, which can affect drying rates and coating quality.



**Scheme 2.4** Dip coating method to coat kraft paper in solution followed by curing.

### 2.4.3 Spray Coating

Spray coating is a versatile and efficient technique for applying thin and uniform coatings onto paper substrates. This method involves atomizing a liquid coating solution into fine droplets and spraying it onto the paper surface. The process is widely used in research and industrial applications due to its ability to coat large areas quickly and its adaptability to different coating formulations.

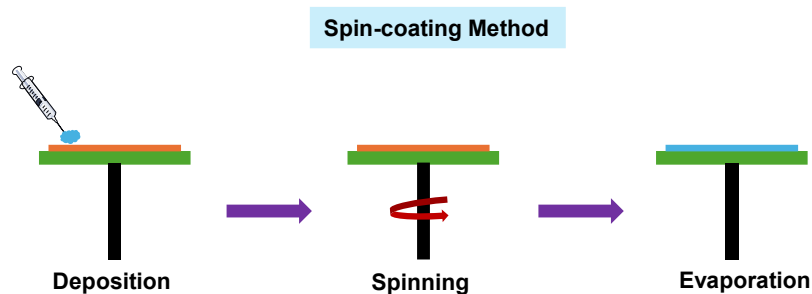


**Scheme 2.5** Spray coating method to coat kraft paper.



#### 2.4.4 Spin Coating

Spin coating is a widely used technique for depositing uniform thin films onto flat substrates. Spin coating relies on centrifugal force to spread a liquid solution evenly over a substrate. The uniformity and thickness of the resulting film depend on factors such as spin speed, solution viscosity, and spin time.



**Scheme 2.6** Spin coating method (less relevant for paper) followed by evaporation of solvent.

#### 2.5 Water-Resistance Tests

The Cobb 1800 test was performed according to TAPPI 441 protocols and standard tests of ISO535 to measure the water absorption capabilities of the papers.

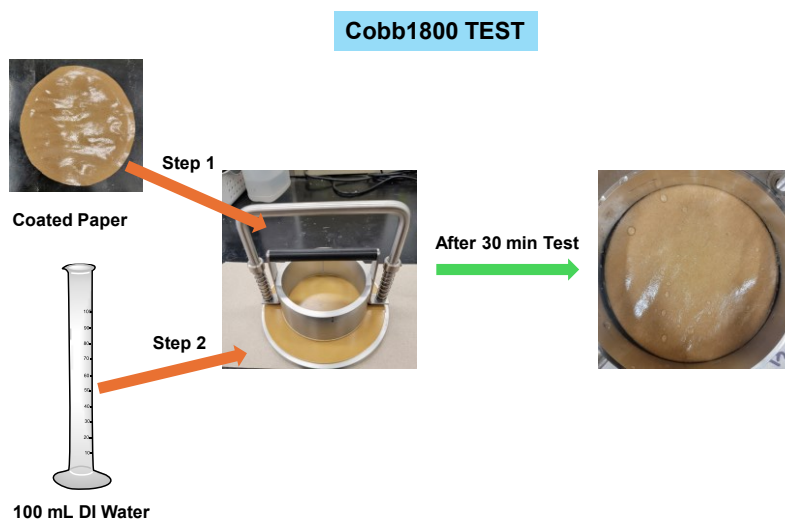


**Figure 2.4** Cobb testing method for 30 mins (Cobb1800), 100 mL of DI water is poured on 100 cm<sup>2</sup> exposed paper under tight conditions so no leakage is possible.

A sample of circular disk paper having a diameter of ~13.00 cm and an area of ~100 cm<sup>2</sup> was exposed to 100 mL of water (deionized) for 1800 s (30 min). The Cobb 1800 value calculation for absorbed water by the paper material was based on the difference in weight of the paper material before and after the test. The reported Cobb 1800 values corresponded to the weight of water that had been absorbed by paper (per square meter of paper) during a 30 min (1800 seconds) time.

## 2.6 Oil/Grease Resistance (Kit Rating)

The oil/grease repellency of paper was measured following the TAPPI UM 557 standards. In this scenario, a series of solutions with kit numbers ranging from 1 (the least aggressive resistance to the coated surfaces) to 12 (the strongest resistance to the coated surfaces) was applied onto the surfaces of the samples and the surface was then cleaned with tissue paper after 15 s.

**Table 2.4** KIT value (oil/grease resistance test) is given if the paper is not stained on the composition given (Castor oil, toluene, n-heptane).

<b>KIT Value</b>	<b>Castor Oil (% vol.)</b>	<b>Toluene (% vol.)</b>	<b>n-Heptane (% vol.)</b>	<b>Surface Tension (dynes/cm)</b>
<b>1</b>	100	0	0	33.9
<b>2</b>	90	5	5	31.2
<b>3</b>	80	10	10	28.8
<b>4</b>	70	15	15	27.6
<b>5</b>	60	20	20	26.3
<b>6</b>	50	25	25	25.3
<b>7</b>	40	30	30	24.8
<b>8</b>	30	35	35	24.4
<b>9</b>	20	40	40	24.1
<b>10</b>	10	45	45	24.0
<b>11</b>	0	50	50	23.8
<b>12</b>	0	45	55	23.4

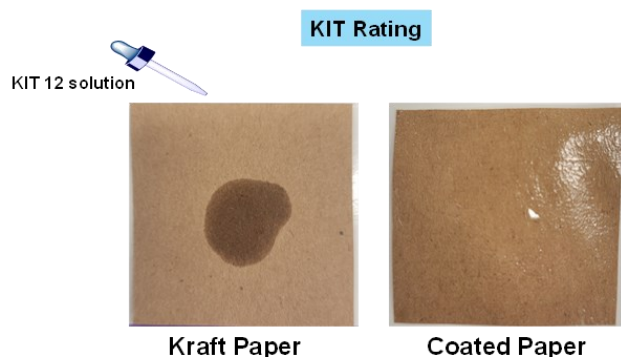


**Figure 2.5** Uncoated kraft paper easily gets stained even with pure castor oil, the coated paper can survive and potentially show maximum KIT rating (12/12).

The regions that were exposed to these solutions were examined and visible spots (normally darkened spots or regions) were taken as an indication that the sample had failed the respective kit rating test.

## 2.7 Physical Testing of Paper

Mechanical properties of paper are important to evaluate its performance as paper packaging go through various kinds of mechanical stress (bending, tearing, stretching, compressing, bursting) during various stages of manufacturing, packaging, transportation and so on. Under these various mechanical stresses, it is essential that paper maintains and resists those external stresses throughout the supply chain so that it ensures the packaged goods are intact throughout the processes. TAPPI standards have been used to perform all the mechanical testing. For instance, Tensile strength (**T 494**), Ring Crush Test (RCT) (**T 822**), Bending Stiffness (BS) (**T 489**) and Internal Tearing Resistance (ITR) (**T 414**) follow the quoted standards.

### 2.7.1 Tensile Strength

Tensile strength of paper measure using Instron, reveals the elastic characteristic of paper. It is an important parameter to evaluate the cellulose fiber quality and fiber bonding between as it plays

a crucial role in guiding the strength of paper. Paper while manufacturing the fibers tends to align along with machine direction (MD) and cross- direction (CD). Usually, the fiber aligned in machine direction can sustain higher stress than in CD. Since the tensile force is applied along the fiber direction, the stress applied is distributed to larger volume of fiber compared to when the same stress is applied to fiber aligned in cross-direction usually has smaller volume and hence the impact is more in CD than MD.

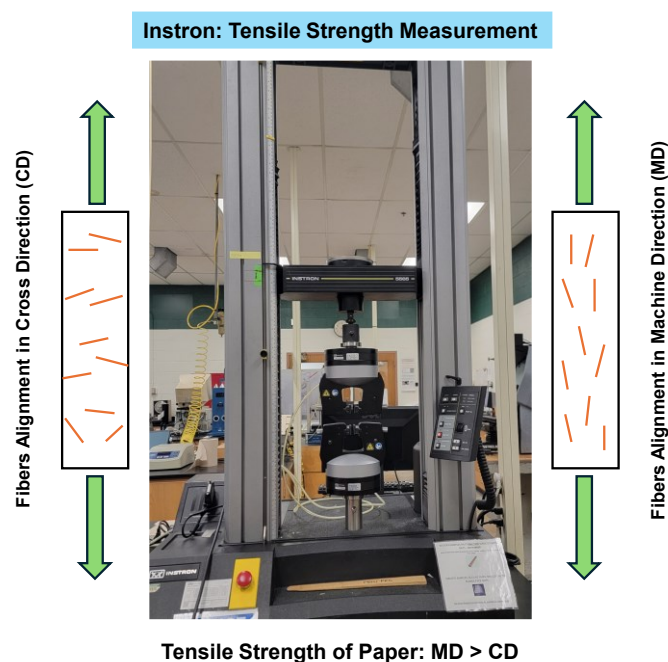


**Figure 2.6** Instron instrument where force is being applied in stretching mode, the fiber alignment (MD and CD) can have significant impact on paper strength. Generally, MD > CD.

### 2.7.2 Ring Crush Test (RCT)

The Ring Crush Test (RCT) is a key method used to measure the edgewise compression strength of materials such as paperboard, corrugated board, and similar products. It is a standard test in the packaging and paper industry to assess the strength of materials that will be used in the construction of packaging products like cartons and boxes.

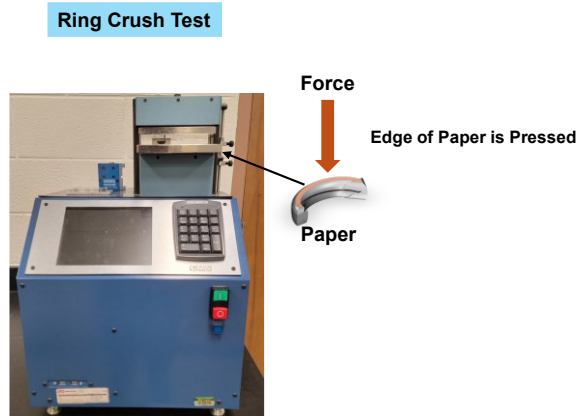


**Figure 2.7** Ring Crush Test (RCT) where force is applied on the edge of paper.

### 2.7.3 Bending Stiffness (BS)

Bending stiffness is a critical property of materials such as paper, paperboard, corrugated board, and other sheet-like materials. It quantifies the material's resistance to bending under an applied force and is essential in determining the durability and performance of packaging materials and structures.



**Figure 2.8** Taber stiffness tester, the paper is deflected by  $15^\circ$  in each direction then measure the stiffness in bending mode.

Bending stiffness is the force required to bend a material to a specified degree or curvature. It reflects how rigid or flexible the material is, with higher stiffness indicating greater resistance to

deformation.

#### 2.7.4 Internal Tearing Resistance (ITR)

Internal Tearing Resistance refers to the ability of a material, such as paper, fabric, or composites, to resist the propagation of a tear when subjected to stress. This property is crucial in applications where durability and reliability are key, such as packaging materials, printing paper, and industrial textiles. This test method determines the force required to tear multiple sheets of paper through a specified distance, perpendicular to the plane of the paper, using an Elmendorf-



**Figure 2.9** Elmendorf-type tearing tester.

type tearing tester. The results obtained are used to calculate the approximate tearing resistance of a single sheet.

#### 2.8 Biodegradation

Biodegradation refers to the natural breakdown of the material into simpler, environmentally benign substances by microorganisms such as bacteria, fungi, or enzymes. Coated paper is commonly used in packaging, printing, and labeling and is often treated with materials like plastic, wax, or clay to enhance properties such as durability, oil/water resistance. These coatings can influence the biodegradability of the paper. For instance, plastics like polyethylene (PE) or waxes

can significantly delay or inhibit biodegradation, on the other hand coating based on biobased polymers such as starch, cellulose, zein can easily be degraded. But it is not necessary that all types of biobased polymer can be degraded easily. The data for CO<sub>2</sub> evolution and % mineralization is mainly utilized to quantify the degradation process. The formula for the calculation of % mineralization is provided in Appendix A. According to the ASTM D6400-22 and D6868 protocols, if the % mineralization of a given material exceeds 90%, then it is considered to have good biodegradability. The aerobic biodegradation has been performed and was evaluated in compost under following conditions ( $58 \pm 2$  °C and  $50 \pm 5\%$  RH) by measuring the amount of evolved CO<sub>2</sub> using a direct measurement respirometer (DMR) equipped with a non-dispersive infrared gas analyzer (NDIR).

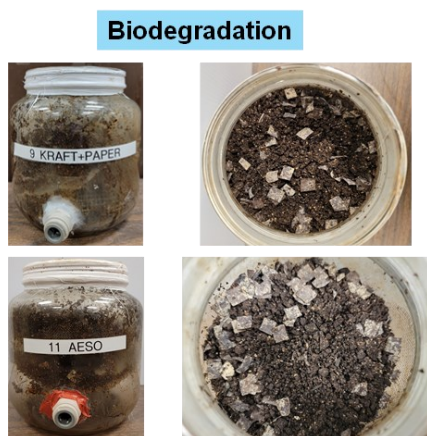


**Figure 2.10** The bioreactor was filled with 400 g of already conditioned compost followed by addition of 8 g of kraft paper and coated paper for testing.

## 2.9 Repulpability and Recyclability

Repulpability and recyclability of coated paper add significant value and crucial to establish circular economy. The repulpability truly stands for recovery of >80% of fiber yield by weight during the processing of coated paper following the standard test procedure while recyclability stands for blending of minimum 20% of fiber yielded from repulping process alongwith

uncoated (virgin) paper and form handsheet out of it. The handsheet must pass all the standard tests. Details have been discussed in Appendix B (section B.3).

## 2.10 Vermicomposting

Vermicomposting (home-composting) is an eco-friendly method of composting that uses worms, usually red wigglers (*Eisenia fetida*), to decompose organic waste into nutrient-rich fertilizer. This process turns kitchen scraps, garden waste, and other organic materials into a valuable soil amendment known as vermicast or worm castings. Worm castings are an excellent source of nitrogen, phosphorus, potassium, and beneficial microbes. It enhances soil structure, aeration, and moisture retention, diverting organic waste from landfills and helping reduce greenhouse gas emissions.



**Figure 2.11** Vermicomposting demonstration. Shredded leaves, water, waste food, worms are mixed, and coated paper is added to compost in the ambient condition. Temperature range (60-80 °F) is ideal for composting.

A sustainable and natural process with minimal environmental impact. The Vermicomposting



method is a more sustainable approach compared to industrial biodegradation. Although quantification is not possible for home composting type degradation, visual disappearance gives clear indication that sample has been fully composted. Also, the cost for testing biodegradation is huge while vermicomposting can be performed with little cost comparatively.

### **CHAPTER 3: A PLANT OIL-BASED ECO-FRIENDLY APPROACH FOR PAPER COATINGS AND THEIR PACKAGING APPLICATION**

A version of this chapter is published as:

Kumar, V.; Khan, A.; Rabnawaz, M., A plant oil-based eco-friendly approach for paper coatings and their packaging applications. *Prog. Org. Coatings* **2023**, *176*, 107386.

### 3.1 Abstract

The use of plant oil-coated paper could provide a greener approach to develop packaging materials in contrast to reliance on synthetic polymers-coated papers such as nylon, polystyrene (PS), polyethylene (PE), polytetrafluoroethylene (PTFE), polypropylene (PP), epoxy (commonly known as *plastic*), including plastic–paper hybrid materials. As described herein, we have successfully demonstrated the use of acrylated epoxidized soybean oil (AESO) for paper coating applications that exhibited excellent oil and water resistance as reflected by KIT rating (12/12) and Cobb 1800 ( $\sim 2 \text{ g/m}^2$ ) analysis. The coating steps include doctor-blade casting of AESO and 2 wt% of photoinitiator (2-hydroxy-2-methylpropiophenone) onto paper substrates followed by UV curing that yields highly crosslinked polymeric coating on the surface of paper. Fourier-transform infrared (FTIR) data confirms the crosslinking of AESO monomers, where the C=C stretching frequency ( $\sim 1638$  and  $809 \text{ cm}^{-1}$ ) disappears after UV treatment. Mechanical properties measurements show retention of  $>80\%$  in tensile strength in the coated sample as compared to the uncoated paper. Further analysis such as ring crush test, bending stiffness, and internal tearing resistance measurements demonstrate that AESO-coated paper offers a significant improvement over uncoated paper in terms of mechanical stability. Thermogravimetric analysis indicates that the crosslinked AESO-matrix is stable even at an elevated temperature ( $\sim 340^\circ\text{C}$ ), which demonstrates the stability of this polymeric material on paper substrates, thus increasing its utility in food packaging by mitigating the risk of the coating material leaching into food at high temperatures.

### 3.2 Introduction

Originating from plants as a natural renewable resource, paper-based materials have been widely used in packaging/non-packaging sectors.<sup>45,48–50</sup> Papers exhibit facile recyclability, economic

viability, and environmentally friendly features when compared to conventional plastics.<sup>18,45,51</sup> Due to its porous nature, virgin paper experiences deterioration in its barrier properties and tensile strength as it readily permits the permeation of liquids and gaseous molecules due to the presence of hydroxyl (-OH) groups and the hydrophilic characteristics of cellulose fibers, thus limiting their applicability.<sup>18,48</sup> To overcome the shortcomings mentioned and accelerate paper utilization in day-to-day life, various coating materials have been investigated and fabricated on the surfaces of paper.<sup>18,32,49,52,53</sup> The hybrid material prepared offered numerous advantages and could be a potential replacement for plastic-based packaging products. Traditionally, paper is laminated using fluorinated chemicals, synthetic plastic, a wax layer, paraffin, and so on.<sup>45,54</sup> Latexes and poly(fluoroalkyl) substances (PFAS) are some examples of fluorinated chemicals used for this purpose.<sup>49,55–57</sup> Despite the hazardous nature of these substances and restrictions on recycling, these applied coatings improve the water-resistance of the paper substrate, thereby mitigating their disadvantages to some extent.<sup>49,53</sup>

The chemistry of these packaging/non-packaging papers were also modulated via chemical modifications to convert the normally hydrophilic paper into a hydrophobic material through esterification, acetylation, metal chelation, and so forth. However, these approaches require harsh chemical conditions as well as expensive protocols.<sup>42</sup> An alternate and more environmentally friendly route could involve the use of biopolymers as coating ingredients such as chitosan, zein, starch, and so forth.<sup>58,59</sup> Although these polymers are biocompatible, non-toxic, biodegradable, and renewable in nature, their poor resistance to water or oils limits the practical applications of these packaging papers.<sup>60</sup> The various approaches that have been developed for paper coatings in recent years are summarized in **Table 3.1**. These methodologies were developed to achieve improved oil/grease and water resistance and can potentially offer replacements for the petroleum-derived

**Table 3.1** Comparison of Cobb Value and KIT rating from literature and this work.

Sample	Methodology	Cobb Values	Kit Rating	References
<b>This Work</b>				
<b>Crosslinked-AESO</b>	Single layer: coating of AESO followed by crosslinking under UV irradiation	$\sim 2 \text{ g m}^{-2}$ (cobb 1800)	12/12	This Work
<b>Previous Work</b>				
<b>PDMS-NCO</b>	Dual layer: PDMS-NCO chemical grafting with Melamine	NA	NA	52
<b>Chitosan-PDMS</b>	Dual layer: chitosan coating applied to fill the pores of the paper, followed by a polydimethylsiloxane (PDMS) coating	NA	12/12	61
<b>Chitosan-g-PDMS</b>	Chitosan-graft-polydimethylsiloxane (chitosan-g-PDMS) formed via copolymerization	$9.89 \pm 0.32 \text{ g m}^{-2}$ (cobb 60)	11.7/12	49
<b>Chitosan-g-castor oil</b>	Chitosan-graft-castor oil (CHI-g-CO) via copolymerization reaction	$29.16 \text{ g m}^{-2}$ (cobb 60)	9/12	42
<b>Zein/Chitosan-g-PDMS</b>	Zein used as a filler for chitosan-graft-PDMS (CHI-g-PDMS)	$21 \text{ g m}^{-2}$ (cobb 60)	11/12	18
<b>Chitosan-Zein</b>	Dual layer: chitosan-zein-based coating	$4.88 \text{ g m}^{-2}$ (cobb 60)	12/12	53
<b>Starch-Zein</b>	Dual layer: starch-zein based coating	$4.81 \text{ g m}^{-2}$ (cobb 60)	12/12	50
<b>PVOH-Zein</b>	Dual layer: Oleophobic PVOH applied in a bottom layer and zein as a subsequently applied hydrophobic top layer.	$3.00 \text{ g m}^{-2}$ (cobb 60)	12/12	64
<b>Chitosan-Sunflower</b>	Chitosan-graft-sunflower oil (CS-g-SO)	$8.00 \text{ g m}^{-2}$ (cobb 60)	7.66/12	40
<b>PVOH/Chitosan-g-PDMS</b>	Blends of poly(vinyl alcohol) and chitosan-graft-polydimethylsiloxane copolymer	$\sim 20 \pm 2.1 \text{ g m}^{-2}$ (cobb 60)	7.6/12	62

Table 3.1 (cont'd)

<b>Starch/Chitosan-g- PDMS</b>	Blends of corn-starch (S) and a novel chitosan-graft-polydimethylsiloxane (CP) copolymer	$13 \pm 0.9 \text{ g m}^{-2}$ (cobb 60)	12/12	<sup>63</sup>
<b>PKO</b>	Palm kernel oil formulation was prepared by mixing with a solvent and furfuryl alcohol (FA).	NA	NA	<sup>32</sup>

materials that are currently employed for paper coating applications.<sup>49,53</sup> However, to ensure that these coatings are suitable for large-scale adoption in industry, many factors still need to be considered and effectively addressed. Notably, most of the approaches described above involve multiple steps, the use of organic solvents, dual-layer coatings, the grafting of chemicals and so on, thus making the process less economical and eco-friendly.

Our group has recently developed some potential strategies involving dual-layer approaches as well as grafting/blending, hence offering several advantages in comparison to the conventional coatings applied onto paper which utilize materials such as latex, wax, paraffin, or low-density polyethylene (LDPE).<sup>18,49,53,61</sup> For instance, we developed plastic- and fluorine-free coating strategies for oil and water-repellent paper substrates using biodegradable composites of chitosan-*graft*-polydimethylsiloxane (chitosan-g-PDMS) and polyvinyl alcohol (PVOH).<sup>49,62,63</sup>

The resultant coated paper displayed good resistance to water, as demonstrated by its water contact angle (WCA) of  $119 \pm 6.3^\circ$  and Cobb 60 value of  $\sim 20 \pm 2.1$  gsm. In the subsequent work, an abundant biopolymer corn-starch blend was utilized with the graft copolymer chitosan-*graft*-PDMS. Due to the analogous chemistry of corn-starch and paper, the obtained coated papers showed a considerable decrease in water absorptivity and oil repellency, which was indicated by a KIT value of 12/12.<sup>63</sup> In another case, PDMS-NCO grafted coatings with melamine as a primer

were developed, which displayed good water-resistance and had a WCA of  $\sim 125^\circ$ .<sup>61</sup>

Plant-based oil is a cheap and plentiful resource that can be used as an alternative to petroleum-based paper coatings.<sup>65</sup> Plant oil-based coatings are not only biodegradable, but also non-toxic and eco-friendly.<sup>34</sup> One such example worth mentioning is soybean oil, which has a huge total production capacity that exceeded by **25.7** billion pounds in 2021. The chemical structure of soybean oil enables it to undergo various chemical alterations generating low molecular weight polymeric blends that are useful for applications such as plasticizers, paints, inks, biodiesel, lubricants, and coatings.<sup>21,65</sup> A two-step chemical modification (epoxidation and acrylation) of soybean oil results in acrylated epoxidized soybean oil (AESO).<sup>21</sup> Here in this work, commercially available AESO-monomers were polymerized on the surface of kraft paper by UV light using a photoinitiator. The obtained coated papers were optimized for their tensile strength and elongation properties to determine the consistency of the papers. Thermogravimetric analysis (TGA) analysis was employed to explore the thermal stability of the coated materials. Further analysis such as bending stiffness, ring crush test, and internal tearing resistance measurements demonstrate that the coated paper exhibits a significant improvement over the uncoated paper in terms of stability. The reported coated kraft paper exhibits high oil/grease and water resistance, with a KIT value of 12/12 and a Cobb 1800 value of  $\sim 2$  g/m<sup>2</sup>, respectively.

### **3.3 Materials and Methods**

#### **3.3.1 Materials**

Acrylated epoxidized soybean oil (AESO) (containing 4,000 ppm of the inhibitor monomethyl ether hydroquinone) was purchased from Sigma Aldrich. 2-Hydroxy-2-methylpropiophenone (a photoinitiator) was acquired from Genocure DMHA. Both of these chemicals were used without any further treatment or purifications/modifications. Paper (35-liner Kraft) was

purchased from Uline.

### **3.3.2 Methods**

A 20 mL vial was charged with AESO (10 g) and Genocure DMHA (photoinitiator) (2 wt%, ~0.2 g) using a magnetic bar. The reaction vial was stirred at ~ 70 °C for 5 min with the aim of melting and mixing. The mixture was then cast onto kraft paper substrates (with dimensions of ~13x13 cm<sup>2</sup>) with different loads (0.5, 1.0, 1.5, and 2.0 mL). Coating was done via the doctor-blade casting technique using a glass slide followed by immediately passing through the UV chambers for 4-5 cycles. The coated papers were named AESO-0.5, AESO-1.0, AESO-1.5, and AESO-2.0 based on their loadings (**Table 3.2**). Subsequently, these coated samples were used for further characterization and all other measurements. The results obtained were compared with uncoated kraft paper.

## **3.4 Characterization**

### **3.4.1 Fourier-transform infrared (FTIR) analysis**

An FTIR spectrometer of model FT/IR-6600typeA has been used to record the spectra of our samples. To improve the signal-to-noise ratio, the FTIR spectra were recorded in the range of 500–4000 cm<sup>-1</sup> with the use of 32 scans and a resolution of 4 cm<sup>-1</sup>.

### **3.4.2 Basis Weight and Thickness Measurement**

The Mass per square meter of the kraft paper (KP), AESO-0.5, AESO-1.0, AESO-1.5, and AESO-2.0 were calculated following the ASTM D646 protocol. Similarly, the weight of each of the papers samples was noted before and after application of the coating process. The paper was cut into a circular disc shape with a diameter of ~13.00 cm and an area equal to ~132.66 cm<sup>2</sup>. The loading of coated material was calculated by using the difference between the coated sample and uncoated kraft paper (control) using the following equation. The coating load was expressed



in g/m<sup>2</sup>.

$$\text{Coating Load} = \text{basis weight (coated paper)} - \text{uncoated paper}$$

$$\text{Where basis weight} = \text{weight (g)/area (m}^2\text{)}$$

The thickness of all the samples was recorded in  $\mu\text{m}$ , which was measured by a micrometer (Testing Machine Inc., New Castle, DE) at five different spots and the final value in **Table 1** refers to the average of these measurements.

### **3.4.3 Water-Resistance Tests**

The Cobb 1800 test was performed according to TAPPI 441 protocols and standard tests of ISO535 to measure the water absorption capabilities of the AESO-coated papers. A sample of circular disk paper having a diameter of  $\sim 13.00$  cm and an area of  $\sim 132.66$  cm<sup>2</sup> was exposed to 100 mL of water (deionized) for 1800 s (30 min). The Cobb 1800 value calculation for absorbed water by the paper material was based on the difference in weight of the paper material before and after the test. The reported Cobb 1800 values corresponded to the weight of water that had been absorbed by paper (per square meter of paper) during a 30 min (1800 seconds) time period.

### **3.4.4 Contact Angles (CAs)**

An advanced automated goniometer (590-U1, Ramé-Hart Instrument Co., USA). was used to measure the static contact angles (CAs) for all AESO-coated samples. The CAs of the coated surfaces were recorded by using deionized water with  $\sim 10$   $\mu\text{L}$  droplet volumes. The contact angles of these droplets were measured after 5 min with an average of at least three measurements being performed on the same specimens at different spots.

### **3.4.5 Oil/Grease Resistance (KIT Rating)**

The oil/grease repellency of AESO-coated papers was measured following the TAPPI UM 557 standards. In this scenario, a series of solutions with kit numbers ranging from 1 (the least

aggressive resistance to the coated surfaces) to 12 (the strongest resistance to the coated surfaces) was applied onto the surfaces of the samples and the surface was then cleaned with tissue paper after 15 s. The regions that were exposed to these solutions were examined and visible spots (normally darkened spots or regions) were taken as an indication that the sample had failed the respective kit rating test. The solution (with the highest number) that does not stain the coated surface is reported as the “KIT rating” for that sample.

#### **3.4.6 Tensile Measurements**

The tensile properties of the AESO coated samples and kraft paper (KP) or of the control were measured using an Instron Series 5565 (Instron, MA, USA) instrument via the TAPPI (Tensile properties of paper and paperboard) standard T494 procedure. All tensile measurements were performed by placing paper specimens between the two-grips of the Instron with a gap separation by 7.1 inch. The paper dimensions (10.23” x 1”) were kept constant among all the samples. A constant rate of 12.75 mm/min was applied during the stretching process. TS value was reported in MPa and the plot between strain and stress was obtained via the Instron Bluehill Software package (Instron, MA, USA).

#### **3.4.7 Ring Crush Test (RCT)**

RCT was implemented via a TMI crush tester. All ring crush test (RCT) measurements were carried out by following the TAPPI standard T882 protocol on AESO-coated samples in the machine direction (MD) as well as the cross direction (CD). The sample with dimensions of 0.5”x6” was cut and then fitted into a ring shape sample holder. Model 1210, Instron, MA, USA is used for the RCT.

#### **3.4.8 Bending Stiffness (BS)**

Bending stiffness (BS) capacities of the AESO-coated samples were carried out by using a Taber

stiffness tester (model 150-D, Teledyne Taber, NY, USA) ensuing the TAPPI standard T489 procedure. The sample dimensions of 1.5” x 2.75” were cut using a sample cutter. The paper was bent by 15° using a total force of 500 Taber stiffness units from the other side. The reported data was collected by using the following equation.

$$\text{Bending Moment} = (\text{Average of left and right reading}) \times P$$

Where  $P = 5$  when the weight is marked as 500 Taber stiffness units.

#### **3.4.9 Internal Tearing Resistance (ITR)**

ITR measurements were carried out via the TAPPI standard T414 protocol by using an ME-1600 Manual Elmendorf-type tearing tester. Two plies of the same sample were used for the ITR test. The reported data was collected by using the following equation.

$$\text{Average tearing force, grams} = (16 \times \text{scale reading}) / \text{number of plies}$$

#### **3.4.10 Thermogravimetric Analysis (TGA)**

Samples (10-15 mg) were taken for thermogravimetric analysis of AESO sample and UV crosslinked AESO samples by using a thermogravimetric analyzer (TA Instruments, Q50). The N<sub>2</sub> flow rate was kept at 40 mL/min and the temperature increased from 25 to 600 °C using a ramping rate of 10 °C/min.

#### **3.4.11 Optical Transmittance**

UV-Vis spectrometer was used for the percent transmittance (%T) of the AESO-0.5, cast on a glass slide. A blank glass slide was used as a reference and the %T value (at the wavelength of 550 nm) was taken as 100%. The UV-Vis spectrometer used was Perkin-Elmer Lambda 25.

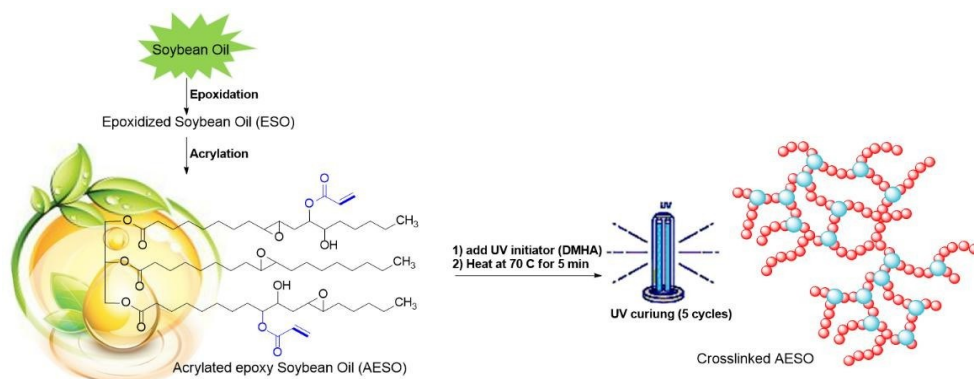
#### **3.4.12 UV-curing**

AESO-coated paper samples were also subjected to the UV-LED curing process. A UV- LED NC1 unit manufactured by Heraeus Noblelight from Cambridge, UK, was used for these curing

processes.

### 3.5 Results and Discussion

In response to the search for greener ways to coat paper substrates while ensuring that they are well-protected against water and oil/grease, the focus has been shifted from petroleum-derived materials toward plant-based renewable, biodegradable, low-cost, bio-compatible, and environmentally friendly sources. Along with other research groups, our lab has shown tremendous effort to contribute to this direction. We have summarized a list of previous approaches in Table 3.1. To obtain high-performance paper coating, we have applied AESO-derived soybean plant oil onto kraft paper. The main reason for the selection of AESO for the coating purposes was their ready availability as well as low cost and biocompatibility. Moreover, the presence of the unsaturated functional sites of AESO provides additional capabilities to obtain high-performance paper coating via UV curing.



**Scheme 3.1.** Schematic representation of the conversion of AESO to the crosslinked AESO by using 2-Hydroxy-2-methylpropiophenone (photoinitiator) in the presence of UV light.

A well-established method for the conversion of soybean oil to epoxidized soybean oil (ESO) followed by the ring opening reaction of ESO with acrylic acid to yield AESO has been demonstrated (Scheme 3.1). Following Scheme 3.1, commercially available AESO (~10 g) was mixed with GENOCURE\* DMHA (a photoinitiator) (~2 wt%, 200 mg) in a reaction flask.

Subsequently, the mixture was heated at 70 °C for 5 min to allow proper mixing. Furthermore, the mixture was cast onto kraft paper via the “doctor-blade method” and exposed immediately to UV radiation for 5 s. This UV treatment was repeated five times for each of the samples. The formulations of the coated paper were based on the loading of the samples. AESO formulations with four different concentrations of 0.5, 1.0, 1.5, and 2.0 mL were cast onto kraft paper substrates with dimensions of 13 x 13 cm<sup>2</sup> (**Figure 3.1A-3.1C**). **Table 3.2** demonstrates the thickness, base weight, as well as loading used for AESO-coated samples along with their names. The coated samples were immediately passed through a UV chamber of the UV curing machine. The extent of UV curing of the AESO occurring upon UV irradiation through free-radical crosslinked polymerization (**Scheme 3.1**) was monitored via FTIR spectroscopy, as shown in **Figure 3.2**. The spectrum of AESO showed a characteristic peak at 1625-1660 cm<sup>-1</sup> due to the stretching vibrations of the acrylated carbon-carbon double bond (C=C) that is associated with soybean oil.

**Table 3.2** Thickness, basis weight, and coating load of uncoated kraft paper and AESO-coated papers.

Sample Code	Thickness (μm)	Basis Weight (g/m <sup>2</sup> )	Coating Load (g/m <sup>2</sup> )
Uncoated Paper	175.4 ± 2.2	125.13 ± 0.0	----
AESO-0.5	227.3 ± 5.7	156.34 ± 0.5	31.20 ± 0.5
AESO-1.0	235.0 ± 6.2	185.06 ± 3.0	59.92 ± 2.9
AESO-1.5	270.7 ± 10.2	215.46 ± 1.3	90.33 ± 1.3
AESO-2.0	321.0 ± 0.6	239.48 ± 4.8	114.35 ± 5.0

Subsequently, the disappearance of these acrylated carbon-carbon double bonds upon exposure to UV radiation confirms the consumption of these double bonds of the copolymer (AESO). Likewise, the peak in the sample of AESO at ~800 cm<sup>-1</sup> can be attributed to the vinyl fragment

of the acrylic acid. Upon exposure to UV radiation, this out-of-plane absorption peak of deformation of the C=C bond of the vinyl part of the acrylic acid has also completely disappeared.

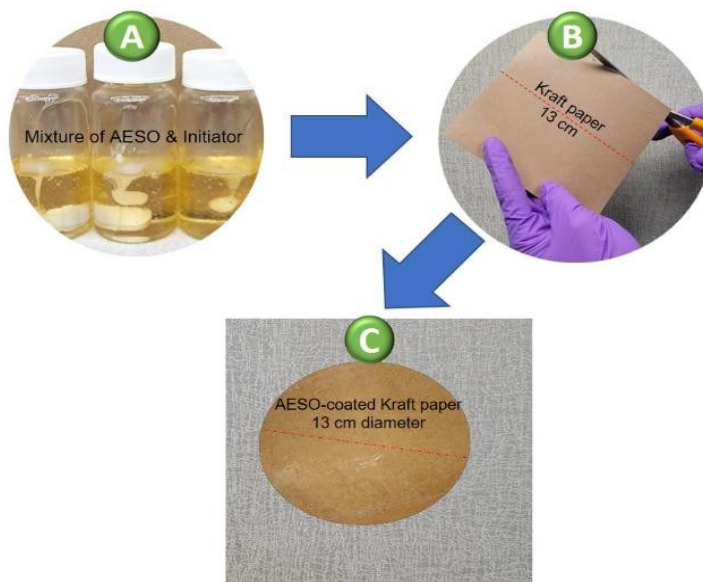


**Figure 3.1** A) Photographs of the resultant yellow blend of 10 mL AESO and DMHA photoinitiator; B) Kraft paper for casting with dimensions of 13 cm x 13 cm; C) crosslinked AESO-coated kraft paper in a disc shape with diameter of 13 cm.

The loading of the coated material is a crucial parameter, as it is an indicator of whether cost-effective process suited for industrial applications. To evaluate the loading level of coating material, the basis weight of each sample has been calculated. The method for basis weight calculation has been provided and is described in the material and Method section. The calculated basis weights are summarized in **Table 3.2**. The basis weight of the AESO-0.5 sample is  $\sim 156$  g/m<sup>2</sup> as compared to  $\sim 125$  g/m<sup>2</sup> for kraft paper (uncoated paper). The loading was calculated by taking the difference between the basis weight of the coated sample and kraft paper, and thus the loading obtained for AESO-0.5 is  $\sim 31$  g/m<sup>2</sup>. Similarly, the loading for the other coated samples including AESO-1.0, AESO-1.5, and AESO-2.0 have been calculated, and these values are listed

in Table 3.2.

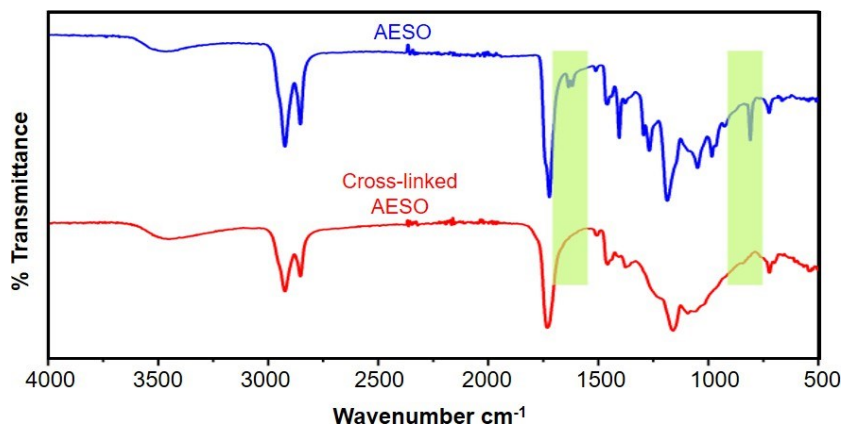


**Figure 3.2** FTIR spectra of AESO and crosslinked-AESO were recorded in the range of 500-4000  $\text{cm}^{-1}$ . The highlighted rectangular portion indicates that peaks near  $\sim 1650$  and  $\sim 800 \text{ cm}^{-1}$  represent the C=C vibrational frequency in the AESO sample that disappeared in the crosslinked film obtained after UV curing.

The highest loading value corresponds to the AESO-2.0 sample and is  $\sim 114 \text{ g/m}^2$ . The low values for Cobb 1800 measurement are an excellent demonstration of water resistance and is widely used method in the coating industry for water resistance. Hence, we determined the Cobb 1800 values of our AESO-coated papers and their respective control (uncoated kraft paper) (**Figure 3.3A**). The water absorptivity of uncoated or unmodified paper was recorded at  $72.4 \text{ g/m}^2$ , which significantly decreased to  $5.5 \text{ g/m}^2$  (corresponding to a decrease by  $\sim 90\%$ ) when coated with AESO followed by UV curing. The Cobb 1800 value was further decreased to  $3.54 \text{ g/m}^2$  for AESO-1.0 coated paper.

This significant advancement in water resistance can be attributed to the almost complete masking of the paper's pores by the soybean oil, as the concentration of the AESO was doubled in comparison to the previous sample (AESO-0.5). In subsequent water resistance measurements, the Cobb 1800 values for AESO-1.5 and AESO-0.2 were determined and found to be 2.71 and 2.18

g/m<sup>2</sup>, respectively. It has been also validated from these measurements that further increases of the AESO content on kraft paper had no significant effect on the water absorptivity. The above Cobb 1800 measurements revealed that the total improvement of water absorptivity was approximately 97% compared to that of unmodified paper. (**Figure 3.3 A**).

The water resistance of the coated papers was also confirmed by the hypothetical measuring of the time-dependent contact angle for all our coated samples. The WCAs for all coated samples have been recorded above ~90-92° as compared to the uncoated kraft papers where it was below 90°. More importantly, the time-dependent study indicates that the WCAs of the uncoated paper decrease with time, while those of the coated sample are retained for several minutes. Overall, Cobb 1800 and time dependent WCA studies reveal that the coated paper exhibits superior water resistance in contrast to the uncoated kraft paper.

TAPPI T559 protocol was used to determine kit values (oil resistance) for the AESO- coated paper samples and compared with that of the uncoated kraft paper (the control). The kit test is a standard test that is frequently used in the coating and paint industry. Kit rating values can be in the range from 0-12, with a higher value corresponding to better oil/grease resistance for a given sample. Therefore, the best oil resistance on this scale corresponds to a kit rating of 12/12. The oil resistance (kit rating) for uncoated paper was found to be 0/12. This low value was observed because the kraft paper itself did not exhibit any oil or grease-resistance. Interestingly, the introduction of AESO to kraft paper followed by UV curing treatment yielded a substantial improvement in the oil resistance, as manifested in **Figure 3.3 B**. For example, the kit rating of AESO-0.5 was observed to reach as high as 8/12. By increasing the content of AESO on the kraft paper, the kit rating of the AESO-coated paper could be substantially further to 12/12. This significant improvement in oil and grease resistance is due to almost all the paper's pores being



masked by the AESO. Meanwhile, the AESO-1.5 and AESO-2.0 samples were also exposed to the kit solvents and the kit rating recorded for these samples were 12/12 for both. These results indicate that the crosslinked AESO covered almost the entire surface area of the paper substrate. The mechanical stability of coated paper is of great importance for real-world or industrial applications. It is one of the essential criteria that must be studied to analyze the durability and robustness of coated samples that can ensure longevity as well as a wide range of packaging applications for coated paper.

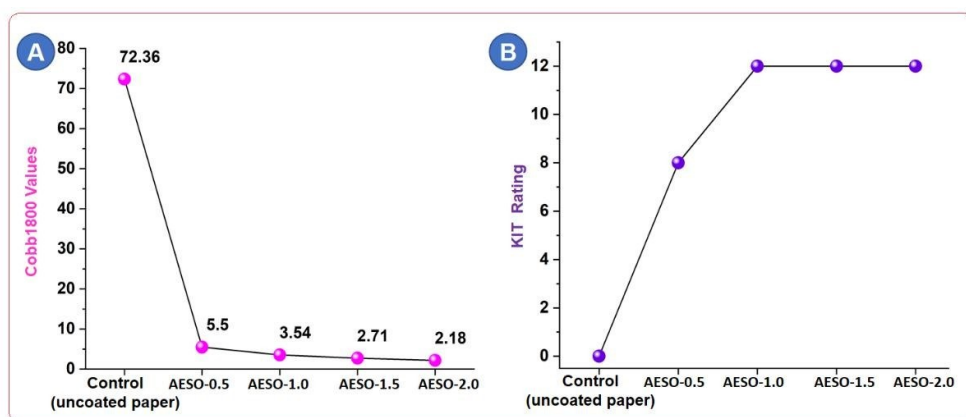


**Figure 3.3 A)** Cobb 1800 values representing the water resistance of uncoated and coated samples with four different AESO concentrations for 1800 s. **B)** Kit rating values measured for uncoated and coated samples, where the value of 12/12 corresponds to the best oil/grease resistance.

Consequently, the mechanical properties of the AESO-coated paper and uncoated kraft paper (control) were also evaluated in this study to investigate the effect of soybean-copolymer on paper. For this purpose, AESO-coated papers (AESO-0.5, AESO-1.0, AESO-1.5, and AESO-2.0) and unmodified paper samples were evaluated for their tensile/mechanical strength, bending resistance, ring crush test performance as well as their tearing force resistance.

The tensile strength of the uncoated paper was found to be  $54.26 \pm 1.62$  MPa. Subsequently,

the tensile strength of the AESO-coated paper was also measured, and a slight decrease in the tensile strength was recorded for the coated samples. **Figure 3.4A** illustrates that the tensile strengths of the AESO-coated samples decrease while the thickness of the coated paper is increased.

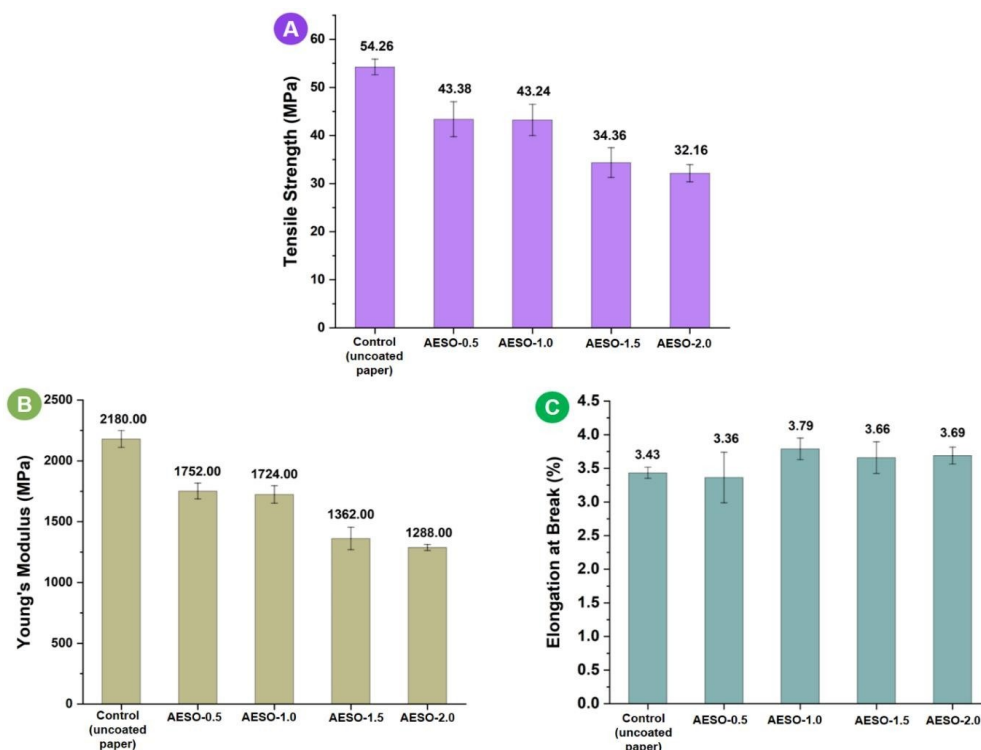


**Figure 3.4.** **A)** Tensile strength (MPa) measurements for the uncoated paper (control) and AESO-coated samples. Each sample being tested three times in machine-direction (MD); **B)** Young's Modulus measurements for the uncoated paper (control) and AESO-coated papers; **C)** % Elongation (Elongation at break) measurements for the uncoated paper (control) and AESO-coated samples.

However, it is noteworthy that the AESO-1.0 sample retains ~81% of the tensile properties exhibited by uncoated paper. The trend observed for Young's modulus is very similar to that of the tensile strength (**Figure 3.4B**), but an increment in the elongation percentage at break has been noted. For instance, the uncoated sample exhibits an elongation percentage of  $3.43 \pm$

0.08% at break, and the corresponding value increased to  $3.69 \pm 0.12\%$  for the AESO-2.0 sample. This increment could be attributed to the polymeric nature of crosslinked AESO that enabled the embed coated sample to become elongated to a slightly greater extent than the uncoated sample (**Figure 3.4C**).

The ring crush resistances of coated or uncoated paper strip were measured via ring crush tests (RCTs) that were performed according to the ISO 12192 and TAPPI 822 protocols. The RCT value was measured in both the machine direction (MD) and the cross direction (CD). It was found that the unmodified Kraft paper exhibited a ring crush resistance of 28.5 lbs in the MD and 23.2 lbs in the CD. These values gradually increased for the AESO-coated papers when the thickness of the coatings increased. The histogram plot for RCT is presented in **Figure 3.5A** to compare the values along the MD and the CD. There is a growing trend in RCT values for both the MD and the CD for all the coated samples with respect to the uncoated Kraft paper, which demonstrates the enhanced performance of the AESO-coated samples. Bending stiffness (BS) is one of the important mechanical properties that defines the flexural strength or bending moment of paper per unit of width producing unit curvature. Therefore, the BS of the samples were measured and compared with one another, as shown in **Figure 3.5B**. The bending resistance for uncoated paper (control) was found to be 49.5 g.cm in the MD and 26.5 g.cm in the CD. When the AESO-coated papers were tested, it was found that with an increase of AESO-coating thickness, the bending stiffness also increased gradually. For example, AESO-2.0 showed a BS of 94.5 g.cm in the MD and 41.0 g.cm in the CD, showing a growing trend in both directions. Overall, the mechanical properties of AESO-coated paper did not change significantly relative to the uncoated kraft paper, although offering enhanced water and oil resistance.

To find other mechanical properties of AESO-coated papers we also have conducted tear

resistant tests which correspond to the force required to break a paper strip in a perpendicular direction. In this scenario, internal tearing resistance (ITR) measurements for the uncoated paper (control) were recorded at 200 g in the MD while they were observed at 128 g in the CD.

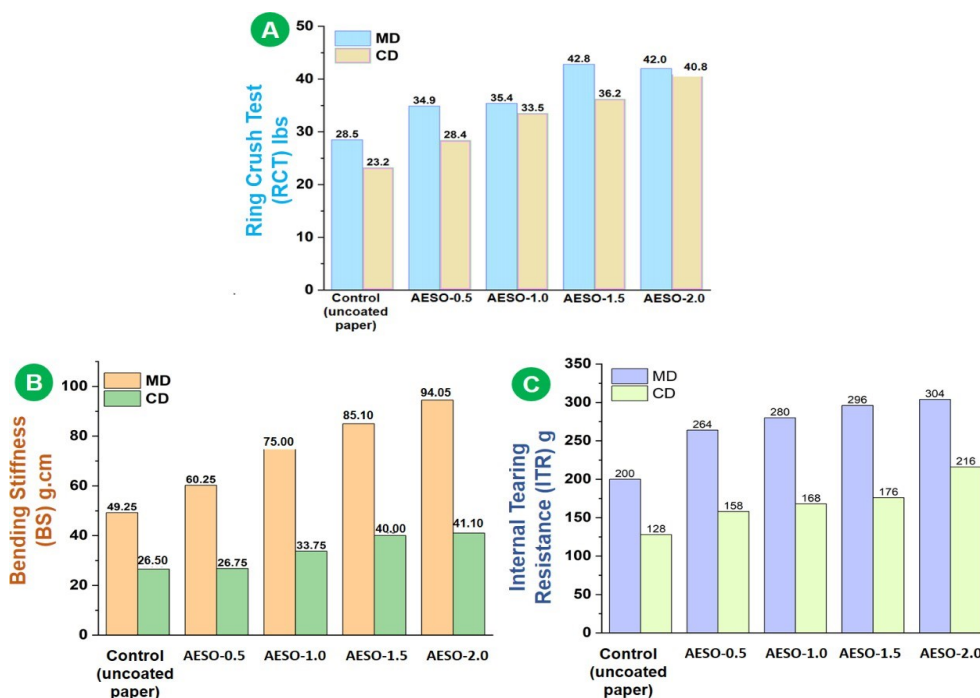


**Figure 3.5. A)** Ring crush test (RCT) measurements for the uncoated paper (control) and AESO-coated papers in in both the machine direction (light blue color) and the cross direction (yellow color). **B)** Bending Stiffness (BS) measurements for the uncoated paper (control) and AESO-coated samples. These measurements were performed in the MD (orange color) and in the CD (green color); **C)** Internal tearing resistance (ITR) measurements for the uncoated paper (control) and AESO-coated papers in in both the MD (light blue color) and the CD (light green).

Comparing these values of the uncoated paper with that of AESO-coated paper (AESO-0.5), the IRT were recorded at 264 g in the MD and 158 g in the CD (**Figure 3.5C**). The tearing force required to rupture AESO-0.5 paper in the MD increased by approximately 32% as compared to uncoated kraft paper whereas it was observed to increase by 40% for AESO-1.0, 48% for AESO-

1.5, and 52% for AESO-2.0. Similarly, the tearing resistance was also recorded in the CD and a growing trend was observed for the AESO-coated paper unlike the uncoated paper.

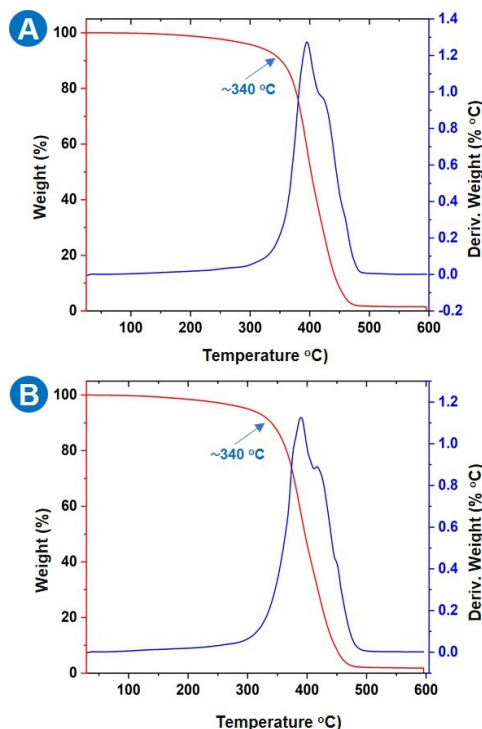


**Figure 3.6. A)** Thermogravimetric analysis (TGA) of the AESO sample (before UV curing) A)

Thermogravimetric analysis (TGA) of the crosslinked AESO (after UV curing). These measurements were recorded over a temperature range from 25 to 600 °C at a ramping rate of 10 °C/min.

In a nutshell, it can be claimed that there is improvement in BS, RCT, and ITR performance for the AESO-coated samples in contrast to the uncoated paper. Additionally, the high retention of tensile strength ( $\geq 80\%$ ) exhibited by the coated sample compliments the superior overall performance of the coated paper in comparison with the uncoated paper.

Thermogravimetric analysis (TGA) analysis for AESO (before UV curing) and crosslinked AESO (after UV curing) samples were performed to evaluate thermal stability. The film of crosslinked

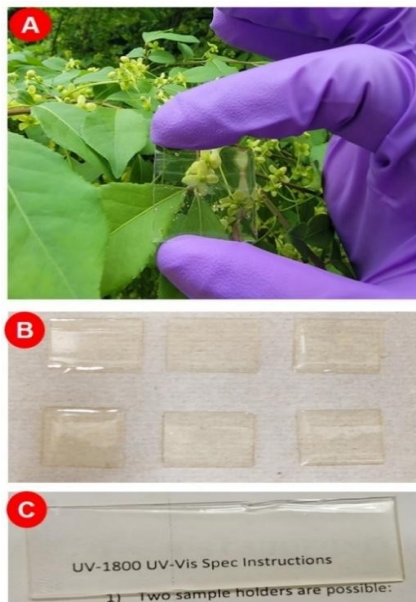


**Figure 3.7.** **A)** Photograph of an AESO-coated glass slide kept in front of green leaves to reveal the transparent nature of film; **B)** AESO-coated film on Uline kraft paper roll towel; **C)** AESO-coated films kept on written text.

AESO was peeled off from the coated surface and tested over a temperature range from 25 to 600 °C using a ramping rate of 10 °C/min. **Figure 3.6A** displays the TGA curve obtained for the AESO sample (before UV curing). This TGA curve indicates that decomposition of the sample started at ~340 °C and complete loss was observed at ~460 °C. Subsequently, the crosslinked AESO sample was also characterized via TGA to determine whether its thermal properties had changed after UV curing. The TGA curve in **Figure 3.6B** indicates that decomposition of the sample started at ~340 °C and was complete at ~460 °C. Comparing both curves, it appears that no significant thermal changes had occurred due to the UV curing treatment. The % weight loss graph at ~350 °C indicates that AESO-coated papers can be used for numerous industrial or practical applications without becoming damaged.

Water and oil repellency, mechanical flexibility, and thermal stability are some of the important

factors that expand the applicability of coatings. In addition to the above properties, optical transparency or clarity further increases their suitability for applications in industry. In this respect, the optical clarity of the AESO films was also investigated. Ultraviolet-visible (UV-Vis) spectroscopy was used to determine the % transmittance of the AESO films at 550 nm.<sup>66</sup> For reference, an uncoated glass slide was used, and its transmittance was taken as 100%. Parallel to the reference slide, an AESO-coated slide ( $\sim 700\ \mu\text{m}$ ) was set in the spectrometer. The percent transmittance (%T) of AESO-coated sample has been recorded and found to be  $\sim 99 \pm 1\%$  (**Figure 3.7A-C**).

### 3.6 Conclusion

In summary, an environmentally friendly, readily available, and bio-based co-polymer of acrylated epoxidized soybean oil (AESO) has been casted onto kraft paper and subsequently subjected to UV curing treatment in the presence of a photoinitiator. The crosslinked AESO-coated films were analyzed by FTIR spectroscopy. TGA characterization revealed that the coated matrix had excellent thermal stability. Meanwhile, the outstanding Cobb 1800 value ( $\sim 2\text{gm/m}^2$ ) together with the high kit rating (12/12) demonstrated that the AESO-coated paper samples exhibited water and oil/grease repellency, respectively. The mechanical properties of the coated samples were also compared to that of uncoated kraft paper, and they were found to retain approximately 81% of the tensile strength while exhibiting enhanced ring crush resistance, bending stiffness (BS), and internal tearing resistance (ITR). In addition to the above desirable features, the high optical transparency (99% transmittance at 550 nm) can further increase their potential for applications in industry and as food packaging materials. Our results could foster further development of the paper coating industry using natural and abundant vegetable oil.

## **CHAPTER 4: SUSTAINABLE PACKAGING WITH WATERBORNE ACRYLATED EPOXIDIZED SOYBEAN OIL**

A version of this chapter is published as:

Khan, A<sup>#</sup>.; Kumar, V<sup>#</sup>.; Anulare, J.; Dam, M.; Wayman, I.; Rabnawaz, M., Sustainable Packaging with Waterborne Acrylated Epoxidized Soybean Oil. *ACS Sustainable Resour. Manage.* **2024**, 1 (5), 879-889. (# - *Equal Contribution*)



#### 4.1 Abstract

Packaging is responsible for ~46% of total plastic waste, and thus, sustainable packaging alternatives are urgently required. Reported herein is coated as a sustainable packaging material using waterborne acrylated epoxidized soybean oil (AESO) to coat Kraft paper. The waterborne AESO was cast onto kraft paper and was then photo-cured. Upon curing, the coated paper was tested for its oil and water repellency as well as its mechanical properties. Biodegradability studies were also conducted for the AESO-emulsion coated paper, and our findings suggest that its biodegradability reaches >90% within 90 days. The coating process was also evaluated for its compatibility with paper printing processes and its resistance to hot oil. Overall, the AESO-emulsion coated paper offers desirable water and oil resistance and mechanical properties, offers biodegradability, and is also cost-effective. This work thus provides a sustainable alternative to the currently wasteful packaging made with plastic or plastic-coated paper. This work also fits numerous principles of green chemistry, such as waste prevention (no microplastics), the use of safer solvents (water), the promotion of renewable feedstock, and the design of packaging that is biodegradable.

#### 4.2 Introduction

Nearly ~36% of plastics are used in the packaging sector owing to their low cost, easy processability, and flexibility (**Figure 4.1 A**).<sup>67</sup> However, the use of plastics has led to environmental concerns (**Figure 4.1 B**) due to the presence of non-biodegradable chemical moieties (because of strong -C-C units in the polymer backbone) in many of these materials.<sup>68–70</sup> In addition, conventional plastics are primarily derived from non-renewable (petroleum derivatives) resources.<sup>71–74</sup> On the other hand, paper is a plant-based renewable material derived from cellulose, and it can be easily recycled, has good mechanical properties, and is eco-

friendly.<sup>75</sup> These properties provide strong motivation to maximize their application in packaging and non- packaging sectors.<sup>1,76</sup> However, paper in its unmodified form has poor water and oil resistance. Therefore, there is a strong interest in creating a modified paper that performs like plastic but retains the e-friendly properties of paper.<sup>77</sup>

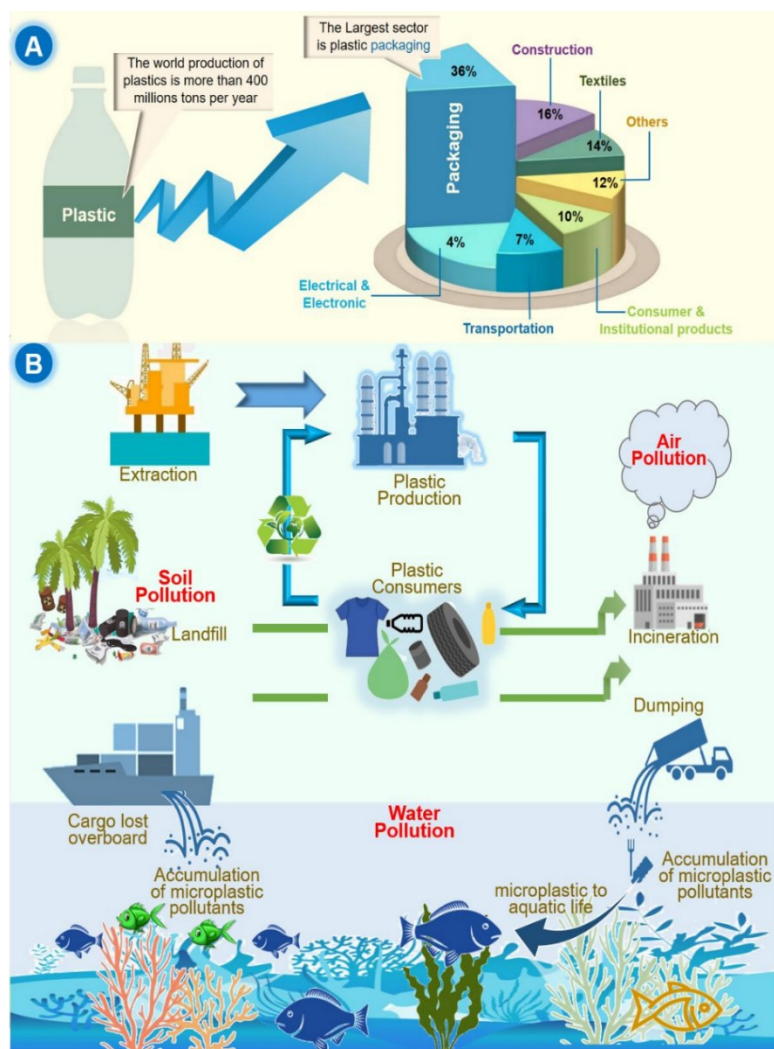


**Figure 4.1** Uses of plastics and the issues they pose to the environment. **A)** Plastic is used in our daily lives for both packaging and non-packaging applications. **B)** Environmental concerns related to plastics and their waste.

Coated- and laminated paper are widely used in industry for packaging applications as they combine the performance of plastics with the sustainability of paper.<sup>78</sup> For example, coated paper

substrates offer better oil and water resistance than their uncoated counterparts, making them suitable for packaging applications such as cups, plates, straws, aseptic cartons, food wrappers, etc.<sup>79–81</sup> However, coated- and laminated paper are difficult to recycle because the coating must be separated from paper pulp. As a result, coated paper is sent to landfills or incinerated. In addition, polyethylene (PE) and perfluorinated alkyl substances (PFAS) are widely employed in paper cups/plates and fast-food wrapper applications, respectively.

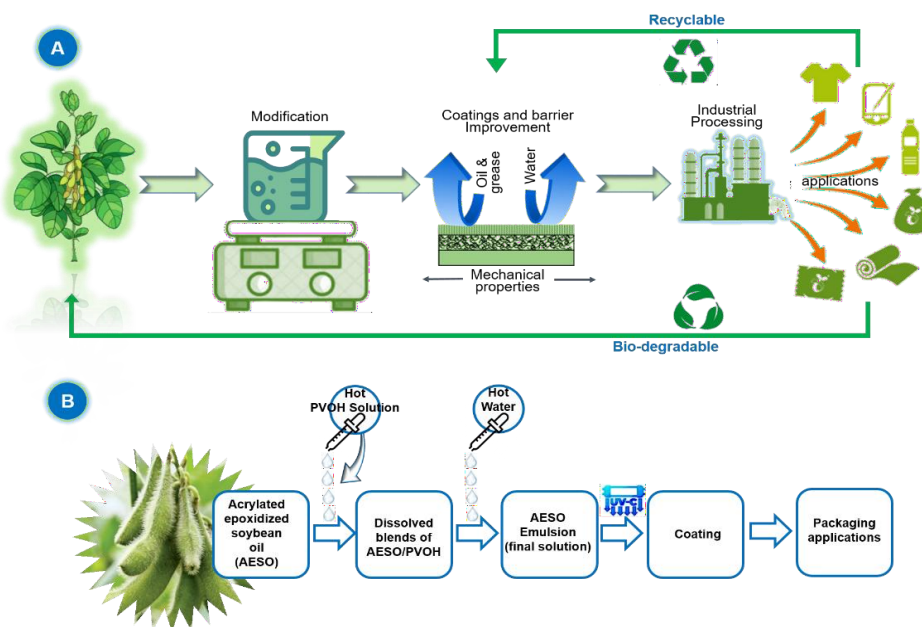


**Figure 4.2** Flow schemes depicting the preparation of plant-based polymers and AESO-emulsion. **A)** Schematic representation of plant-based polymers, their development, packaging applications, recyclability, and biodegradation. **B)** Flow scheme showing our AESO, its use to prepare an emulsion, its application onto paper substrates, and its subsequent packaging applications.

However, PE has the potential to form persistent microplastics, while PFAS has carcinogenic concerns. There is a strong need to replace PE and PFAS with bio-based, non-toxic, recyclable, and biodegradable paper coating material.<sup>82,83</sup> Researchers have recently devoted enormous

efforts toward replacing these non-degradable plastic layers with natural renewable biopolymers, such as zein, starch, chitosan, and so forth.<sup>50,62</sup> These biopolymers are degradable, and hence, they pose a much smaller threat to the environment than conventional plastics.<sup>84</sup> Additionally, they can be easily peeled from the surface of the paper, thus facilitating repulping/recycling processes.<sup>63</sup> Plant-based oils are emerging as eco-friendly coatings for paper substrates (**Figure 4.2 A**).<sup>53,85</sup> We have recently used AESO for a simple yet very effective paper coating with outstanding water and oil resistance properties.<sup>13</sup> These results were indeed exciting, but a high coating loading was required because AESO was the sole coating material. For example, the minimal loading was  $\sim 31 \text{ g/m}^2$ , and the maximum loading reached  $\sim 114 \text{ g/m}^2$ . In addition, the reported coating was not waterborne, despite waterborne coatings being preferred for paper substrates in industry.<sup>86</sup> For example, the global market value of waterborne coatings has been estimated to be about \$99.2 billion in 2021 and is expected to expand at an annual growth rate of 4.0% from 2022 to 2027.

Herein, we report on a practical approach to produce waterborne paper coatings using food- safe biodegradable emulsifying agents (**Figure 4.2 B**). To find a good emulsifier, such as one that imparts stable emulsion, minimal effect on water and oil resistance, and food safe, we screened many emulsifiers. Polyvinyl alcohol (**PVOH**) stood out as the most suitable emulsifier for AESO. AESO-emulsion coated paper was tested for its water resistance and oil resistance, mechanical properties, printing performance, and biodegradation.

### 4.3 Results and Discussion

Plant oils are readily available, environmentally benign, and biodegradable, thus making them an ideal substitute to formulate bio-based pre-polymers.<sup>87</sup> As the name indicates, plant oils are liquids that can migrate from paper if they are used for paper coating applications. Polymerizable plant oils such as acrylated soybean oil address this problem as after curing, AESO becomes a

hard material. Both heat and ultraviolet (UV)-curing techniques can be used to polymerize AESO. The UV-curing approach has received tremendous attention thanks to its applicability in industrial processes such as the curing of adhesives, inks, and coatings due to its very short reaction time (less than 60 s).<sup>88</sup> Lately, our exploration focused on utilizing plant-based soybean oil (acrylated epoxidized soybean oil or **AESO**) for producing coated paper through photocuring, resulting in impressive Cobb-1800 values and kit ratings of approximately  $\sim 2 \text{ g/m}^2$  and  $\sim 12/12$ , respectively.<sup>13</sup> However, the amount of AESO used in this approach was rather high (1-2 grams) for the  $13 \times 13 \text{ cm}^2$  kraft paper, making it less feasible for industrial applications and less attractive from a sustainability standpoint. The reason for using large coating loads was due to the absence of solvent thinners (organic solvent diluents). This motivated us to develop waterborne AESO emulsions in the presence of polyvinyl alcohol (PVOH) for paper coating, thus replacing any organic solvents using an environment-friendly approach.

PVOH can be used for the aqueous dispersions of several organic gels, oils, and polymers. However, the films or coatings of these blended substrates have poor water resistance due to their hydrophilic nature. To adjust the hydrophilicity of the PVOH chains and the hydrophobicity of the AESO-emulsion, we conducted a series of experiments. In our initial study, 5 g of AESO and 2 wt% of a UV initiator were mixed via stirring for 2 min at  $70^\circ\text{C}$  (**Scheme A.S1**). Subsequently, 5 mL of a hot PVOH solution (10% w/v) in hot water was added in a dropwise manner to the AESO mixture. Conversely, there was no emulsion present at any stage of the addition. However, when a hot 0.5 mL solution of PVOH was added in a dropwise manner to the AESO mixture followed by another 4.5 mL of hot water, we obtained a desirable emulsion. Thus, the addition of PVOH solution followed by the addition of hot water in a dropwise manner results in emulsion formation.

Considering the optimization details outlined in the SI (**Tables A.S3 and A.S4**), we decided to focus on three AESO-emulsions (A, B, and C), each formulated by using a different amount of 10% PVOH solution. For example, AESO-emulsions A, B, and C were created by incorporating 0.5, 1.0, and 2.0 mL of 10% PVOH solution, respectively into the vial that contains 5.0 g of AESO. The formulation, the amount of PVOH utilized and the quantity of hot water employed for each emulsion are depicted in **Figure 4.3**. These AESO-emulsions were then coated onto starch-coated kraft paper (13 x 13 cm<sup>2</sup>) using 0.5 mL of each and were subsequently UV-cured. The starch coating serves two functions: first, it prevents the coating emulsion (AESO/water) from deep permeation and leakage through the paper by filling the pores in uncoated kraft paper; second, starch also improves the oil resistance of the paper. The analysis of an emulsion (WSO-P2.0) was conducted by using a Nikon Eclipse Ni upright microscope. The result of the analysis indicates that the average size of the emulsion droplets was found to be approximately  $14.84 \pm 8.14 \mu\text{m}$ . (**Figure 4.4A and 4.4B**). The emulsion stability test was also conducted for all prepared samples. For example, the photographs of WSO- P0.5, WSO-P1.0 and WSO-P2.0 emulsions after 5 min were taken and it was found that all the prepared emulsions were very stable (**Figure A.S10**) However, after 24 hrs the phase separation was found for WSO-P0.5, WSO-P1.0. This phase separation was very low for the WSO-P2.0 sample. These findings indicate that WSO-P2.0 was a more stable emulsion than WSO-P0.5, WSO-P1.0. **Figure 4.4C** describes the use of FTIR spectroscopy to monitor the degree of UV curing of AESO-emulsion and acrylated epoxidized soybean oil (AESO) via radical crosslinked polymerization. The FTIR spectrum of AESO primarily displayed a characteristic peak at 1630- 1655 cm<sup>-1</sup> corresponding to the stretching vibrations of the C=C (acrylated carbon-carbon double bond). As these acrylated C=C double bonds were subsequently consumed upon exposure to UV radiation, they had thus

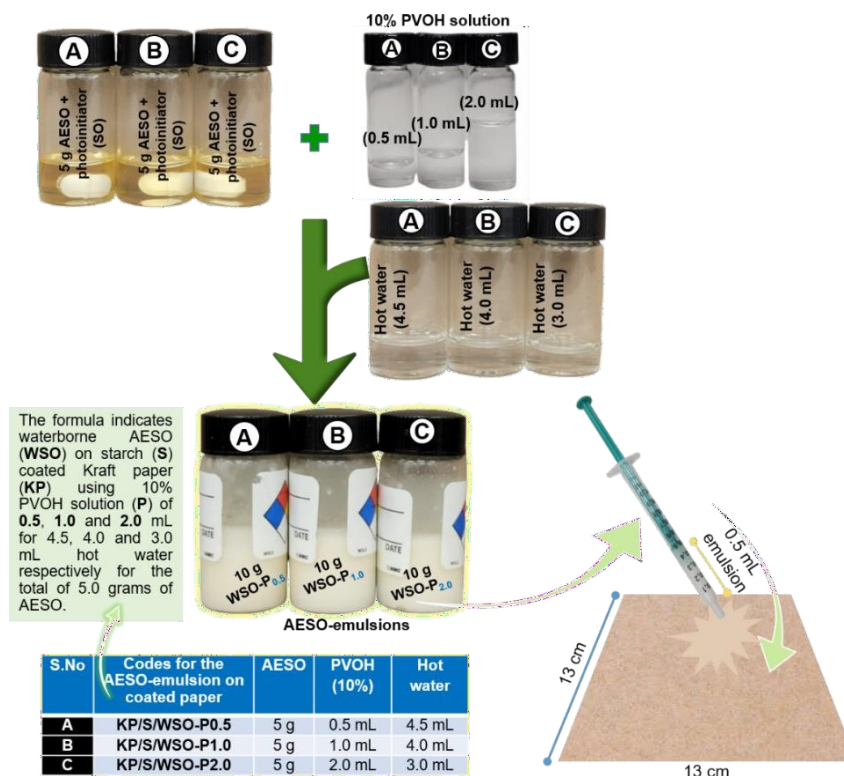


**Figure 4.3** Procedure employed to coat paper substrates. Vials containing a mixture of AESO and the photoinitiator, each of these three vials having the same composition. Next, three vials of 10 wt% PVOH solutions (0.5 mL, 1.0 mL, and 2.0) were added dropwise to the AESO, followed by a 2<sup>nd</sup> batch of water addition. The obtained white emulsion was cast on starched-coated paper (13 x 13 cm<sup>2</sup>) using the amounts of 0.5 mL with the aim of finding the best coating load for water and oil resistance properties.

completely disappeared from the FTIR spectrum of the blend obtained after the crosslinking reaction (green spectrum). Similarly, the peak appearing in the non-cured AESO sample at  $\sim 800$  cm<sup>-1</sup> can be ascribed to the vinyl fragment of the acrylic acid. This peak also disappeared upon exposure to UV radiation, indicating complete consumption of the vinyl moiety of the acrylic acid. This information provides insight into the degree of polymerization and crosslinking that

occurred during the UV curing process, which is important for optimizing the properties of the resulting material.

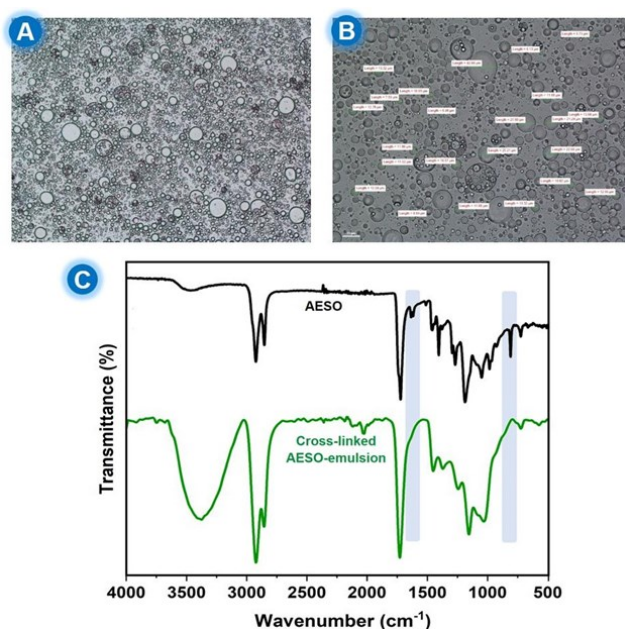


**Figure 4.4.** Optical images of the emulsion and FTIR analysis of both AESO and cured AESO-emulsion. **A)** Brightfield-transmitted light images of the WSO-P2 emulsion (200 μm scale); **B)** Zoom image of the figure A (100 μm scale). These images were recorded via a Nikon Eclipse Ni upright microscope using a 10 x Plan Apo objective (NA 0.3) and a Nikon DS-Fi2 color camera; and **C)** FTIR analysis of the AESO (black spectrum) and cross-linked AESO-emulsion (WSO-P2.0) (green spectrum).

The Cobb test is a TAPPI standard approach for determining water resistance. Cobb-600 (the amount of water in grams absorbed per square meter coated surface during a period of 600 s) and Cobb-1800 (the amount of water in grams absorbed per square meter coated surface during a period of 1800 seconds) were measured using a commercial Cobb Tester. **Figure 4.5 A** shows the Cobb-1800 (red) and Cobb-600 (blue) values for the kraft paper (KP) and starch-coated kraft paper (KP/S) that were used as controls, as well as the three final solutions of A, B, and C that had been



cast onto KP/S. These samples were named **KP/S/WSO-P0.5**, **KP/S/WSO-P1.0**, and **KP/S/WSO-P2.0** for the three final solutions of A, B, and C, respectively. Sample codes, thickness, basis weight and loading estimation for the controls (uncoated Kraft paper and starch Kraft coated paper), and AESO-emulsion coated samples are shown in **Table A.S5**. The graph indicates that KP and KP/S (used as controls) have Cobb-600 values of  $\sim 60$  and  $63.6 \text{ g/m}^2$ , respectively. The latter has a higher Cobb-600 value due to the hydrophilic nature of starch. This value was decreased by almost 75% (i.e., from  $63.6$  to  $16.2 \text{ g/m}^2$ ) for the KP/S/WSO-P0.5 sample. An even lower Cobb-600 value of  $\sim 9.4 \text{ g/m}^2$  was recorded when the water resistance of the KP/S/WSO-P2.0 was tested. A similar trend was observed when the Cobb-1800 protocol was employed to measure the water resistances of the control samples (KP and KP/S) as well as the coated samples. The red plot shown in **Figure 4.5 A** indicates that both KP and KP/S have Cobb-1800 values of  $\sim 80$  and  $75.3 \text{ g/m}^2$ , respectively. However, AESO-emulsion coated samples showed a drastic decrease in Cobb-1800 values, and the lowest value ( $\sim 13.5 \text{ g/m}^2$ ) was recorded for the KP/S/WSO-P2.0 sample. To investigate the coating load effect of the waterborne AESO-emulsion, the final solutions were also casted on KP/S using 0.2, 0.3 and 0.4 mL followed by determination of Cobb-600 and Cobb-1800 analysis (**Table A.S6**).

To compare the AESO-emulsion coated paper for the Cobb-1800 values with our recently developed waterborne polybutyl succinate (PBS)-coated paper (blends of PBS and PVOH).<sup>83</sup> The results indicated that the AESO-emulsion coated paper developed in this study, had a Cobb-1800 value of  $13.5 \text{ g/m}^2$ , whereas the PBS-coated paper was published with a Cobb-1800 value of  $15.5 \text{ g/m}^2$ . The water resistance properties of certain commercially available coated paper were also compared with those of AESO-emulsion coated paper. The Cobb-1800 values and loading per square meter for each are provided in **Table A.S7**.

The Cobb-600 and Cobb-1800 values described above indicate that our coated samples have good water repellency. This can be especially useful in applications where the paper will be exposed to water, such as the case with disposable cups. However, oil/grease resistance is another important parameter that must be considered in the packaging industry. The standard kit rating test is a useful tool for evaluating the oil/grease resistance of packaging materials and can provide valuable insights into their performance. The kit ratings recorded for our coated samples were 7/12, whereas a value of 0/12 was observed for the kraft paper (control). Kit values have a maximum range of 0-12, where a rating of 0/12 corresponds to the weakest oil/grease resistance, and a higher rating suggests that the coating has improved the oil/grease resistance of the paper. Consequently, it was evident that the paper samples bearing our coatings exhibited enhanced oil/resistance relative to their uncoated counterparts. These findings suggest that the cross-linked AESO-emulsion covered almost all paper's surface including the cracks and pores (see scanning electron microscopy (SEM) analysis of the KP, KP/S and KP/S/WSO-P2.0 coated samples in **Figure A.S9**).

Mechanical properties are an important consideration when selecting papers for packaging applications, as they help to ensure that the packaging can withstand the stresses and strains of handling and transportation while also protecting the product from damage. There are several mechanical properties that are important to consider when evaluating the suitability of a paper for packaging, such as the tensile strength, tear resistance, bending stiffness, elongation at break, and ring crush test. Generally, the mechanical properties are evaluated in machine direction (cellulose fiber aligned in the direction of applied tensile force in elongation mode) and cross-direction (cellulose fiber aligned perpendicular to the applied tensile force). The tensile strength is the maximum stress that the paper can withstand before breaking or tearing. The average tensile

strength (**Figure 4.5B**) of uncoated paper was  $55.86 \pm 1.56$  MPa (for the machine direction (MD),

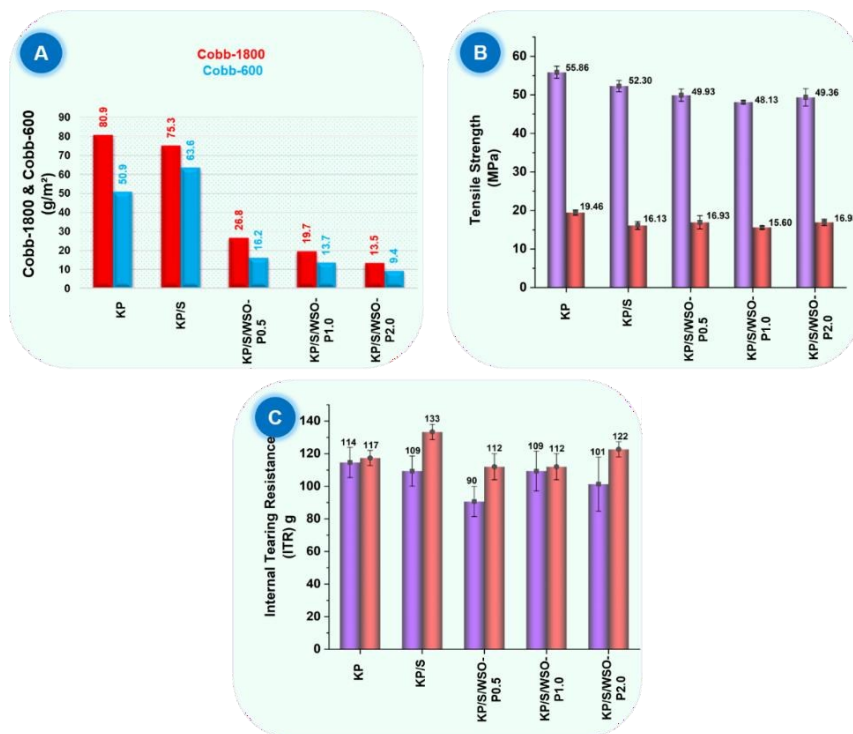


**Figure 4.5** Water resistance and mechanical properties of uncoated and coated paper samples.

A). Water resistance properties (Cobb-1800 (red) and Cobb-600 (blue) values) for the kraft paper (KP), starch- coated kraft paper (KP/S), and three AESO-emulsion coated samples (KP/S/WSO-P0.5, KP/S/WSO-P1.0, and KP/S/WSO-P2.0) B). Tensile properties for the KP, KP/S, KP/S/WSO-P0.5, KP/S/WSO-P1.0, and KP/S/WSO-P2.0 samples in the machine direction (MD) (violet color) and the cross direction (CD) (red). C) Tearing resistance properties for the KP, KP/S, KP/S/WSO-P0.5, KP/S/WSO-P1.0, and KP/S/WSO-P2.0 samples in the machine direction (MD) (violet color) and the cross direction (CD) (red).

and this value decreased to  $49.36 \pm 2.27$  MPa for the sample KP/S/WSO-P2.0. Therefore, the coated sample retained ~90% of the tensile strength with respect to the uncoated sample in the MD. The internal tearing test (ITR) is a method used to measure the resistance of the paper to

tearing from within the paper structure. This test is important because the internal strength of the paper can impact its ability to withstand handling during manufacturing, transportation, and storage. Therefore, ITR measurements were performed to determine the force required to tear a paper strip in a perpendicular direction, and the results are presented in **Figure 4.5C**. The ITR values were measured in both the machine direction (MD) and the cross direction (CD). The value recorded for the coated sample KP/S/WSO-P2.0 was found to be  $101.33 \pm 16.65$  g as compared to  $114.66 \pm 9.23$  g for KP (MD). This finding also suggests that ~90% of the tearing resistance was retained even after coating. Other mechanical properties, such as ring crush test (RCT) performance, material's stiffness by Young's modulus, percent elongation at break, and bending stiffness (BS), were measured for the KP, KP/S, KP/S/WSO-P0.5, KP/S/WSO-P1.0, and KP/S/WSO-P2.0 samples both in the MD and the CD (**Figure A.S2-A.S5**). It can be stated that the AESO-emulsion coated samples retained ~85% of the mechanical properties exhibited by their uncoated counterparts as observed via BS, RCT, and ITR measurements. A slight decrease in the mechanical properties of the coated paper can be attributed to reduced inter fiber interactions in paper fiber by the AESO- emulsion coating. Other factors such as increasing the thickness of coated materials also can lead to lower mechanical properties as the coated material itself has lower tensile modulus. Thus, in turn, contributes to an overall reduction in mechanical properties of the coated papers compared to the uncoated KP.<sup>13,83</sup> By evaluating and optimizing these mechanical properties, manufacturers can produce coated papers that meet the specific performance requirements of different packaging applications. This can help ensure that the packaged product is protected from damage while also helping to reduce waste and improve overall sustainability in the packaging sector. In addition to mechanical testing, thermal stability and decomposition behavior of our coated materials was also determined via thermogravimetric

analysis (TGA) and Differential scanning calorimetry (DSC) study (**Figure A.S6** and **A.S7**).

Biodegradability is a critically important issue that must be considered to avoid any microplastic issues.

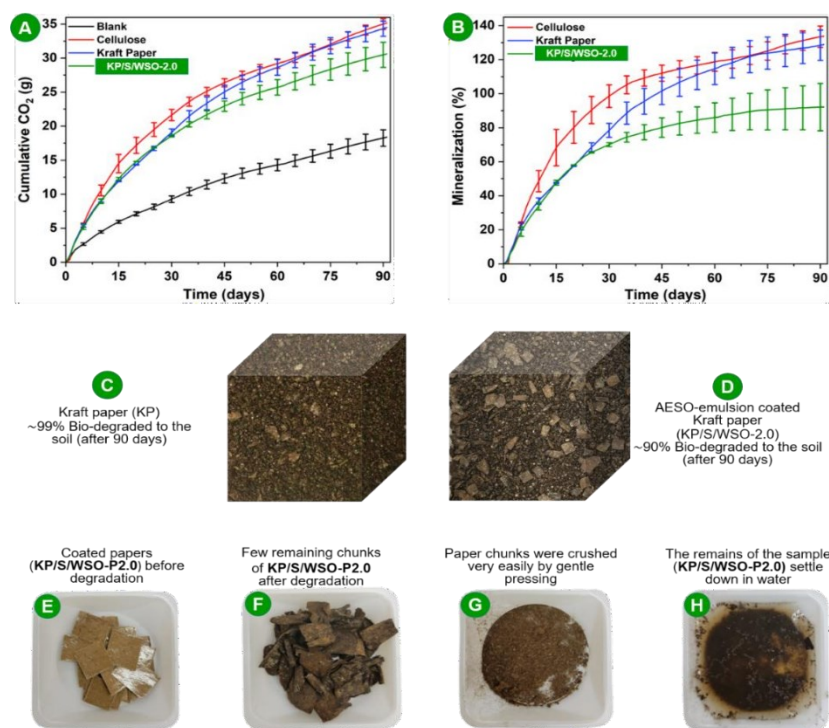


**Figure 4.6** Biodegradability data for uncoated and coated paper samples. Cumulative CO<sub>2</sub> evolution (**A**) and mineralization (**B**) of blank, cellulose, unmodified kraft paper (KP), and coated paper substrate (KP/S/WSO-P2.0). These tests were performed under simulated composting conditions. Photographs of the biodegraded control sample (**C**), and KP/S/WSO-P2.0 (**D**). Photographs of the coated samples at different stages: **E**) Before biodegradation; **F**) after 90 days of biodegradation; **G**) photograph showing that the biodegraded sample is converted to powder by gentle pressing; and **H**) photograph demonstrating that the powdered which had been dipped into water did not show evidence of the coating material on its surfaces.

Conventional coating materials used for paper modification, such as low-density polyethylene (LDPE), styrene-rubber latex, and polyvinylidene chloride (PVDC), are non-biodegradable, which can lead to persistent microplastic environmental issues. Our coated sample (*KP/S/WSO-P2.0*) was subjected to biodegradation studies.<sup>89,90</sup> For comparison, we used two control samples (kraft paper and cellulose). The data for CO<sub>2</sub> evolution and % mineralization has been collected for a total of 90 days. The amount of CO<sub>2</sub> evolved in the case of cellulose was  $\sim 35.01 \pm 0.78$  g, while in the case of KP, it was  $\sim 34.33 \pm 0.11$  g (**Figure 4.6A**). Interestingly, the *KP/S/WSO-P2.0* sample exhibited a high amount of CO<sub>2</sub> evolution ( $\sim 30.48 \pm 1.84$  g), which indicates  $\sim 88\%$  conversion with reference to the control sample. These results are further corroborated by the % mineralization values (**Figure 4.6B**), which were  $133.44 \pm 6.25\%$  and  $128.45 \pm 8.89\%$  for cellulose and KP, respectively, whereas that for the coated sample (*KP/S/WSO-P2.0*) was  $92.09 \pm 13.88\%$ . The formula for the calculation of % mineralization is provided in the Materials and Methods section. According to the ASTM D6400-22 and D6868 protocols, if the % mineralization of a given material exceeds 90%, then it is considered to have good biodegradability. **Figures 4.6C and 4.6D** show comparative photographs of the control sample (KP) and an AESO-emulsion coated sample (*KP/S/WSO-2.0*) after 90 days of biodegradation. Meanwhile, **Figure 4.6E** is a photograph of *KP/S/WSO-2.0* before biodegradation, and **Figures 4.6F-H** are photographs of biodegraded *KP/S/WSO-2.0* at different stages. Coated paper products that are not easily recyclable can contribute to environmental pollution and waste. Therefore, it is important to develop coating materials that are easily removable during the recycling process. Hot basic water washing is an effective method for repulping paper because it can break down a wide range of paper products, including coated and printed papers. Keeping this in mind, we prepared basic solutions of 2% Na<sub>2</sub>CO<sub>3</sub> and 2% NaHCO<sub>3</sub> (100 mL). These

solutions were added into two Erlenmeyer flasks that each contained 5 g of chopped coated paper (KP/S/WSO-P2.0), as shown in **Figure 4.7A**.

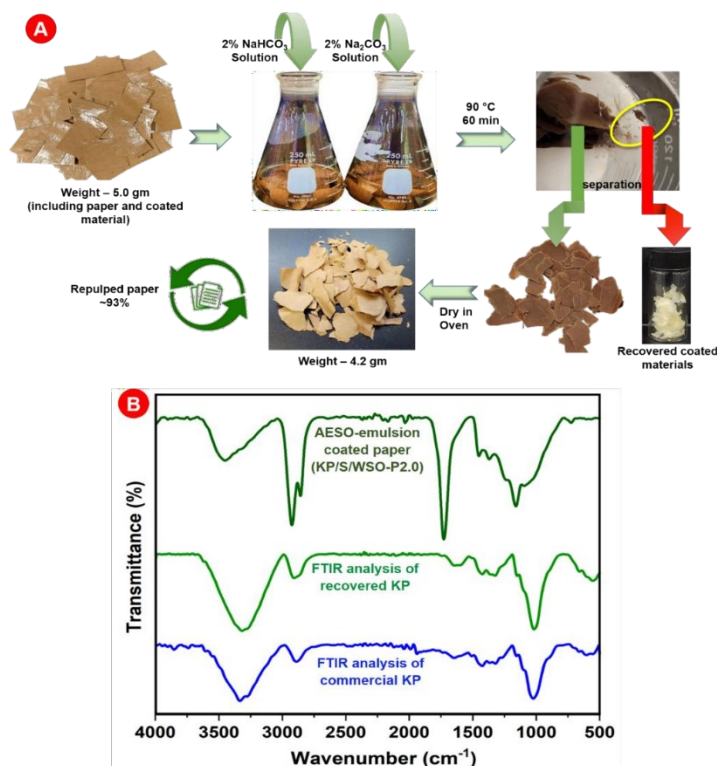


**Figure 4.7** Chemo-degradation and repulpability; **A**) repulpability of the coated sample (KP/S/WSO- P2.0) in basic solution (2% Na<sub>2</sub>CO<sub>3</sub> and NaHCO<sub>3</sub>). The Erlenmeyer flasks were heated at ~90 °C for 60 min and subsequently sonicated, thus ensuring complete removal of the coated materials. The pulp recovery rate was almost 93% once it had been dried in an oven; **B**) FTIR analysis indicates that the peak corresponding to AESO was absent in case of the recovered pulp (green spectrum) and found similar spectrum as it is for the commercial Kraft paper (blue).

Both of these flasks were next heated at ~90 °C for 60 min. It was observed that the AESO-emulsion (coated materials) peeled away from the paper and came out to the top of both conical flasks. The exfoliation process was further accelerated by sonication, which ensures complete

removal of the coated materials from the surface of the paper.



**Figure 4.8** Demonstration of the coating's compatibility with printed substrates. **A)** To determine the transparency level of our coated paper, a sketch was drawn on KP/S using a black marker. **B)** The printing remained intact during the coating process, as can be seen from the photograph of the KP/S/WSO-P2.0 sample.

The exfoliated material was then collected and dried in an oven for further evaluation. FTIR analysis was performed for these samples (**Figure 4.7B**) and it was found that the peak corresponding to AESO was absent from the spectrum of recovered pulp, which was found to be similar spectrum to that of commercial kraft paper. The weight of the recovered pulp was also measured, and it was found that almost 93% of the pulp was recovered.

Printing is a critical aspect of any package as it provides valuable information to the consumer about the product and brand. To demonstrate that coating can be applied onto pre-printed paper, we evaluated the impact of applying our coating onto the printed paper and subsequent curing treatment. For example, a sketch was drawn, and writing was made on KP/S using a black



marker (**Figure 4.8A**), and then this paper substrate was coated with the AESO-emulsion (KP/S/WSO-P2.0). The printing remained intact during the coating process, which suggests that these coatings would be suitable for application onto printed paper substrates (**Figure 4.8B**).

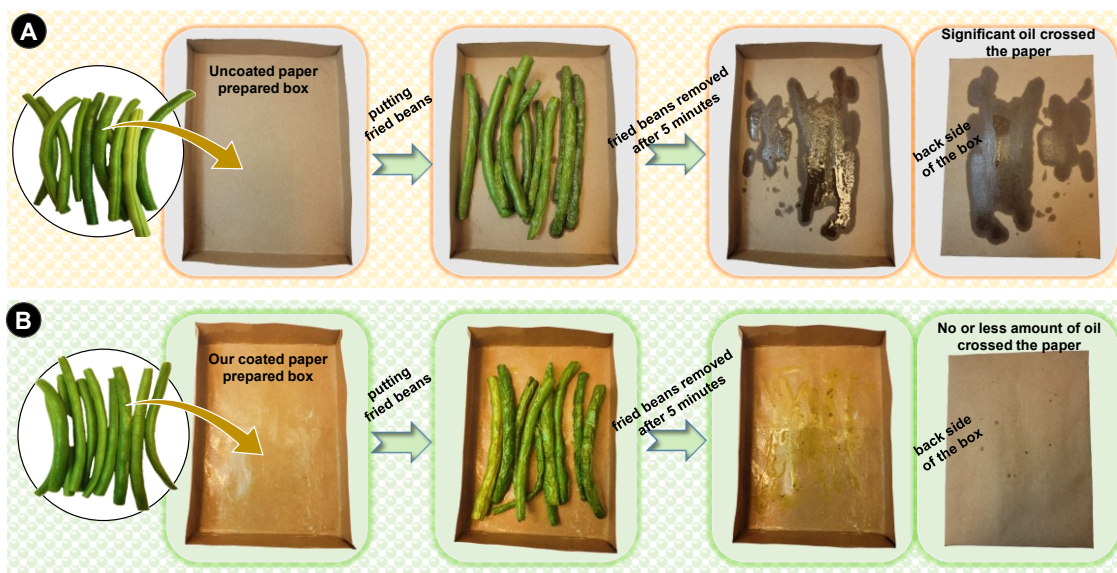


**Figure 4.9** Use of uncoated and coated paper plates to handle oily food. **A)** The impact of placing hot, oily green beans on uncoated paper. The paper became saturated with oil and penetrated through the paper, and oil stains were visible on both the front and back of the paper plate. **B)** The impact of placing hot oily green beans on coated paper prevented the oil from reaching the other side.

Since our AESO-emulsion coated paper showed excellent water and oil/grease-resistant properties, we also demonstrated the impact of placing hot, oily green beans on uncoated and coated paper. As uncoated paper is generally not resistant to oil or moisture, and thus, by placing oily cooked beans, the paper became saturated with oil, which penetrated through the paper. The oil stains were visible on both the front and back of the paper plate (**Figure 4.9A**). Coated paper, on the other hand, was designed to have a degree of resistance to oil and moisture. Consequently,

the coating acted as a shield and prevented the oil from reaching the other side of the paper when oily hot beans were placed on the AESO-emulsion coated paper plate (**Figure 4.9B**). This clearly shows the potential of these coatings for food packaging applications with an appropriate level of oil and moisture resistance.

#### **4.4 Conclusion**

In summary, we have demonstrated the formation of AESO-emulsion and the use of these emulsions for manufacturing water- and oil-resistant paper. After it had undergone UV curing treatment, the coated paper offered excellent oil and water repellency. The coated paper also retained 90% of its mechanical properties as compared to uncoated kraft paper when it was tested for its tensile strength, tearing resistance tests, ring crush tests, material's stiffness by Young's modulus, % elongation at break, and bending stiffness. Interestingly, the coated paper was found to be over 90% biodegradable (with regard to mineralization) in 90 days. The coating process is compatible with pre-printed paper. In addition, the coating was also found to provide good oil resistance to hot oil.

**CHAPTER 5: WATER, OIL AND MICROBE RESISTANT PAPER COATINGS VIA  
MgNP BLEND ACRYLATED EPOXIDIZED SOYBEAN OIL (AESO) EMULSION  
FOR PACKAGING APPLICATIONS**

A version of this chapter is under submission in *Industrial Chemistry & Engineering*:

Kumar, V.; Alkarri, S.; Khan, A.; Hamdani, S.S.; Sharma, R.; Rabnawaz, M., Water, Oil and Microbe Resistant Paper Coatings via MgNP Blend Acrylated Epoxidized Soybean Oil Emulsion For Packaging Applications.

## 5.1 Abstract

Paper having water and oil resistance, as well as anti-microbial properties, can be used for numerous food and medical device packaging applications. Herein, we reported the use of magnesium hydroxide nanoparticles with acrylated epoxidized soybean oil (AESO) and polyvinyl alcohol (PVOH) to produce stable emulsion. The obtained emulsion was then used for paper coating that offers good water and oil resistance. Moisture barrier performance of the coated paper was also investigated. Additionally, the coated paper was tested for anti-microbial properties and demonstrated a  $\sim 4$  log reduction in the population of *Escherichia coli* (E. Coli) that corresponding to kill 99.99% of bacteria. Owing to its water and oil resistance and antimicrobial properties, such coated paper can find waste applications in the food and medical packaging applications.

## 5.2 Introduction

Plastic-based packaging is widely used thanks to its excellent performance-cost balance.<sup>91,92</sup> However, commonly used plastics lack biodegradability and have low recyclability rates, thus, they have led to environmental concerns such as landfilling, the generation of microplastics, and so on.<sup>72,74</sup> This situation has created space for paper to emerge as a promising alternative owing to its high recycling rates and biodegradability in the natural environment.<sup>1,67,69</sup> However, paper inherently has poor water/oil resistance and thus has limited applications in packaging.<sup>23,62,63,93</sup> To be effective for packaging applications, a paper must deliver water/oil resistance (verified by Cobb and KIT tests), offer good gas barrier and moisture properties such as water vapor transmission rates (WVTR) and oxygen transmission rate (OTR).<sup>83</sup> In some cases, anti-microbial properties are also highly desirable, especially for food packaging and medical applications.<sup>94,95</sup> On the other hand, regular paper is not suitable for packaging applications because of its porous and polar nature. These attributes are responsible for the lack of water and oil resistance,

including its inability against gas or moisture barrier.<sup>50,53</sup> Moreover, the regular paper also lacks the necessary antimicrobial properties that are desirable for avoiding cross-contamination during transportation, storage, and delivery.<sup>96</sup>

During the COVID-19 breakout, sanitation was recognized as an essential tool to help combat the spread of the pandemic, and this led to a strong surge in demand for anti-microbial products in the market.<sup>97,98</sup> Paper packaging exposed to moisture and humidity during transportation can provide a suitable environment to accelerate microbial growth, thus potentially leading to the spread of infectious diseases. Microbes can survive for any length of time, ranging from day to year. For instance, it has been reported that *Escherichia coli* (E.coli) can survive from 1.5 h to 16 months on inanimate surfaces.<sup>99,100</sup> Additionally, in hospitals and schools where safety is of utmost importance, the persistence of microbes on paper is a major concern.

Antimicrobial agents can be blended with coating ingredients to activate antimicrobial properties that could inhibit the microbe's growth, benefit food and medical packaging, and reduce the possibilities of cross-contamination during transportation in paper-based packaging. Generally, antimicrobial agents can be categorized into three categories depending on their composition and origin: natural, inorganic, and organic antibacterial. Inorganic antibacterial agents such as zinc oxide (ZnO), titanium oxide (TiO<sub>2</sub>), magnesium oxide (MgO), magnesium hydroxide (Mg(OH)<sub>2</sub>), silver nanoparticles and others which display a broad spectrum of antimicrobial activities, are heat resistant, low cost, and environmentally friendly, making them more durable and safer as compared to other antimicrobial agents.<sup>101–103</sup> Additionally, nanomaterials provide room for tunability in their shape, size, and charge and thus open opportunities for a wide array of antimicrobial effects based on their morphological variations and different interaction mechanisms resulting in the death of microbes.<sup>104–107</sup>

The biosafety of  $\text{Mg}(\text{OH})_2$  has been investigated thoroughly without any oral toxicity in animals. This makes an excellent case to integrate  $\text{Mg}(\text{OH})_2$  into paper packaging for antimicrobial properties.<sup>108,109</sup> Applying antimicrobial coatings thus can help the paper and print industry to restore public confidence and address all those consumer concerns about cleanliness. Moreover, food packaging with built-in antimicrobial features will help to preserve the freshness and longevity of food.<sup>110</sup> Integrating all four salient features in paper (water/oil resistance, gas and vapor barrier performance, and anti-microbial resistance) will provide a strong candidate for various packaging applications from food packaging to medical industries.

Here in this work, we explored the use of magnesium hydroxide nanoparticles combined with acrylated epoxidized soybean oil (AESO) and polyvinyl alcohol (PVOH) to create a stable emulsion. This emulsion was then applied on Kraft paper, resulting in enhancement of their water and oil resistance. The coated paper was also investigated for moisture barrier performance. Additionally, the antimicrobial properties of the coated paper were also tested, showing a  $\sim 4$  log reduction in the population of *Escherichia coli* (*E. coli*). Due to its water and oil resistance and antimicrobial properties, our coated paper has substantial potential for the use in food and medical packaging applications.

## **5.3 Materials & Methods**

### **5.3.1 Materials**

Polyvinyl alcohol (PVOH, Mw- 30000-70000 g/mol, 80-90% hydrolyzed) and acrylated epoxidized soybean oil (AESO) were purchased from Millipore Sigma. The Photoinitiator (2-Hydroxy-2-methylpropiophenone) was obtained from Genocure. Paper (35-liner Kraft) purchased from Uline. Aqua Resources (Florida, USA) gifted  $\text{Mg}(\text{OH})_2$  (Purity: 99.99 %) in dry form and slurry ( $\text{Mg}(\text{OH})_2$  form dispersed in water).

### 5.3.2 Methods

#### 5.3.2.1 Preparation of $\text{Mg}(\text{OH})_2$ suspensions

The coating suspension of  $\text{Mg}(\text{OH})_2$  nanoparticles was obtained commercially in slurry form (7 wt% of  $\text{Mg}(\text{OH})_2$ ) in deionized (DI) water. Using the slurry, a new suspension solution of  $\text{Mg}(\text{OH})_2$  (10 mg/mL) was prepared and used for spraying method. The suspension was vortexed for 30 s and sonicated for 10 min to make the suspension with uniform distribution on  $\text{Mg}(\text{OH})_2$ .

#### 5.3.2.2 Preparation of starch solution

Corn starch (10 g) was dispersed in DI water (90 mL) and heated at 90-100 °C for 35 min. The prepared solution was cast onto kraft paper (KP) using a coating machine (rod no. 8) and left to air, dry for 24 h. The kraft/starch-coated paper was labeled as KP/S.

#### 5.3.2.3 Preparation of waterborne soybean oil blended with magnesium hydroxide nanoparticle ( $\text{MgNP}$ ) for paper coating.

AESO, weighing 5 grams, was placed in a 20 mL vial and mixed with 100 mg (2 wt%) of the photoinitiator. The mixture was then heated at 80 °C for 10 min. In a 2nd vial, a polyvinyl alcohol (PVOH) solution (10 wt% in water) was prepared and used as an emulsifier. Also in a separate flask, 50 mg (1 wt%) and 100 mg (2 wt%) of  $\text{Mg}(\text{OH})_2$  were combined in 3 mL of hot deionized (DI) water ( $T = 80^\circ\text{C}$ ) and sonicated for 5 min to disperse the  $\text{Mg}(\text{OH})_2$  nanoparticles (Nano dimension confirmed using SEM & TEM analysis) in water.

Subsequently, 2 mL of the 10 wt% PVOH solution were added dropwise to the AESO solution, followed by the addition of 3 mL of the  $\text{Mg}(\text{OH})_2$  aqueous solution. The mixture was stirred for an additional 10 min before being cast onto KP/S. The resulting coated KP/S was cured under UV light for 5 cycles (each cycle having approximately 10 s of exposure). The blend of waterborne soybean oil (**WSO**) and  $\text{Mg}(\text{OH})_2$  ( $\text{MgNP}$ ) was labeled as **WSO@MgNP**, and the coated

paper was denoted as **KP/S/WSO@MgNP**.

#### **5.3.2.4 Preparation of waterborne soybean oil sprayed with magnesium hydroxide nanoparticle (MgNP) for paper coating.**

5 grams of AESO were placed into a 20 mL vial, and 100 mg (2 wt%) of the photoinitiator was added. The above mixture was then heated to 80 °C for 10 min. Next, a 10 wt% polyvinyl alcohol (PVOH) solution was prepared (as an emulsifier) and 2 mL of it was added to the AESO solution in a dropwise manner, followed by the addition of 3 mL of hot water. The mixture was stirred for an additional 10 minutes before being applied onto KP/S and followed by spraying the Mg(OH)<sub>2</sub>-suspension (prepared in section 2.2.1) from the top. Finally, the coated paper was cured under UV light for five cycles.

### **5.4 Characterization**

#### **5.4.1 Basis Weight and Thickness Measurement**

The basis weight of the kraft paper (KP), starch coated kraft paper (KP/S), and KP/S coated with WSO@MgNP (termed as KP/S/WSO@Mg@NP) paper were calculated using the ASTM D646 protocol. The paper was cut into a circular disc (diameter = ~13 cm; area = ~132 cm<sup>2</sup>). The load of the coated material was determined by calculating the difference between the coated sample and uncoated KP (control) in g/m<sup>2</sup> using Equations (i) and (ii):

$$\text{Coating Load} = \text{basis weight (coated paper} - \text{uncoated paper)} \quad (\text{i})$$

$$\text{Where basis weight} = \text{weight (g)/area (m}^2\text{)} \quad (\text{ii})$$

The thickness of the samples was documented in a micrometer (μm) based on measurements with a testing instrument (Testing Machine Inc., New Castle, DE) at five different locations. The final values in Table 1 refer to the averages of these measurements.



#### **5.4.2 Fourier-transform Infrared (FTIR) Analysis**

The consumption of double bonds in cured AESO was determined via using FTIR spectroscopy (FT/IR-6600 type A FTIR spectrometer) in ATR (attenuated total reflectance) mode. A total of 32 scans were accompanied at a resolution of  $4\text{ cm}^{-1}$ , with the spectral range set between  $500\text{--}4000\text{ cm}^{-1}$ .

#### **5.4.3 Water-Resistance Test**

Following the guidelines defined in TAPPI 441 and ISO 535 protocols, the water-resistance test (Cobb-1800 test) was implemented to measure water absorption for the coated paper. A circular disc of diameter  $\sim 13\text{ cm}$  was prepared from the coated paper and next was exposed to  $\sim 100\text{ mL}$  of DI water for a total duration of 1800 seconds (30 min). The Cobb 1800 values recorded indicates that the total amount of water absorbed (in grams) by the paper sample per square meter over the course of 30 min.

#### **5.4.4 Oil/Grease Resistance Test**

Oil/grease repellency was measured in accordance with the TAPPI UM 557 standards. The solutions designed to measure resistance for the samples, assigned kit numbers, ranging from 1 (the least resistance) to 12 (the most resistance), were directly exposed to the sample surfaces for 15 seconds, followed by cleaning with tissue paper. The regions that were exposed to the kit solutions underwent investigation. The stains signified area or the presence of darkened spots on the sample had not passed to that specific kit solution are considered to fail. The solution with the highest number that did not stain the coated surface is recorded as the "kit rating" for that particular sample.

#### **5.4.5 Field Emission Scanning Electron Microscope (FESEM) analysis**

Analysis with a Field Emission Scanning Electron Microscope (FESEM) was performed by

utilizing a JEOL 6610LV scanning electron microscope equipped with a tungsten hairpin emitter (JEOL Ltd., Tokyo, Japan). For sample preparation, specimens were mounted on aluminum stubs using adhesive tabs (M.E. Taylor Engineering, Brookville, MD) and subsequently coated with iridium, having a total thickness of  $\sim 3 \mu\text{m}$ .

#### **5.4.6 Energy Dispersive X-ray Spectroscopy (EDX) analysis**

Elemental analysis was carried out via Energy Dispersive X-ray Spectroscopy (EDX) using an Oxford Instruments AZtec system (Oxford Instruments, High Wycombe, Bucks, England), incorporating  $150 \text{ mm}^2$  Silicon Drift Detector (JEOL 7500F SEM). A software version 3.1 was used with an ultra-thin window.

#### **5.4.7 Optical Microscopy**

Thickness measurements were performed using a VHX Optical Microscope (VHX-6000) from KEYENCE.

#### **5.4.8 Leica Stellaris Confocal Microscope**

Brightfield-transmitted light images were collected for emulsion on a Nikon Eclipse Ni upright microscope using a 10 x Plan Apo objective (NA 0.3) and a Nikon DS-Fi2 color camera. Emulsion droplet size was analyzed using the Nikon NIS-Elements AR Imaging Software (version 5.42.03).

#### **5.4.9 Water vapor transmission or permeability**

The permeability of water vapors was recorded by measuring the water vapor transmission rate (WVTR). A Permatran-W (Model 3/34, Mocon Inc. MN, United States) was used for this analysis. The samples were preconditioned for one hour at  $23^\circ\text{C}$  and relative humidity (RH) of 50% prior to actual testing. The paper specimen with specific dimensions of  $2 \times 2 \text{ cm}^2$  was trimmed and fixed on an aluminum mask with an opening of  $0.5 \text{ cm}^2$ . The flow rate of 100 standard cubic

centimeters per min (SCCM) was maintained and the WVTR results were expressed in g/(m<sup>2</sup>-day).

#### **5.4.10 Oxygen transmission rate**

A Mocon Ox-Tran Model 2/22 (Mocon, MN, United States) instrument was used to analyze the oxygen barrier properties for the samples. The samples were prepared and preconditioned similarly to those that were prepared for the WVTR measurements. The tests were performed using nitrogen as a carrier gas. The oxygen transmission rate (OTR) was recorded and expressed in cc/(m<sup>2</sup>-day). The test was recorded in duplicates using both cells (A & B).

#### **5.4.11 Anti-microbial testing method**

For anti-microbial studies, *E. coli* K-12 MG1655 (American Type Culture Collection, Manassas, VA) has been chosen. The stock culture that was maintained at -80 °C was smeared on TSA plates (BBL/Difco, Sparks, MD, USA). Next, these TSA plates were put for incubation at 37°C for 24 h. One colony from this was transferred to 5 mL of TSB (BBL/Difco, Sparks, MD, USA) and incubated for 18 h at 37 °C. Then 1 mL of this culture was taken and centrifuged at 13,000 x g for 5 min and the supernatant was then discarded. Next, cells were put in 1 mL of Phosphate Buffered Saline and followed by the vortex process. Subsequently, cell suspension was taken in a 15 mL tube and PBS (11.5 mL) was added to it. Aliquots of the prepared suspension were then exposed to disks. On each of the single disks, 1 mL of suspension was added that completely covered the disk into the culture broth and pod was then covered. A mini rotator (Benchmark Scientific, Roto Mini Plus R 2024, Sayreville, NJ, USA) was used to attach the pods and then rotated (20 rpm) to agitate the broth and that resulted in liquid renewal on the disks. At different time intervals (0, 4, and 24 h), a 100 µL of suspension was taken out for 1:10 dilutions, and incubated (at 37 °C) for 12 h. The colony forming unit (CFU) number was counted and has been used to estimate the viability of the cell. Neat KP disks were used as a "negative" control sample,

and blended disks (KP/S/WSO@MgNP) with antimicrobial agents (spraying and solution methods) were tested individually for antimicrobial properties.

## 5.5 Results & Discussion

As discussed in the experimental section that AESO was mixed with 2 wt% of the photoinitiator and stirred for 10 min at 80 °C. Next a hot solution of 10% PVOH solution (2 mL) was added followed by the addition of 1 wt% or 2 wt% of the dispersed  $\text{Mg}(\text{OH})_2$  nanoparticles in water (3 mL). This procedure is called the blending-method for developing coated paper and emulsion formed was named as WSO@MgNP (**Figure 5.1A**). On the other hand, when 1 wt% or 2 wt% of the dispersed solution of  $\text{Mg}(\text{OH})_2$  nanoparticles (3 mL) was sprayed on the AESO-PVOH coated paper, the procedure we called spray-method. The resulting coated papers (developed via blending method or spray-method) were then cured under UV light for 5 consecutive cycles. The coated paper was denoted as KP/S/WSO@MgNP.



**Figure 5.1** Preparation of the emulsion **A**) Three vials (from left) contain the composition of AESO and photoinitiator, 10% PVOH solution and magnesium hydroxide nanoparticles (MgNP).

The combination of all these three mixtures was stirred at 80 °C for 10 min to give the final emulsion (WSO@MgNP).

Once the WSO@MgNP was prepared then it was applied onto a kraft paper (KP) in desired loadings and subjected to UV curing (**Figure 5.2**). After curing, the coated paper was tested for its

basis weight and coating loads and the data is shown in **Table 5.1**. KP had a thickness of  $186 \pm 2$   $\mu\text{m}$  and a basis weight of 133.16 gsm.

**Table 5.1** Sample codes for all the paper samples along with the thickness ( $\mu\text{m}$ ), basis weight (gsm), and loading (g).

Sample Code	Thickness ( $\mu\text{m}$ )	Basis Weight (gsm)	Loading (g)
KP	$186 \pm 2$	$133.2 \pm 3.4$	NA
KP/S	$217 \pm 5$	$145.1 \pm 0.8$	$11.9 \pm 4.2$
KP/S/WSO@MgNP	$231 \pm 6$	$155.3 \pm 3.9$	$22.1 \pm 0.4$

After coating with starch, the obtained KP/S had a thickness of  $217 \pm 5$   $\mu\text{m}$ , basis weight of  $145.1 \pm 0.8$  gsm, and net coating load of  $11.9 \pm 4.2$  g. However, when WSO@MgNP was coated onto KP/S, the obtained KP/S/WSO@MgNP had a thickness of  $231 \pm 6$   $\mu\text{m}$ , a basis weight of  $155.3 \pm 3.9$  gsm, and a net coating load of  $22.1 \pm 0.4$  g (**Figure 5.3A**). The basis weight suggests that KP/S/WSO@MgNP has 8.2% of starch, and 7% of WSO@MgNP coating.

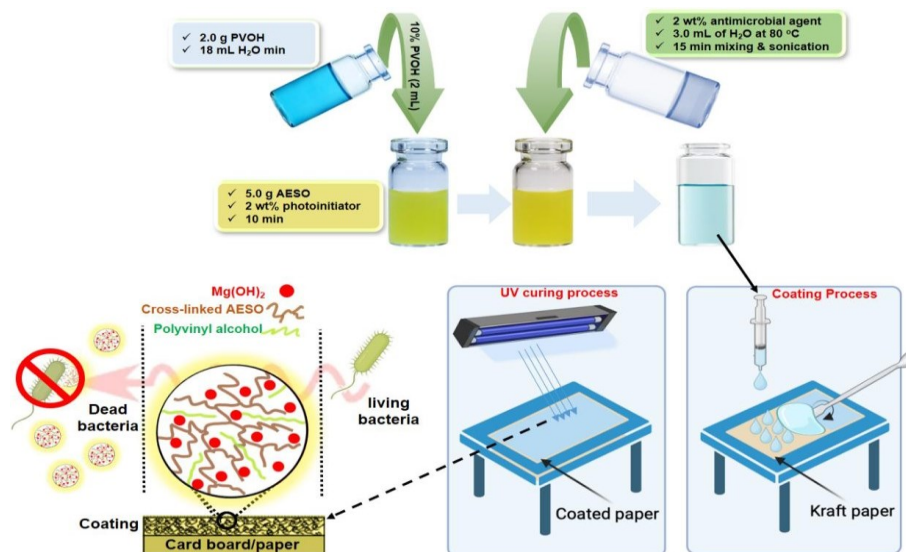


**Figure 5.2** Preparation of the WSO@MgNP followed by the coating process and then curing via UV light.

The curing process was examined by using FTIR spectroscopy. **Figure 5.3B** demonstrates the FTIR analysis of the kraft paper (black spectrum), starch coated kraft paper (red) and WSO@MgNP emulsion (blue spectrum). The last green spectrum of the FTIR involves the UV (ultraviolet) curing process of the emulsion (WSO@MgNP) on KP/S. In the initial stage, the uncured WSO@MgNP exhibited a distinctive peak at  $\sim 1630\text{-}1650\text{ cm}^{-1}$ , which represented the stretching vibrations of the C=C (acrylated carbon-carbon double bond). Similarly, peaks at  $\sim 800\text{ cm}^{-1}$  signify the C=C vibrational frequency of the AESO (blue FTIR spectrum). However, the acrylated C=C double bonds were completely consumed upon exposure to UV radiation, thus no longer observed in the FTIR spectrum of KP/S/WSO@MgNP after the crosslinking reaction, as indicated by the green spectrum in **Figure 5.3B**. Thus, the FTIR analysis provides effective evidence of crosslinking in the AESO-emulsion during UV curing. To measure how tightly a coated film is packed and how thick it is on the surface are very critical for further evaluation of coated papers. We used an optical microscope to investigate closely the structure of paper and coating on it. We checked smoothness of the coating and their continuity, and measured how thick each layer was across its width, as demonstrated in **Figure 5.4** for all three samples. The microscopic analysis showed that KP has thickness of  $\sim 166 \pm 4.2\text{ }\mu\text{m}$  across its width (**Figure 5.4A**). Next, the KP was coated with a thin layer of starch following the method explained in the material and method section. We found that the starch layer was about  $25 \pm 5.5\text{ }\mu\text{m}$  thick. **Figure 5.4B** illustrates the high variation in thickness as well as zig-zag pattern for starch layer on KP. However, this can be avoided by pressing the starch coated paper at elevated temperature ( $\sim 80\text{ }^{\circ}\text{C}$ ). Next WSO@MgNP coating was applied on KP/S thus the starch layer got pressed and became more compact during the process. Furthermore, UV treatment (elevated temperature inside UV chamber) leads to a more compact coating with an average thickness of

$35.75 \pm 6.5 \mu\text{m}$  (**Figure 5.4C**). If the average value of starch layer thickness is excluded from the mean value of total thickness of WSO@MgNP, the value comes around  $\sim 11 \mu\text{m}$ . If the average

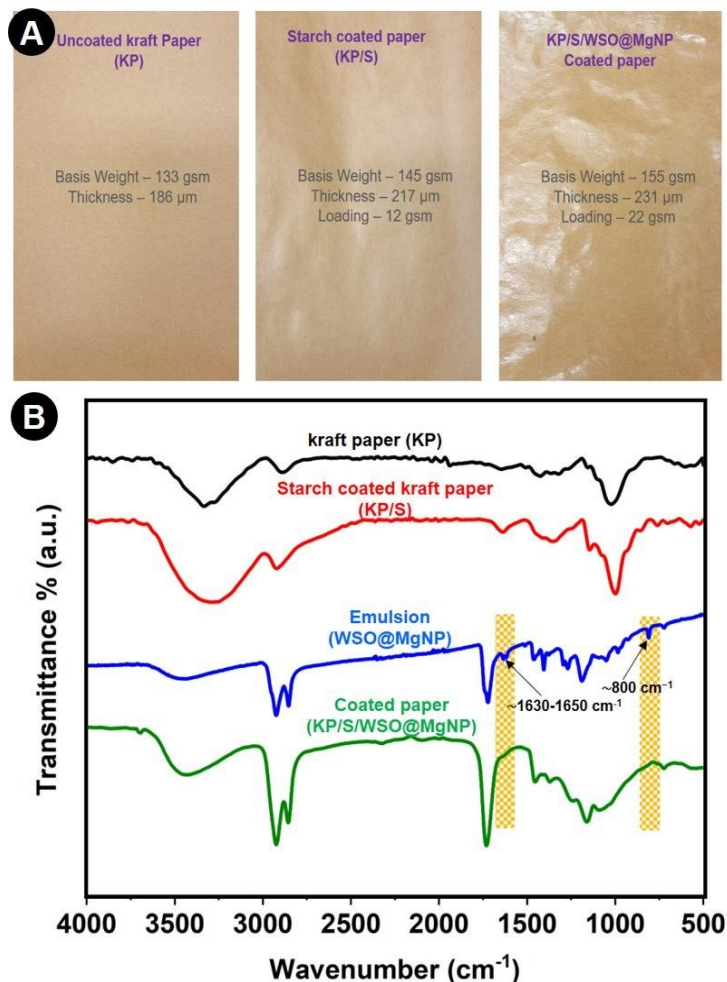


**Figure 5.3 A)** Photographs of kraft paper (KP), starch-coated kraft paper (KP/S), and coated paper (KP/S/WSO@MgNP) along with basis weight, thickness, and loading details and **B)** FTIR analysis of the kraft paper (black spectrum), kraft paper/starch (red), WSO@MgNP emulsion (blue) and coated paper or KP/S/WSO@MgNP (green).

value of starch layer is excluded from the mean value of total thickness of WSO@MgNP, the value comes around  $\sim 11 \mu\text{m}$ . This indicates that the layer in KP/S/WSO@MgNP is compact, uniform, and as thin as  $\sim 11 \mu\text{m}$  (**Figure 5.4C**). The KP/S/WSO@MgNP coated paper was also subjected

to energy dispersive X-ray (EDX) mapping analysis to determine the uniformity of the MgNPs throughout the surface. The carbon and oxygen mapping (**Figure 5.5A, 5.5B**) originates from the content of kraft paper, soybean oil, PVOH and UV-initiator. The EDX mapping (**Figure 5.5C**) and elemental analysis show a very uniform distribution of MgNPs throughout the paper surface and the calculated loading of MgNPs was  $\sim 0.3$  wt%.

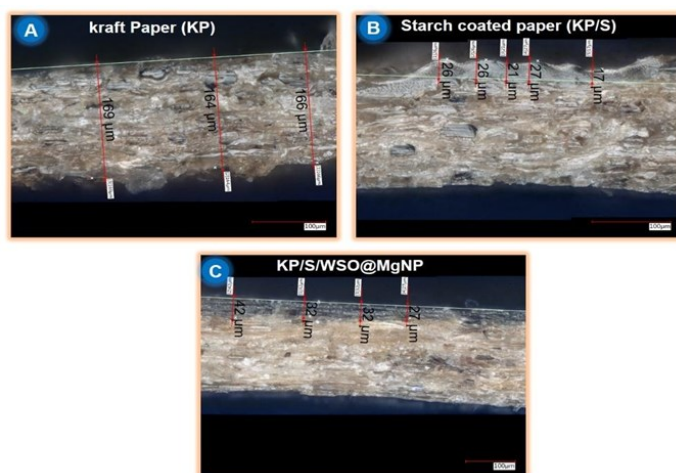


**Figure 5.4** Optical microscope images showing cross-sections of **A)** Kraft Paper, **B)** starch-coated paper, **C)** KP/S/WSO@MgNP.

The FESEM and TEM images of MgNP have also been recorded (**Figure 5.5D & 5.5E**) that suggest the magnesium hydroxide nanoparticles exhibit hexagon like structure and size distribution is in the range of 40-110 nm. The nanoparticle size is chosen as the nano particle will have a larger surface area compared to its bulk. The larger surface area will be instrumental in leveraging the antimicrobial activity of the coated paper. The Cobb 1800 value for KP/S/WSO@MgNP was  $\sim 18$  gsm, a decrease from the earlier report has been observed, possibly due to the interaction of magnesium ions with water molecules providing a path for diffusion (**Figure 5.6A**). The KIT value for the KP/S/WSO@MgNP coated paper is 7/12, suggesting that it has good oil resistance retention. The Cobb and kit test reveals that water/oil resistance has been



retained compared to the previous report even after doping with MgNP (**Figure 5.6B**).

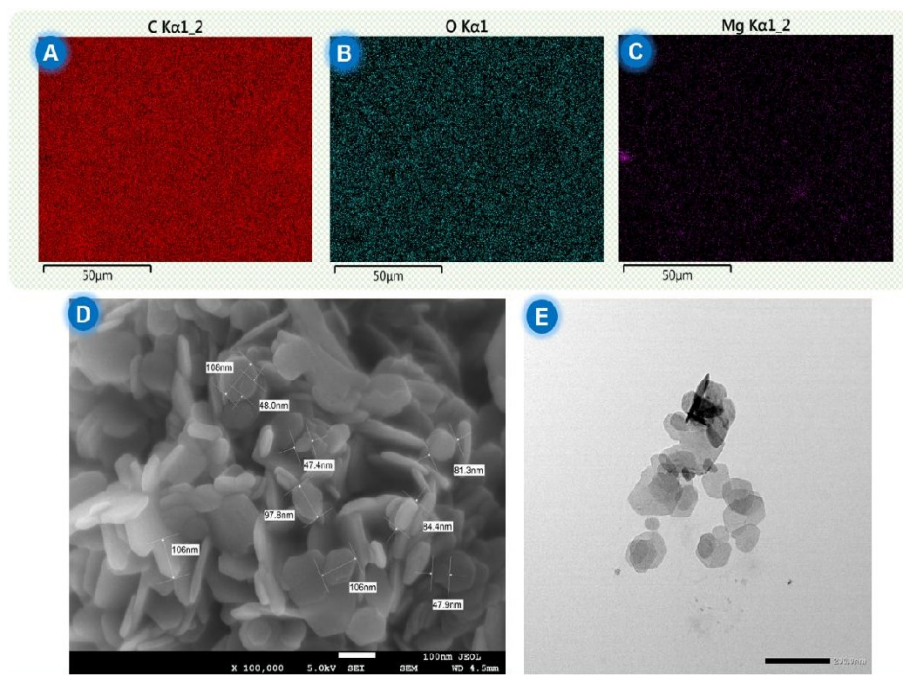


**Figure 5.5** EDX mapping of coated paper representing distribution of elements, (A) carbon, (B) oxygen, and (C) magnesium respectively. FESEM images of magnesium hydroxide ( $\text{Mg}(\text{OH})_2$ ) nanoparticles (MgNP) illustrating sheet like hexagon structure. The particle size of MgNP is in the range of ~40-110 nm. (D). TEM images of MgNP complementing sheet like structure captured by FESEM (E).

Next, the FESEM images of all three samples were captured to observe their surface morphologies. The fiber-like porous structure (**Figure 5.6C**) is visible for kraft paper but disappears after applying the starch coating (**Figure 5.6D**). Further, upon WSO@MgNP coating and curing, a very smooth thin film (**Figure 5.6E**) was achieved that is anticipated to shield the paper against water and oil upon exposure to these liquids. Barrier properties are important parameters to determine the efficacy of coated samples for food/medical packaging applications. The quality of food begins to deteriorate once it has been exposed to moisture and oxygen.

Plastic packaging generally provides a strong shield against moisture/oxygen, thereby preserving the quality and improving the shelf life of food packaging. However, environmental concerns give rise to alternative options of paper-coated material for food-safe packaging. With this in mind, the WVTR and OTR properties of the kraft paper coated with WSO@MgNP were tested to evaluate its barrier performance. The WVTR of kraft paper was  $\sim 775$  g/m<sup>2</sup>·day, and this value dropped to  $\sim 400$  g/m<sup>2</sup>·day after the application of the starch coating, and the subsequent application of the WSO@MgNP coating caused the WVTR to decrease significantly to  $\sim 76$  g/m<sup>2</sup>·day (**Figure 5.7A**). This dramatic reduction ( $>90\%$ ) in water transmission rate indicates a huge improvement in the water vapor barrier performance, owing to the hydrophobic nature of the WSO@MgNP coating.

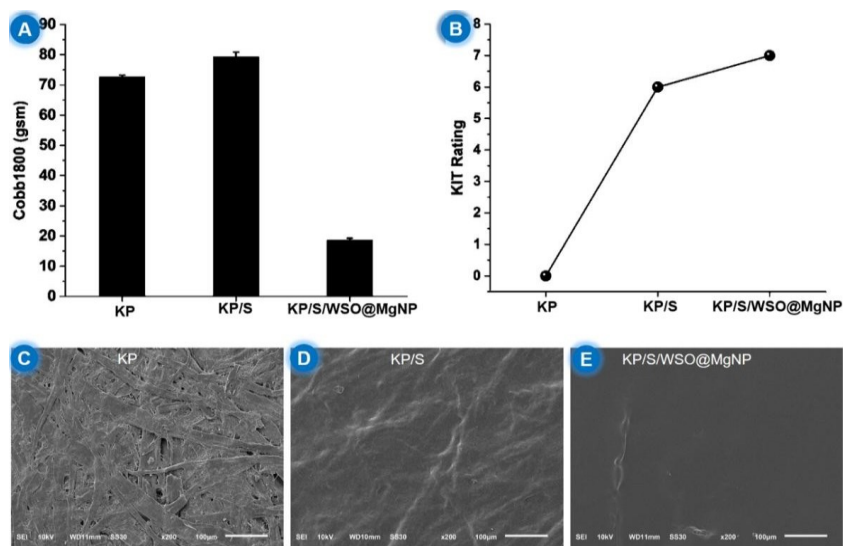


**Figure 5.6** Cobb1800 values for KP, KP/S, and KP/S/WSO@MgNP samples (**A**); Kit ratings of KP, KP/S, and KP/S/WSO@MgNP samples (**B**); FESEM images of (**C**) kraft paper, (**D**) kraft paper coated with starch (KP/S), (**E**) KP/S coated with WSO@MgNP.

The oxygen transmission rate (OTR) measurement is another essential factor to be considered and needs to be evaluated for coated paper. The OTR value of all the samples has been plotted in

**Figure 5.7B.** The OTR tests revealed that the coated paper (KP/S/WSO@MgNP) exhibited no oxygen barrier performance along with kraft paper and kraft-coated starch paper.

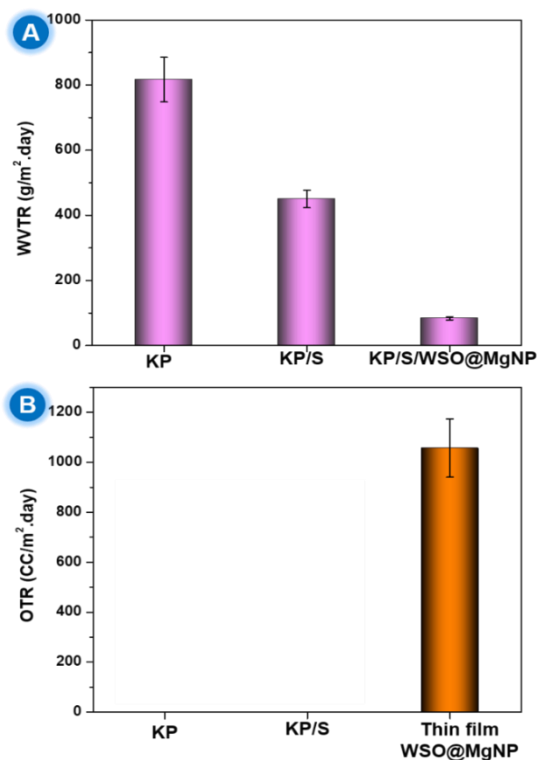


**Figure 5.7 A)** Water vapor transmission rate (WVTR) data for KP, KP/S, and KP/S/WSO@MgNP samples and **B)** Oxygen transmission rates (OTR) of KP, KP/S (shows negligible OTR), and a thin film of UV cured WSO@MgNP.

This poor oxygen barrier performance could be attributed to the lower thickness of the coating as well as the amorphous nature of the coated material, while the control sample itself is very porous and can hardly have any oxygen barrier performance. We then prepared a separate thin film of UV cured WSO@MgNP with a thickness of  $\sim 47 \mu\text{m}$  on a glass slide and measured the OTR value for the film. The film shows  $\sim 1100 \text{ cc/m}^2\cdot\text{day}$  (**Figure 5.7B**) OTR value. Further investigation is needed to improve the OTR performance on coated paper. The OTR experiment on thin film indicates that WSO@MgNP shows some promise for barrier properties for film

packaging applications. However, for paper coatings based on WSO@MgNP improvements in the fabrication process or from a material perspective will be needed in order to achieve suitable OTR performance.  $\text{Mg}(\text{OH})_2$  is an inexpensive and environmentally friendly material. The goal of Lui et al. to create anti-bacterial nanofiber membranes required a prior evaluation of the effects and safety of the  $\text{Mg}(\text{OH})_2$  nanoparticles they intended to use.  $\text{Mg}(\text{OH})_2$  nanoparticles in suspension (not as an anti-microbial membrane) were shown to be effective at eliminating an *E.coli* population (an approximately  $5 \times 10^6$  kill) in a dose dependent manner in 24 h.  $\text{Mg}(\text{OH})_2$  NPs caused oxidative damage to *E.coli* and affected bacteria at an enzymatic and genetic level. Biosafety experiments with  $\text{Mg}(\text{OH})_2$  NPs on rabbits and mice showed no skin irritation, no oral toxicity, no effect on blood physiological markers or animal weight. These workers concluded that  $\text{Mg}(\text{OH})_2$  NPs were safe for future work in creating membranes for tissue engineering. The anti-microbial data for “neat” paper disks (without anti-microbial NPs), anti-microbial NPs spray coated paper disks, coated paper disks with 1 wt%  $\text{Mg}(\text{OH})_2$  NPs (blending method), and coated paper disks with 2 wt%  $\text{Mg}(\text{OH})_2$  NPs (blending method) are presented in (**Figure 5.8**). The anti-microbial activity in “neat” paper disks was completely absent at 4 h and 24 h but rather exhibited a higher growth of bacteria ( $> 1$  log growth for 4 h and 24 h). Meanwhile, the spray-coated paper disks had a  $\leq 2$  log reduction of the *E. coli* K-12 MG1655 population at 4 h, which after 24 h offered a  $\sim 4$  log reduction. The coated paper disks with 1 wt%  $\text{Mg}(\text{OH})_2$  had a less than 1 log reduction at 4 h, and a  $\sim 2$  log reduction at 24 h for the *E. coli* K-12 MG1655 population. For the coated paper disks with 2 wt%  $\text{Mg}(\text{OH})_2$ , a  $\sim 2$  log reduction of the *E. coli* K-12 MG1655 population at 4 h, and a  $\sim 3$  log reduction at 24 h. This trend indicates that a higher  $\text{Mg}(\text{OH})_2$  concentration will result in a higher *E. coli* reduction. The anti-microbial data clearly demonstrate that WSO@MgNP shows a dramatic decrease in microbial growth and has potential in numerous

packaging applications where safety and hygiene are key considerations, especially in food/medical packaging.  $\text{Mg}(\text{OH})_2$  NPs are broad spectrum anti-microbial agents. Dong et al. demonstrated the anti- microbial activity of  $\text{Mg}(\text{OH})_2$  NPs against *E. coli* and the plant-associated bacterium *Burkholderia phytofirmans*. Additional work from our laboratories showed  $\text{Mg}(\text{OH})_2$  and Copper Oxide NPs to be similar in effectiveness against *E. coli*.  $\text{Mg}(\text{OH})_2$  can generate Reactive Oxygen Species (ROS) which overwhelm the bacterial oxidative defense mechanisms and thus mediate cell destruction in multiple ways. However, additional anti-bacterial mechanisms appear to exist. Dong et al. demonstrated previously using semi-permeable (ion permeable) membranes that direct contact is required for killing by  $\text{Mg}(\text{OH})_2$  NPs.

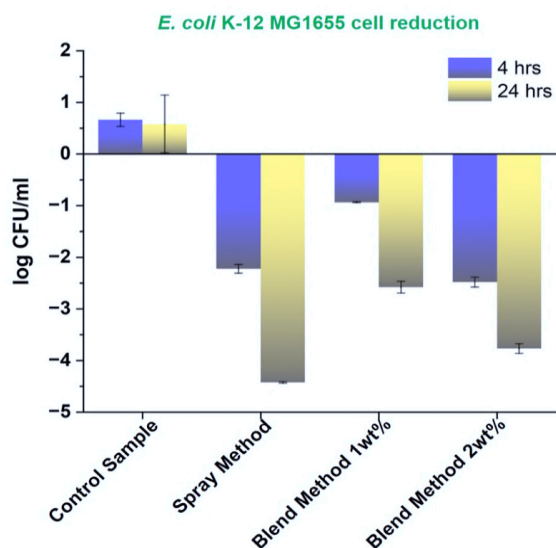


**Figure 5.8** Antimicrobial data for (i) a control sample, (ii) coated paper sprayed with MgNP, (iii) paper coated by the WSO@MgNP blend with 1 wt % MgNPs, and (iv) paper coated by the WSO@MgNP blend with 2 wt% MgNPs.

Consistent with this observation Nakamura et al. were using  $\text{Mg}(\text{OH})_2$  NPs of different sizes and using growth-kill experiments and SEM analysis concluded that the bactericidal effect of  $\text{Mg}(\text{OH})_2$  NPs was due to physical damage caused to the bacteria, not chemical alteration. The

relative effectiveness of the ROS-mediated and physical damage-mediated mechanisms of cell destruction may be altered by nanoparticle size and morphology and the rate of kill may be influenced by factors such as the bacterial stage of growth as reported by Okamoto et al. Such observations imply that nanoparticles may exert their biocidal potential via ROS and physical perturbation in different degrees depending on the nanoparticles' size, morphology or composition. A nanoparticle with modest ROS production may have size and structure such that physical damage is the principal mechanism of biocidal action.

## **5.6 Conclusions**

We have successfully developed the incorporation of food-safe MgNPs into waterborne soybean oil (derived from renewable sources) for paper coating. Excellent antimicrobial resistance as well as good water barrier performance, is achieved. Water/Oil repellency is also remarkable. The integration of four salient features (water/oil repellency, barrier and anti-microbial resistance) in coated papers offers huge potential in food and medical packaging. We anticipate our developed waterborne soybean oil-doped MgNP coating to pave the way for the development of coated paper exhibiting antimicrobial activity which will enhance the performance of coated paper and may provide a viable alternative to plastic packaging. Future studies will focus on potential migration of any ingredient in food simulant condition.

**CHAPTER 6: DESIGN OF COMPOSTABLE AND RECYCLABLE MODIFIED  
SOYBEAN OIL COATED PAPER WITH ENHANCED WATER AND OIL  
RESISTANCE**

A version of this chapter is published as:

Kumar, V.; Shaker, M.; Khan, A.; Sabde, S.; Hamdani, S.S.; Alghaysh, O.M.; Wang, Y.; Li, K.; Abdelwahab, M.A.; Barton, S.; Haidler, J.; Rabnawaz, M., Design of compostable and recyclable modified soybean oil coated paper with enhanced water and oil resistance. *ACS Sustainable Resour. Manage.* **2025**, 2, 98-107.

## 6.1 Abstract

Plastic (especially polyethylene), per- and polyfluoroalkyl substances (PFAS), and modified plant oils, such as acrylated epoxidized soybean oil (AESO), are commonly used for paper coatings due to their excellent packaging performance. However, plastic- and plant oil coated paper is not recyclable, and PFAS is toxic. To address these, a photocurable AESO emulsion was blended with a degradable crosslinker, oligoacrylate lactide/glycolide to enhance the recyclability of the coated paper. In a parallel approach, Epoxidized Soybean Oil (ESO) was modified with glycolic and methacrylic groups to further promote the recyclability of the coated paper. In both cases, emulsions were prepared, cast onto paper, and UV-cured prior to testing for water and oil resistance using Cobb-1800 and kit rating tests, respectively. The coated paper was both repulpable and recyclable, as validated through standard recycling methods. Furthermore, vermicomposting tests confirmed the compostability of coated paper. This work demonstrates a unique, naturally derived packaging alternative for PFAS and plastics in packaging applications.

## 6.2 Introduction

For several decades, we have been relying on plastics for every aspect of our lives, from packaging to transportation.<sup>67,111,112</sup> Owing to ease of processing, lower cost and thermal resistance, plastics have been adopted rapidly in the packaging sector. According to certain estimates, packaging accounts for 34% of all plastic consumption.<sup>70,113</sup> However, this has also created a problem of potential microplastics, landfilling, and environmental pollution.<sup>114–116</sup> Particularly, the packaging sector is self-responsible for 47% of plastic waste generated today.<sup>117,118</sup>

In 2024, the United States NSF (National Science Foundation) Engineering Research Vision Alliance (ERVA) identified three key manufacturing areas significantly affecting carbon



emissions: chemical production, construction materials, and single-use consumer plastics. On one hand, plastic production and consumption are on the rise; on the other hand, recycling rates are very low; for example, in the US, the current plastic recycling rate is less than 10%.<sup>69,70</sup> Due to the headwind in plastic recycling, there has been more interest in biodegradable packaging materials.

In this regard, biodegradable materials such as polyhydroxyalkanoates (PHA), polylactic acid (PLA), polybutylene succinate (PBS), and poly(butylene adipate-co-terephthalate) (PBAT) can offer biodegradability under certain conditions, and are also difficult to recycle.<sup>83,101,119</sup> In response to the growing concerns about plastics and microplastics, there has been a renewed interest in paper-based packaging.<sup>12</sup> One reason for the growth of the paper industry is the increasing consumer sentiment against plastic. Another reason is that paper is naturally derived and biodegradable without contributing to microplastic pollution. Paper packaging can also offer net-zero packaging solutions that are beneficial for the climate, thanks to the CO<sub>2</sub> absorption by plants during their growth. Finally, paper is as affordable as plastic and recyclable, with nearly 68% of paper being recycled in the U.S. alone.

Contemporary paper-based packaging that offers performance comparable to that of plastics relies on paper coated or laminated with plastic materials.<sup>120</sup> Some examples of this coated paper are polyethylene-coated laminated paper, wax-coated paper,<sup>118,121,122</sup> acrylic-coated paper, and PFAS-coated paper.<sup>29,123</sup> While these coated and laminated paper offer packaging desirable functions, they lose their recyclability and biodegradability. There is certainly a growing demand in designing paper that offers packaging performance while also retaining recyclability and biodegradability. The estimated value of the global paper packaging market stood at around \$348.08 billion USD in 2022 and is expected to grow to \$488.64 billion USD by 2030, thus

corresponding to a compound annual growth rate (CAGR) of ~4.38%. The paper packaging market usually includes the intended applications from various fields such as food and beverage, e-commerce, electrical and electronics, home care, automotive, healthcare, and so on.

Naturally bioderived polymers have been used to replace non-degradable plastics for paper coating.<sup>124</sup> For example, the paper has been coated with zein, starch, chitosan and tested for its packaging performance.<sup>62,63</sup> However, such polymers failed to offer the necessary water resistance to the coated paper. In addition, sustainable bio-derived materials often face challenges related to cost considerations, as they are often more expensive than conventional alternatives. The lack of a reliable supply of bio-based alternatives is yet another challenge, which also leads to price fluctuations. However, with increasing awareness of the adverse impact of petroleum-derived resources on global climate change, there has been a shift toward more sustainable bio-based alternatives in recent years. Over time, supply chain and cost issues are expected to be resolved as customer demand for sustainable materials grows in the coming years.

Recently, plant-based oils are gaining significant interest as a coating material for paper because of their superior water and oil resistance.<sup>24,32,43,46,47</sup> Globally soybean oil productions are estimated ~59.62 million metric tons out of which US alone contribute ~20% (~12.3 million metric tons). For example, our group reported the use of AESO for paper coating with excellent water/oil resistance properties; however, the coating load was too high (~31 g/m<sup>2</sup>).<sup>13</sup> Recently, we published waterborne coated paper using AESO emulsion that was stabilized via polyvinyl alcohol (PVOH), that offered excellent water and oil resistance and are food-safe.<sup>125</sup> Even the coated paper has good water and oil resistance and offers biodegradation but the recycling aspect was challenging and detail investigation was missing.<sup>125</sup>

Here in this work, we explored a novel approach for the paper coating by incorporation of

degradable linker in modified soybean oil via extrinsic and intrinsic methods. The extrinsic method where a photocurable AESO emulsion was blended with a degradable crosslinker oligoacrylate lactide (AOLA) or oligoacrylate glycolide (AOGL) to enhance the degradability/recyclability of the coated paper. In a parallel approach (intrinsic) modification of epoxidized soybean oil (ESO) with glycolide followed by methacrylation was carried out with aim to promote the degradability and recyclability of the coated paper. Hexagonal boron nitride (H-BN) nanosheets were utilized as emulsifiers to stabilize the AESO blends and modified ESO.<sup>126</sup> Excellent water/oil resistances were observed as the Cobb1800 were in the range of ~5-11 gsm and KIT rating was ~12/12. The coated paper was found to be easily repulpable as well as recyclable. Vermicomposting results confirmed that coated paper is compostable too. Thus, this work has the potential to replace contemporary per- and polyfluoroalkyl substances (PFAS), acrylic, and polyethylene-based coated paper.

## **6.3 Results and Discussion**

### **6.3.1 Soybean oil modification approaches**

AESO coated paper is not easily recyclable because of the crosslinked nature of AESO after UV/light exposure.<sup>127</sup> In a previous article, an attempt to recover pulp resulted in a thin coating of cured AESO peeling off from the coated paper surface that appears like plastic, which could be problematic from the industrial perspective as separation could pose a challenge. To navigate this problem, a new idea was introduced: creating modified soybean oil crosslink coating on paper with degradable linkers. These degradable linkers do not interfere with the recycling of the coated paper, nor do they interfere with its biodegradation. In this work, chemical modification of soybean oil to create degradable linkers has been pursued mainly via two approaches, the extrinsic and intrinsic approaches, as shown in **Figure 6.1**.

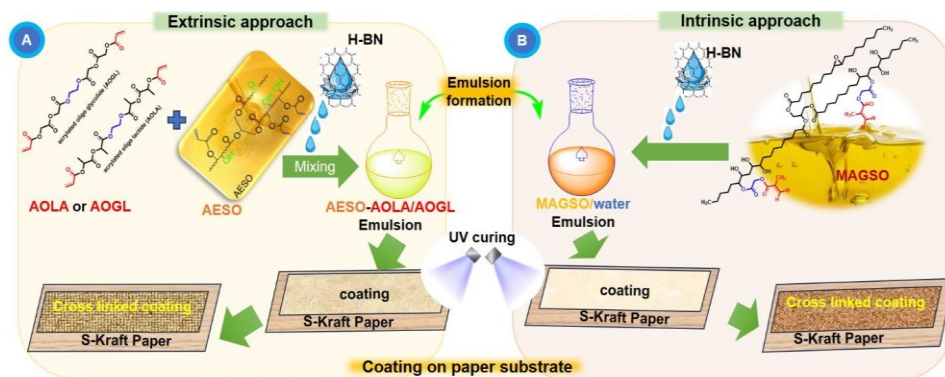
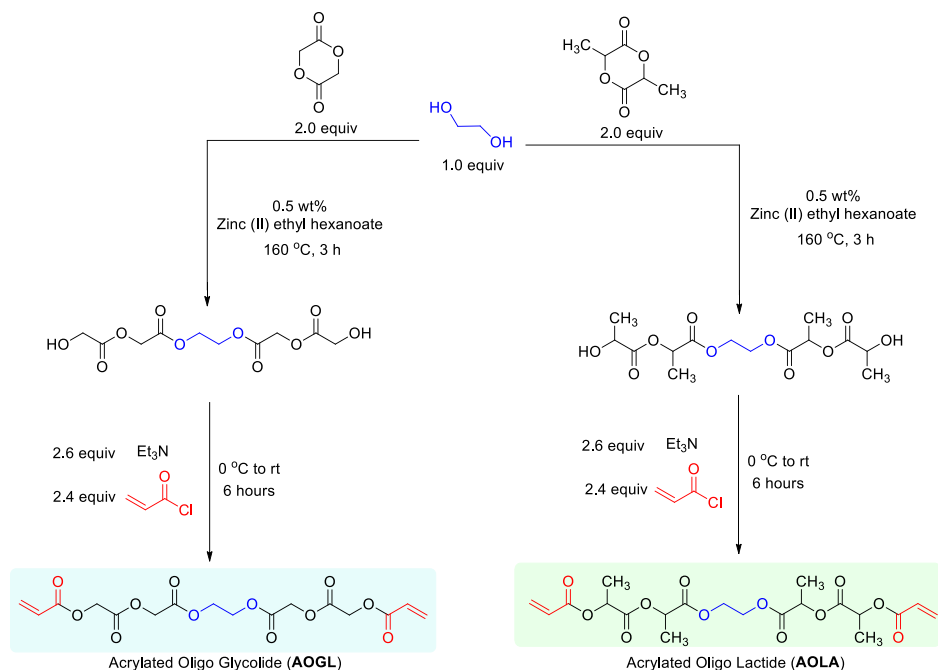


**Figure 6.1** Illustration of A) extrinsic and B) intrinsic for waterborne paper coating.

### 6.3.2 Extrinsic Approach

The extrinsic approach involves the synthesis of additional cross-linkers, acrylated oligo lactide (AOLA) and acrylated oligo glycolide (AOGL). As shown in **Scheme 6.1**, first, lactide/glycolide was reacted with ethylene glycol to form the corresponding terminal diols. This was followed by reacting the diols with acryloyl chloride to obtain the AOLA and AOGL. The chemical structures of AOGL and AOLA are confirmed by  $^1\text{H}$ -NMR analysis in the Supporting Information (SI), Figure B.S9 - B.S12. In the case of AOLA, the peaks around 6.46, 6.18, and 5.91 ppm are assigned for the terminal vinyl group, the lactide ( $-\text{CH}$ ) and ( $-\text{CH}_3$ ) proton are at 4.32 and 1.58 ppm, respectively, and peaks at 4.37 ppm are assigned for ethylene units. The  $^1\text{H}$  NMR analysis confirmed the AOGL chemical structure, with acryl protons found at 6.54 and 6.23 ppm, as well as 5.94 ppm (d,  $-\text{CH}_2=\text{CH}-$ ), a peak corresponding to glycolide ( $-\text{CH}_2$ ) being observed at 4.84 ppm, and ethylene protons being found at 4.40 ppm. Once the crosslinkers (AOLA and AOGL) were prepared, they were blended with AESO in a weight ratio of 1:1 (Figure 6.1A). The photographs of the preparation of AOLA-AESO and AOGL-AESO emulsions are shown in SI, Figure B.S1. The H-BN dispersed in Water/IPA was added to obtain the desired emulsion where H-BN acts as solid particle stabilizer and can be described as inverse pickering emulsifier.<sup>128</sup>



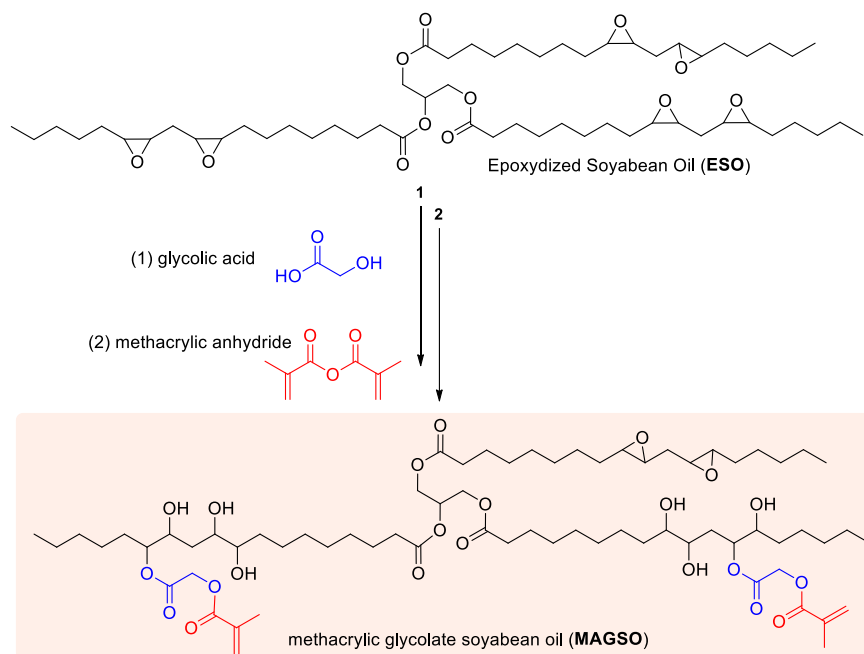
**Scheme 6.1** Synthetic route of the acrylated oligo glycolide (AOGL) and acrylated oligo lactides (AOLA) materials.

The waterborne emulsion of AOLA-AESO or AOGL- AESO was then coated onto starch-coated kraft paper to prepare KP/S/AOLA-AESO and KP/S/AOGL-AESO. This paper was then UV cured, and cross-linking happens in the presence of a photoinitiator. AOLA and AOGL act as reactive organic diluents as well as cross linkers during the curing process to improve the coating properties and able to be hydrolyzed in recycling process of the cross-linked coating.<sup>129</sup>

### 6.3.3 Intrinsic approach

The intrinsic approach means a direct chemical functionalization/modification of epoxidized soybean oil (ESO), as shown in **Scheme 6.2**. Briefly, the chemistry of modification of epoxidized soybean oil begins with reaction of ESO with glycolic acid. The glycolic acid reacts with epoxy functional group present in backbone of soybean oil chemical structure and the ring-opening transesterification step yield glycolate and hydroxy- units. The reaction has been monitored using  $^1\text{H-NMR}$  (**Figure B.S13**). Peak at 3.36 ppm assigned for -CH proton of glycerol unit, -CH units

bearing the glycolate found to be at 4.90 ppm and -CH<sub>2</sub> of glycolic units assigned at 4.12 ppm.



**Scheme 6.2** The synthesis of the methacrylated glycolate soybean oil (MAGSO).

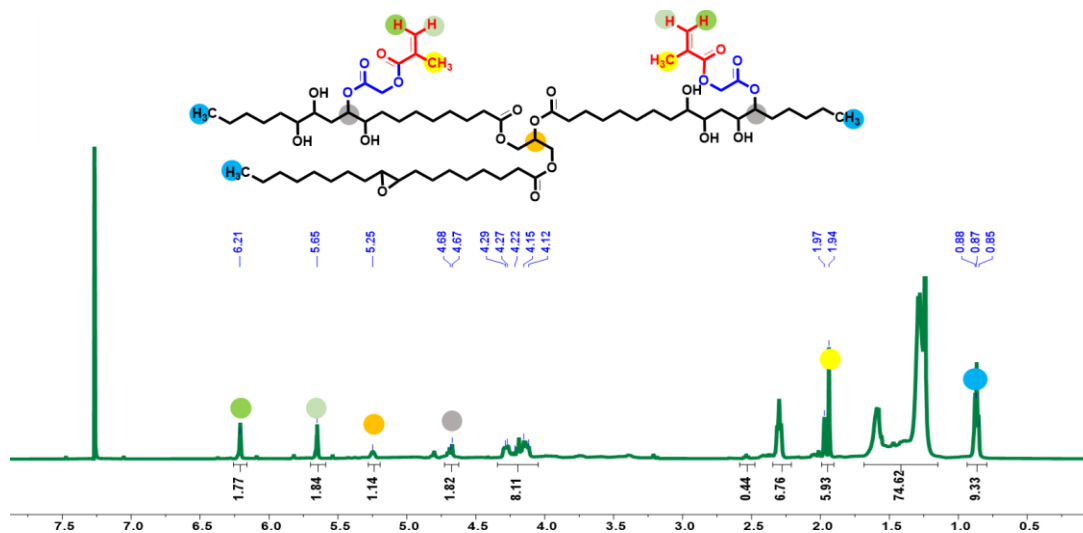


**Figure 6.2** <sup>1</sup>H-NMR spectrum (CDCl<sub>3</sub> is used as solvent, frequency- 500 MHz) of methacrylated glycolate soybean oil (MAGSO).

In the next step, the hydroxy of glycolate unit attached to ESO reacted with methacrylic anhydride resulting in the formation of methacrylate glycolate soybean oil (MAGSO), (**Scheme 6.2**). Protons of acryl units assigned to be at 6.21 and 5.65 ppm while peak at 4.81 ppm corresponding to -CH proton of the newly formed methine proton comes after the opening of epoxy ring. The methyl of acrylic group was found to be at 1.94 ppm (**Figure 6.2**).

The introduced C=C functionality per ESO in MAGSO sample is  $\sim 2$ . This value is lower than commercial AESO where the value can vary from 2.16-2.77 depending upon the extent of acrylation.<sup>34,39</sup> Wu et al. reported ESO that was grafted with HEMAMA (hydroxyethyl methacrylated maleate) where C=C functionality was reached to 5.51-6.05.<sup>130</sup> The lower functionality in MAGSO could aid in degradation during the recycling and composting process. After successful preparation of MAGSO, it was directly dispersed in water in the presence of H-BN. The obtained waterborne emulsion of MAGSO, shown in **Figure 6.3**, was coated on starch coated paper, and UV crosslinked in a similar manner as described in the extrinsic approach (**Figure 6.1B**).



**Figure 6.3** MAGSO is mixed with H-BN solution to form emulsion.

The glycolate units work as spacers between the ESO backbone structure and the methacrylate unit. This spacer offers the modified MAGSO chemical structure, the ability to hydrolyze easily after curing process which gives it more advantage in recyclability and repulpability.

### 6.3.4 Characterization of the coated paper

After successfully obtaining coated kraft paper via intrinsic and extrinsic approaches, further evaluation such as coating load, basis weight and thickness of all the three coated paper (KP/S/AOLA-AESO (extrinsic approach), KP/S/AOGL-AESO (extrinsic approach) and KP/S/MAGSO (intrinsic approach) has been performed. The thickness, basis weight and the loading of the sample has been summarized in **Table 6.1**. It is evident that the thickness of the coated papers is  $\sim 8\text{-}10\ \mu\text{m}$  with reference to starch coated kraft paper (KP/S), give an indication, that fabrication process is cost-effective and yielded a thin cured coated layer. The basis weight which represent the mass of paper in grams per square meter (gsm) is  $129.2 \pm 1.6$  gsm for the kraft paper while for all the coated samples it lies in the range of  $\sim 150\text{-}152$  gsm that reflects the total loading (including starch content) is  $\sim 20\text{-}22$  gsm while excluding the starch amount the loading level of cross-linked coatings left only around  $\sim 10\text{-}15$  gsm. This lower loading of the cured modified soybean oil drops the cost of coating process and gives competitive advantage of using these materials as compared to other biobased commercially available materials.

**Table 6.1** Paper coated sample composition, thickness, basis weight and loading respectively.

Sample #	Sample Name	Thickness ( $\mu\text{m}$ )	Basis Weight (gsm)	Loadin g (g)
1	KP	$185.7 \pm 1.5$	$129.2 \pm 1.6$	NA
2	KP/S	$216.3 \pm 2.5$	$139.0 \pm 1.6$	$9.8 \pm 2.3$
3	KP/S/AESO-AOLA	$222.4 \pm 1.5$	$151.1 \pm 1.5$	$11.4 \pm 1.1$
4	KP/S/AESO-AOGL	$223.3 \pm 2.1$	$150.6 \pm 2.6$	$11.7 \pm 4.1$
5	KP/S/MAGSO	$222.2 \pm 1.5$	$151.7 \pm 2.7$	$11.3 \pm 3.9$

### 6.3.5 Water- and Oil-Resistance

Coated paper via intrinsic and extrinsic approach (KP/S/AOLA-AESO, KP/S/AOGL- AESO and KP/S/MAGSO) respectively, were subjected to water resistance test by following Cobb1800 test to determine the efficacy of coated paper. The Cobb1800 reflects the amount of water absorbed



by the coated paper in 1800 sec, as known, the lower the Cobb1800 value, the better the performance of coated paper will be proved.

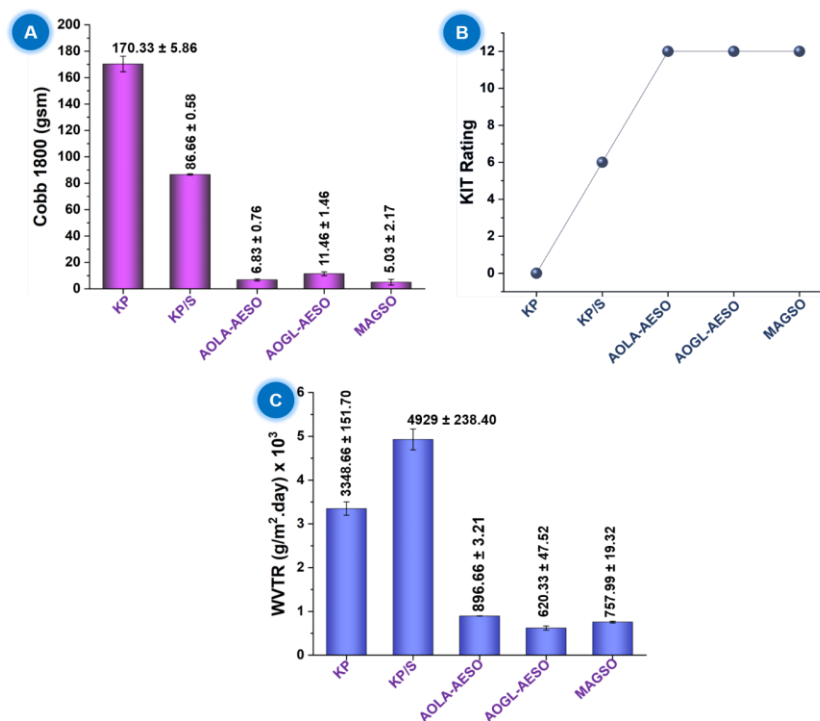


**Figure 6.4.** A) Water resistance analysis (Cobb 1800) of the coated samples against to the controls; B) Oil resistance analysis (KIT rating) of the coated samples against to the controls and C) Water vapor transmission rate (WVTR) of the coated samples against the controls.

The Cobb1800 value was presented in **Figure 6.4A**. The uncoated kraft paper shows value of  $\sim 177.33 \pm 5.86$  gsm in 1800 sec, this value is on way higher side owing to the porous structure of cellulose matrix as well as the hydroxyl group present that provide path for diffusion of water molecules through the formation of hydrogen bonding with the cellulose matrix. The Cobb1800 dropped to  $86.66 \pm 0.58$  gsm for KP/S because the pores were filled up by starch layer but the value still significantly high mainly owing to the hydrophilic characteristic of starch. The coated paper KP/S/AOLA-AESO, KP/S/AOGL-AESO and KP/S/MAGSO showed significant reduction in water adsorption Cobb1800 values  $6.83 \pm 0.76$  gsm,  $11.46 \pm 1.46$  gsm and  $5.03 \pm 2.17$  gsm

respectively, nearly 94-98% reduction in the amount of water adsorption compared to the control uncoated kraft paper. Addition of acrylate oligomers AOLA and AOGL to AESO become an integral fragment of the cured coating and provide specific properties. These oligomers impact the kinetic rate of polymerization as well as significantly increase the cross-link density as aided by higher concentration of double bond present in the system.<sup>130,131</sup> Increasing the cross-link density dramatically improving the packing density of the cured coating which completely masks pores in KP/S and dramatically reduced the Cobb1800 value. This has been demonstrated by performing the Cobb1800 determination with only cured AOLA and AOGL individual ingredient coating on KP/S, expecting low cross-link density and the result indicates the evaluated Cobb1800 value is in the range of ~30-32 gsm (**Table B.S1**).

MAGSO coating material has self-cross linker methacrylate groups, which help to obtain a uniformed cross linked coating structure after UV curing process, leading to a uniform coating, which enhanced water resistance of coated KP/S/MAGSO paper by dramatic reduction of the porosity of the starch coated layer. Coated paper with enhanced water-resistant properties can be useful for a range of applications where the coated paper will be in contact with water for a prolonged period. However, oil resistance is equally important and must be evaluated essentially relevant for the food packaging industry. The standard KIT rating test has been performed for oil/grease resistance of coated paper.<sup>132</sup> The KIT ratings of all the coated samples (KP/S/AOLA-AESO, KP/S/AOGL-AESO and KP/S/MAGSO) were 12/12 reflecting maximum oil resistance ability (**Figure 6.4B**) whereas a value of 0/12 was observed for the kraft paper control (KP) that signifies absence of oil resistant. Thus, it can be concluded that the coating layer truly acts as a barrier for oil to penetrate through the paper pores. As shown in **Figure 6.4C**, the coated kraft paper (KP/S/AOLA-AESO, KP/S/AOGL- AESO and KP/S/MAGSO) has been tested for Water

vapor transmission rate (WVTR) properties. The WVTR of kraft paper is  $\sim 3200 \text{ g/m}^2\cdot\text{day}$  that increases to  $\sim 4500 \text{ g/m}^2\cdot\text{day}$  upon starch coating and later the KP/S/AOLA-AESO and KP/S/AOGL-AESO coating WVTR significantly reduces the to  $\sim 600 \text{ g/m}^2\cdot\text{day}$  and  $\sim 550 \text{ g/m}^2\cdot\text{day}$ . This huge reduction ( $>85\%$ ) in water transmission rate indicates huge improvement owing to the hydrophobic nature of coated material thanks to the high cross-link density of the coating layer.

### 6.3.5 Repulping and Recyclability process

KP/S/AOLA-AESO paper has been chosen for exploring the repulpability method based on industrial process. In the repulping process, the screen is not rejecting the coated ingredient composed of cured AOLA-AESO as they degrade into fine powder during the process and thus the coated paper can be easily processed and recycled via the pulp recovery method. The results obtained are very promising and truly align with the concept of circular economy. The general appearance of repulping and rejects during the test are shown in **Figure 6.5**. The percentage yield of the repulping process is 97.3%, which confirmed that KP/S/AOLA-AESO coated paper has passed the test (**Table 6.2**).



**Figure 6.5** Industrial scale repulpability of the coated paper KP/S/AOLA-AESO.

Next, lab scale recyclability test was performed in this study. Detailed procedures have been provided in section 3, **SI**. In brief, 20% coated sample and 80% uncoated base paper are mixed

and repulped in a lab-scale pulper at pH ~7 and 125 °F. The pulped suspension is passed through a vibration flat screen with 0.010-inch slots. Hand sheets are made from screen accepts. The properties including Coefficient of Friction (Slide Angle), Short Span Compression Strength (STFI), Burst Strength, Water-Drop Penetration, and Stickies are investigated following TAPPI standards.

**Table 6.2** Results of repulping process, the yield is ~97% indicates KP/S/AOLA-AESO pass the test.

Content	Units	KP/S/AOLA-AESO
Moisture	(wt%)	7.40
Sample Charged	(g)	25.00
Screen Rejects	(g)	0.54
Screen Accepts	(g)	19.10
Yield of sample	(wt%)	97.3%
Pass/Fail		Pass

The results have been summarized in **Table 6.3** and are compared to a control sample, which is a 100% base paper pulped and screened using identical conditions. Interestingly, the repulped paper shows at par performance as compared with the control sample. Thus, validates that repulped paper can be easily recycled without loss of any performance for commercial purposes.

**Table 6.3** Performance comparison of AOLA-AESO repulped paper with control kraft paper.

Performance	Control Kraft Paper	AOLA-AESO recycled paper
Coefficient of Friction (°)	26.40	33.40
Water drop penetration (sec)	4.00	1.40
Stickies (counts)	38.00	39.00
Burst Strength (lb/inch)	36.70	34.00
Burst Strength (index value)	0.265	0.275
Short span compression strength (STFI) (lb/inch)	8.85	8.11
Short span compression strength (STFI) (lb/inch)	0.064	0.066

### 6.3.6 Vermicomposting of KP/S/MAGSO sample

Vermicomposting is a cost-effective method using earthworms and microbes to manage organic waste, producing vermicompost as a beneficial biofertilizer for agricultural soils.<sup>133</sup> Using vermicompost guarantees that organic matter is recycled effectively, which helps reduce waste, eases the load on landfills, and advances the circular economy.<sup>134</sup>

Earthworms play a crucial role in maintaining ecological balance as they positively impact chemical, biological and physical properties of the soil. Several studies have highlighted the harmful impacts of microplastics on soil organisms like earthworms, including intestinal damage, DNA damage, oxidative stress, avoidance behavior, impairment of spermatogenesis, reduced coelomocyte viability, inhibited growth, and decreased reproduction.<sup>135</sup>



**Figure 6.6** Vermicomposting process of KP/S/MAGSO papers shredded into (0.5 cm x 4.0 cm) sized sheets.

The vermicomposting of shredded paper is one of the important sources of food for microbes and worms. We have performed vermicomposting of KP/S/MAGSO coated papers. The

vermicompost mixture was prepared by mixing a certain proportion of food waste, water, worms, and compost (**Figure 6.6**). Worms along with shredded leaves, waste food mixed and then sprinkled with water, the prepared mixture is then mixed with our coated paper and then left for two months. It is worth mentioning that the vermicomposting process has been conducted for KP/S/MAGSO papers in different shredded sizes, (1.5cm x 15cm), (15cm x 15cm), (1.5cm x 1.5cm) and (0.5 cm x 4.0 cm) diameters **Figure B.S6**. All shredded papers were added to the prepared mixture respectively, as illustrated in **Figure B.S7**. The analysis of vermicomposting process was conducted by I) visual observation of worms; II) earthworms' growth parameter (cocoon); III) physicochemical properties of vermicompost obtained from the coated and control samples. After two months, the large sized papers (1.5cm x 15cm) and (15cm x 15cm) were not fully decomposed and needed more time to completely disappear (**Figure B.S7**). The small paper samples (strips) (0.5cm x 4cm) shredded were almost fully composted with only a few chunks remaining. Additionally, the biodiversity looks very rich (**Figure 6.6**). Species of fly larvae, juveniles, centipede exoskeleton, plant sprouts, pot worms and tons of cocoons have been found. Earthworms are still in good health and active. Small squares (1.5cm x 1.5cm) have been composted similar to (0.5 cm x 4.0 cm) sized sheets with similar observations. In general, we found paper is decomposed and eaten by worms. It is observed that the coating material did not hinder the growth of worms and was completely consumed in 60 days. Moreover, these vermicompost can be used as an organic manure for farming purposes. The cost of vermicomposting is roughly ~800 \$ for one cubic yard. The detailed elemental analysis (**Table B.S5 & B.S6**) of vermicomposting has been conducted in lab to know the exact nutrients value that can be provided to soil when it will be used as organic manure. In general, C/N ratio is quantitative way to assign the quality of compost, the lower C/N ratio is preferred as it will

provide high amount of nitrogen content. For vermicomposting process mainly, C/N ratio can lie in between 25-30:1. The C/N ratio obtained for KP/S/MAGSO sample is close to 18.4:1, implies that the compost generated has a much better C/N ratio and thus open up opportunity to generate revenue by selling the compost.

## **6.4 Conclusion**

In summary, cross-linked AOLA-AESO, AOGL-AESO, and MAGSO systems were successfully developed for paper coating using extrinsic and intrinsic approaches.  $^1\text{H}$  NMR characterization confirmed the successful synthesis of the desired degradable linkers for coating. All coated papers demonstrated excellent water resistance (Cobb-1800: 5–11 g/m<sup>2</sup>), a kit rating of 12/12, and over 85% reduction in their WVTR values. The coated papers passed certified repulping and recyclability tests, thus validating the effectiveness of our degradable crosslinker approach. KP/S/MAGSO-coated paper was also successfully tested in the vermicomposting process, where it was found to complete compost within two months. The coated paper does not possess thermal sealing and oxygen barrier properties, which will be addressed in future studies. Despite the lack of sealing and good oxygen barrier properties, the current coated paper is suitable for applications such as disposable plates, food wrappers, and similar uses.

## CHAPTER 7: CONCLUSIONS AND FUTURE OUTLOOK

### 7.1 Conclusions

Sustainable packaging is of the utmost importance as the concern over plastic waste generation has been rising every year. With the estimated plastic recycling rate ~9% is surely alarming. Innovation in paper packaging such as imparting water/oil resistance alongwith biodegradation, repulpability and recyclability as discussed throughout the thesis is one way to overcome the concern rising from plastic waste. As discussed, modified soybean oil as coating ingredient has potential to replace conventional plastic/PFAS based coated paper packaging. The concept can be further extended to other plant oils/waste cooking oils and so on to bring similar innovations as well as new chemical modifications in water medium will be interesting.

In Chapter 3, we demonstrated the first example of successful UV curing of neat acrylated epoxidized soybean oil (AESO) on kraft paper using photoinitiator motivates further investigation on modified soybean oil. The loading was quite high (lowest ~31 gsm, highest ~114 gsm), as the packaging industry demands to be coating load in the range of ~8-20 gsm. We also demonstrated water resistance properties for longer period of time (Cobb1800, 30 mins) and excellent KIT rating (12/12). Tensile properties are compromised with higher level of loading, and this could be attributed to lower modulus properties of cured AESO itself. Motivated by lowering the AESO loading level as well as maintaining decent water and oil resistance properties along with maintaining mechanical properties we investigated waterborne AESO coating in the next chapter.

In Chapter 4, we demonstrated a waterborne emulsified AESO system using polyvinyl alcohol (PVOH) as an emulsifier. PVOH is US FDA approved as well as biodegradable in nature thus it became a perfect choice to emulsify the AESO in water. Emulsion of AESO was optimized with



different amounts of water and PVOH and the optimized system demonstrated excellent Cobb1800 ~ 13 gsm, KIT rating -7/12. The water/oil resistance has been compromised compared to neat AESO; however, the loading level is low comparatively. We also investigated biodegradation properties of AESO coated paper in detail and compared with the control sample, interestingly the AESO coated paper degraded more than 90% within 90 days as evident by ~90% CO<sub>2</sub> released compared to the control sample for same time frame. Hot beans served on coated plates as well as coating on printed paper without affecting the printing demonstrate that its practical applications. Additionally, mechanical properties are retained more than 90% compared to the control sample. Chemo-degradation of coated paper has been demonstrated, however, the coated AESO leaches out as plastic although it is biobased, it could pose a significant challenge during processing in industry and might affect repulpability and recyclability of coated paper. Antimicrobial properties are very relevant, especially for medical/food packaging applications. During Covid 19, we witnessed how disease can spread by contaminated surface.

In chapter 5, we investigated and incorporated food-safe magnesium nanoparticles (MgNPs) into waterborne AESO for paper coating applications. This innovative coating was evaluated for its antimicrobial properties and demonstrated approximately a 4-log reduction in the population of *Escherichia coli* (E. coli), effectively eliminating 99.99% of the bacteria. Water and oil resistance has been maintained to a good extent as Cobb1800 ~18 gsm and KIT ~7/12. The combination of these four key features—antimicrobial resistance, water and oil repellency, and moisture barrier performance—positions the coated paper as a promising solution for food and medical packaging. Our waterborne soybean oil-doped MgNP coating holds significant potential to revolutionize coated paper by offering antimicrobial functionality, improving performance, and presenting a sustainable alternative to conventional plastic packaging.

In chapter 6, intrinsic and extrinsic modification of soybean oil has been demonstrated using degradable linker. All the degradable linker synthesized has been monitored and confirmed using  $^1\text{H}$ -NMR analysis. For extrinsic modification, oligo lactide/glycolide acrylate has been used to cross-link acrylates unit of AESO. The presence of ester units in oligo lactide/glycolide is susceptible to hydrolytic cleavage in the presence of basic solutions and indeed the coating material instead of peeling off as plastic, it separated in powder form. Similar observation has been found when intrinsic modification path has been followed where epoxidized soybean oil (ESO) has been modified with glycolic acid followed by methacrylic anhydride. The coating material peeled off as powder instead of plastic like appearance. Further recyclability and repulpability tests corroborate the same observation as there has not been any peeled off coating layer has been observed. Finally, a simple vermicomposting method has been adopted and coated paper has been shown to be completely degraded and compost formed is of high quality that can be used in farming and add significant value for the crops.

## **7.2 Future Outlook**

Surface coating has been proven as seen throughout the thesis is a great way to impart water/oil resistance. Water/oil resistance, repulpability, recyclability, biodegradation, vermicomposting of the coated paper has been investigated to claim for a sustainable packaging. Some other properties such heat sealing, not improved mechanical properties are some challenges that still need to be addressed. Other studies such as migration of any component in various food simulants can be studied to further strengthen the concept.

Other tests such as dynamic mechanical analysis (DMA) can be utilized to understand the cross-linking density as well as temperature/solvent dependent modulus behavior that is crucial to understand the coated paper durability in extreme and more practical conditions.

## REFERENCES

- (1) Deshwal, G. K.; Panjagari, N. R.; Alam, T. An Overview of Paper and Paper Based Food Packaging Materials: Health Safety and Environmental Concerns. *Journal of Food Science and Technology*. Springer October 1, s, pp 4391–4403.  
<https://doi.org/10.1007/s13197-019-03950-z>.
- (2) Kóczán, Z.; Pásztor, Z. Overview of Natural Fiber-Based Packaging Materials. *Journal of Natural Fibers*. Taylor and Francis Ltd. **2024**.  
<https://doi.org/10.1080/15440478.2023.2301364>.
- (3) Macht, J.; Klink-Lehmann, J.; Venghaus, S. Eco-Friendly Alternatives to Food Packed in Plastics: German Consumers' Purchase Intentions for Different Bio-Based Packaging Strategies. *Food Qual Prefer* **2023**, *109*. <https://doi.org/10.1016/j.foodqual.2023.104884>.
- (4) Jain, P.; Hudnurkar, D. M. Sustainable Packaging in the FMCG Industry. *Cleaner and Responsible Consumption* **2022**, *7*. <https://doi.org/10.1016/j.clrc.2022.100075>.
- (5) Duarte, P.; Silva, S. C.; Roza, A. S.; Dias, J. C. Enhancing Consumer Purchase Intentions for Sustainable Packaging Products: An in-Depth Analysis of Key Determinants and Strategic Insights. *Sustainable Futures* **2024**, *7*. <https://doi.org/10.1016/j.sftr.2024.100193>.
- (6) Zhu, Z.; Liu, W.; Ye, S.; Batista, L. Packaging Design for the Circular Economy: A Systematic Review. *Sustainable Production and Consumption*. Elsevier B.V. July 1, 2022, pp 817–832. <https://doi.org/10.1016/j.spc.2022.06.005>.
- (7) Oloyede, O. O.; Lignou, S. Sustainable Paper-Based Packaging: A Consumer's Perspective. *Foods* **2021**, *10* (5). <https://doi.org/10.3390/foods10051035>.
- (8) Perumal, T.; Krebs de Souza, C.; Nihues, T. C.; Jain, P.; Gaikwad, K. K.; Roy, S. A Review on Biopolymer-Based Oil and Water-Resistant Functional Paper Coating for Food Packaging. *Food Biosci* **2025**, *63*, 105656. <https://doi.org/10.1016/j.fbio.2024.105656>.
- (9) Upadhyay, A.; Lucia, L.; Pal, L. Harnessing Total Chemical-Free Paper and Packaging Materials Barrier Properties by Mechanical Modification of Cellulosic Fibers for Food Security and Environmental Sustainability. *Appl Mater Today* **2023**, *35*.  
<https://doi.org/10.1016/j.apmt.2023.101973>.
- (10) Kansal, D.; Hamdani, S. S.; Ping, R.; Sirinakbumrung, N.; Rabnawaz, M. Food-Safe Chitosan-Zein Dual-Layer Coating for Water- And Oil-Repellent Paper Substrates. *ACS Sustain Chem Eng* **2020**, *8* (17), 6887–6897.  
<https://doi.org/10.1021/acssuschemeng.0c02216>.

- (11) Iselau, F.; Malmberg-Nyström, K.; Holmberg, K.; Bordes, R. Parameters Influencing Hydrophobization of Paper by Surface Sizing. *Nord Pulp Paper Res J* **2018**, *33* (1), 95–104. <https://doi.org/10.1515/npprj-2018-3015>.
- (12) Jahangiri, F.; Mohanty, A. K.; Misra, M. Sustainable Biodegradable Coatings for Food Packaging: Challenges and Opportunities. *Green Chemistry*. Royal Society of Chemistry April 5, 2024, pp 4934–4974. <https://doi.org/10.1039/d3gc02647g>.
- (13) Kumar, V.; Khan, A.; Rabnawaz, M. A Plant Oil-Based Eco-Friendly Approach for Paper Coatings and Their Packaging Applications. *Progress in Organic Coatings*. Elsevier B.V. March 1, **2023**. <https://doi.org/10.1016/j.porgcoat.2022.107386>.
- (14) Ziani, K.; Ioniță-Mîndrican, C. B.; Mititelu, M.; Neacșu, S. M.; Negrei, C.; Moroșan, E.; Drăgănescu, D.; Preda, O. T. Microplastics: A Real Global Threat for Environment and Food Safety: A State of the Art Review. *Nutrients*. MDPI February 1, **2023**. <https://doi.org/10.3390/nu15030617>.
- (15) Carnero, A. R.; Lestido-Cardama, A.; Loureiro, P. V.; Barbosa-Pereira, L.; de Quirós, A. R. B.; Sendón, R. Presence of Perfluoroalkyl and Polyfluoroalkyl Substances (Pfas) in Food Contact Materials (Fcm) and Its Migration to Food. *Foods*. MDPI AG July 1, **2021**. <https://doi.org/10.3390/foods10071443>.
- (16) Gaines, L. G. T. Historical and Current Usage of Per- and Polyfluoroalkyl Substances (PFAS): A Literature Review. *American Journal of Industrial Medicine*. John Wiley and Sons Inc May 1, **2023**, pp 353–378. <https://doi.org/10.1002/ajim.23362>.
- (17) Rosenmai, A. K.; Taxvig, C.; Svingen, T.; Trier, X.; van Vugt-Lussenburg, B. M. A.; Pedersen, M.; Lesné, L.; Jégou, B.; Vinggaard, A. M. Fluorinated Alkyl Substances and Technical Mixtures Used in Food Paper-Packaging Exhibit Endocrine-Related Activity in Vitro. *Andrology* **2016**, *4* (4), 662–672. <https://doi.org/10.1111/andr.12190>.
- (18) Hamdani, S. S.; Li, Z.; Rabnawaz, M.; Kamdem, D. P.; Khan, B. A. Chitosan -Graft-Poly(Dimethylsiloxane)/Zein Coatings for the Fabrication of Environmentally Friendly Oil- And Water-Resistant Paper. *ACS Sustain Chem Eng* **2020**, *8* (13), 5147–5155. <https://doi.org/10.1021/acssuschemeng.9b07397>.
- (19) Hamdani, S. S.; Li, Z.; Sirinakbumrung, N.; Rabnawaz, M. Zein and PVOH-Based Bilayer Approach for Plastic-Free, Repulpable and Biodegradable Oil- And Water-Resistant Paper as a Replacement for Single-Use Plastics. *Ind Eng Chem Res* **2020**, *59* (40), 17856–17866. <https://doi.org/10.1021/acs.iecr.0c02967>.
- (20) Mori, R. Replacing All Petroleum-Based Chemical Products with Natural Biomass-Based Chemical Products: A Tutorial Review. *RSC Sustainability*. Royal Society of Chemistry January 3, **2023**, pp 179–212. <https://doi.org/10.1039/d2su00014h>.

- (21) Hernandez, S.; Viguera, E. Acrylated-Epoxidized Soybean Oil-Based Polymers and Their Use in the Generation of Electrically Conductive Polymer Composites. In *Soybean - Bio-Active Compounds*; InTech, **2013**. <https://doi.org/10.5772/52992>.
- (22) Ho, Y. H.; Parthiban, A.; Thian, M. C.; Ban, Z. H.; Siwayanan, P. Acrylated Biopolymers Derived via Epoxidation and Subsequent Acrylation of Vegetable Oils. *International Journal of Polymer Science*. Hindawi Limited 2022. <https://doi.org/10.1155/2022/6210128>.
- (23) Tambe, C.; Graiver, D.; Narayan, R. Moisture Resistance Coating of Packaging Paper from Biobased Silylated Soybean Oil. *Prog Org Coat* **2016**, *101*, 270–278. <https://doi.org/10.1016/j.porgcoat.2016.08.016>.
- (24) Tian, X.; Wu, M.; Wang, Z.; Zhang, J.; Lu, P. A High-Stable Soybean-Oil-Based Epoxy Acrylate Emulsion Stabilized by Silanized Nanocrystalline Cellulose as a Sustainable Paper Coating for Enhanced Water Vapor Barrier. *J Colloid Interface Sci* **2022**, *610*, 1043–1056. <https://doi.org/10.1016/j.jcis.2021.11.149>.
- (25) Zubair, M.; Pradhan, R. A.; Arshad, M.; Ullah, A. Recent Advances in Lipid Derived Bio-Based Materials for Food Packaging Applications. *Macromolecular Materials and Engineering*. John Wiley and Sons Inc July 1, **2021**. <https://doi.org/10.1002/mame.202000799>.
- (26) Gharby, S. Refining Vegetable Oils: Chemical and Physical Refining. *Scientific World Journal*. Hindawi Limited **2022**. <https://doi.org/10.1155/2022/6627013>.
- (27) zaaboul, F.; Zhao, Q.; Xu, Y. J.; Liu, Y. F. Soybean Oil Bodies: A Review on Composition, Properties, Food Applications, and Future Research Aspects. *Food Hydrocolloids*. Elsevier B.V. March 1, **2022**. <https://doi.org/10.1016/j.foodhyd.2021.107296>.
- (28) Orsavova, J.; Misurcova, L.; Vavra Ambrozova, J.; Vicha, R.; Mlcek, J. Fatty Acids Composition of Vegetable Oils and Its Contribution to Dietary Energy Intake and Dependence of Cardiovascular Mortality on Dietary Intake of Fatty Acids. *Int J Mol Sci* **2015**, *16* (6), 12871–12890. <https://doi.org/10.3390/ijms160612871>.
- (29) Vijayan, S. P.; Aparna S; Sahoo, S. K. Effect of Beeswax on Hydrophobicity, Moisture Resistance and Transparency of UV Curable Linseed Oil Based Coating for Compostable Paper Packaging. *Ind Crops Prod* **2023**, *197*. <https://doi.org/10.1016/j.indcrop.2023.116645>.
- (30) He, W.; Zhu, G.; Gao, Y.; Wu, H.; Fang, Z.; Guo, K. Green Plasticizers Derived from Epoxidized Soybean Oil for Poly (Vinyl Chloride): Continuous Synthesis and Evaluation in PVC Films. *Chemical Engineering Journal* **2020**, *380*.

<https://doi.org/10.1016/j.cej.2019.122532>.

- (31) Yang, X.; Cheng, F.; Fan, Y.; Song, Y.; He, N.; Lai, G.; Gong, Z.; Shen, J. Highly Transparent Acrylate Epoxidized Soybean Oil Based UV–Curable Silicone–Modified Coatings with Good Thermal Stability and Flame Retardancy. *Prog Org Coat* **2022**, 165. <https://doi.org/10.1016/j.porgcoat.2022.106769>.
- (32) Zeng, K.; Gu, J.; Cao, C. Facile Approach for Ecofriendly, Low-Cost, and Water-Resistant Paper Coatings via Palm Kernel Oil. *ACS Appl Mater Interfaces* **2020**, 12 (16), 18987–18996. <https://doi.org/10.1021/acsami.0c00067>.
- (33) Thakur, S.; Misra, M.; Mohanty, A. K. Sustainable Hydrophobic and Moisture-Resistant Coating Derived from Downstream Corn Oil. *ACS Sustain Chem Eng* **2019**, 7 (9), 8766–8774. <https://doi.org/10.1021/acssuschemeng.9b00689>.
- (34) Cheng, Q. Y.; An, X. P.; Li, Y. D.; Huang, C. L.; Zeng, J. B. Sustainable and Biodegradable Superhydrophobic Coating from Epoxidized Soybean Oil and ZnO Nanoparticles on Cellulosic Substrates for Efficient Oil/Water Separation. *ACS Sustain Chem Eng* **2017**, 5 (12), 11440–11450. <https://doi.org/10.1021/acssuschemeng.7b02549>.
- (35) Silva, F. M.; Pinto, R. J. B.; Barros-Timmons, A. M.; Freire, C. S. R. Tung Oil-Based Coatings towards Sustainable Paper Packaging Materials. *Prog Org Coat* **2023**, 178. <https://doi.org/10.1016/j.porgcoat.2023.107476>.
- (36) Loesch-Zhang, A.; Bellmann, M.; Lachmann, K.; Biesalski, M.; Geissler, A. Plasma Polymerization of Vegetable Oils onto Paper Substrates of Varying Porosity for Improved Hydrophobicity. *Adv Mater Interfaces* **2024**. <https://doi.org/10.1002/admi.202400507>.
- (37) Shang, Q.; Chen, J.; Liu, C.; Hu, Y.; Hu, L.; Yang, X.; Zhou, Y. Facile Fabrication of Environmentally Friendly Bio-Based Superhydrophobic Surfaces via UV-Polymerization for Self-Cleaning and High Efficient Oil/Water Separation. *Prog Org Coat* **2019**, 137. <https://doi.org/10.1016/j.porgcoat.2019.105346>.
- (38) Kępa, K.; Amiralian, N.; Martin, D. J.; Grøndahl, L. Grafting from Cellulose Nanofibres with Naturally-Derived Oil to Reduce Water Absorption. *Polymer (Guildf)* **2021**, 222. <https://doi.org/10.1016/j.polymer.2021.123659>.
- (39) Loesch-Zhang, A.; Cordt, C.; Geissler, A.; Biesalski, M. A Solvent-Free Approach to Crosslinked Hydrophobic Polymeric Coatings on Paper Using Vegetable Oil. *Polymers (Basel)* **2022**, 14 (9). <https://doi.org/10.3390/polym14091773>.
- (40) Kansal, D.; Rabnawaz, M. Fabrication of Oil- and Water-Resistant Paper without Creating Microplastics on Disposal. *J Appl Polym Sci* **2021**, 138 (3).

<https://doi.org/10.1002/app.49692>.

- (41) Nurul Syahida, S.; Ainun, Z. M. A.; Ismail-Fitry, M. R.; Nur Hanani, Z. A. Development and Characterisation of Gelatine/Palm Wax/Lemongrass Essential Oil (GPL)-Coated Paper for Active Food Packaging. *Packaging Technology and Science* **2020**, 33 (10), 417–431. <https://doi.org/10.1002/pts.2512>.
- (42) Li, Z.; Rabnawaz, M.; Khan, B. Response Surface Methodology Design for Biobased and Sustainable Coatings for Water- And Oil-Resistant Paper. *ACS Appl Polym Mater* **2020**, 2 (3), 1378–1387. <https://doi.org/10.1021/acsapm.9b01238>.
- (43) Chen, L.; Li, P.; Guan, J.; Xu, C.; Xu, C. A.; Yang, Z. Castor Oil-Based Paper Packaging Coating with Water Resistance and Degradability Obtained by Thiol-Ene Click Reaction. *J Appl Polym Sci* **2024**, 141 (17). <https://doi.org/10.1002/app.55269>.
- (44) S, A.; Suresh, T.; Sahoo, S. K. Development of Moisture/Oil-Resistant Biocoatings from Waste Cooking Oil for Packaging Applications: Scientific Upcycling with Circular Economy Potential. *ACS Sustainable Resource Management* **2024**. <https://doi.org/10.1021/acssusresmgt.4c00392>.
- (45) Parvathy, P. A.; Sahoo, S. K. Hydrophobic, Moisture Resistant and Biorenewable Paper Coating Derived from Castor Oil Based Epoxy Methyl Ricinoleate with Repulpable Potential. *Prog Org Coat* **2021**, 158. <https://doi.org/10.1016/j.porgcoat.2021.106347>.
- (46) Gao, W.; Wu, T.; Cheng, Y.; Wang, J.; Yuan, L.; Wang, Z.; Wang, B. Highly Water-Resistant Paper via Infiltration with Polymeric Microspheres from Nanocellulose-Stabilized Plant Oil-Derived Monomer. *Int J Biol Macromol* **2024**, 267. <https://doi.org/10.1016/j.ijbiomac.2024.131539>.
- (47) Arshad, M.; Shankar, S.; Mohanty, A. K.; Todd, J.; Riddle, R.; Van Acker, R.; Taylor, G. W.; Misra, M. Improving the Barrier and Mechanical Properties of Paper Used for Packing Applications with Renewable Hydrophobic Coatings Derived from Camelina Oil. *ACS Omega* **2024**, 9 (18), 19786–19795. <https://doi.org/10.1021/acsomega.3c07213>.
- (48) Jing, X.; Li, X.; Jiang, Y.; Zhao, R.; Ding, Q.; Han, W. Excellent Coating of Collagen Fiber/Chitosan-Based Materials That Is Water- and Oil-Resistant and Fluorine-Free. *Carbohydr Polym* **2021**, 266. <https://doi.org/10.1016/j.carbpol.2021.118173>.
- (49) Li, Z.; Rabnawaz, M.; Sarwar, M. G.; Khan, B.; Krishna Nair, A.; Sirinakbumrung, N.; Kamdem, D. P. A Closed-Loop and Sustainable Approach for the Fabrication of Plastic-Free Oil- And Water-Resistant Paper Products. *Green Chemistry* **2019**, 21 (20), 5691–5700. <https://doi.org/10.1039/c9gc01865d>.

- (50) Kansal, D.; Hamdani, S. S.; Ping, R.; Rabnawaz, M. Starch and Zein Biopolymers as a Sustainable Replacement for PFAS, Silicone Oil, and Plastic-Coated Paper. *Ind Eng Chem Res* **2020**, *59* (26), 12075–12084. <https://doi.org/10.1021/acs.iecr.0c01291>.
- (51) Guzman-Puyol, S.; Tedeschi, G.; Goldoni, L.; Benítez, J. J.; Ceseracciu, L.; Koschella, A.; Heinze, T.; Athanassiou, A.; Heredia-Guerrero, J. A. Greaseproof, Hydrophobic, and Biodegradable Food Packaging Bioplastics from C6-Fluorinated Cellulose Esters. *Food Hydrocoll* **2022**, *128*. <https://doi.org/10.1016/j.foodhyd.2022.107562>.
- (52) Li, Z.; Rabnawaz, M. Fabrication of Food-Safe Water-Resistant Paper Coatings Using a Melamine Primer and Polysiloxane Outer Layer. *ACS Omega* **2018**, *3* (9), 11909–11916. <https://doi.org/10.1021/acsomega.8b01423>.
- (53) Kansal, D.; Hamdani, S. S.; Ping, R.; Sirinakbumrung, N.; Rabnawaz, M. Food-Safe Chitosan-Zein Dual-Layer Coating for Water-and Oil-Repellent Paper Substrates. *ACS Sustain. Chem. Eng.* **2020**, *8* (17), 6887.
- (54) Wang, K.; Zhao, L.; He, B. Chitosan/Montmorillonite Coatings for the Fabrication of Food-Safe Greaseproof Paper. *Polymers (Basel)* **2021**, *13* (10). <https://doi.org/10.3390/polym13101607>.
- (55) Vaswani, S.; Koskinen, J.; Hess, D. W. Surface Modification of Paper and Cellulose by Plasma-Assisted Deposition of Fluorocarbon Films. *Surf Coat Technol* **2005**, *195* (2–3), 121–129. <https://doi.org/10.1016/j.surfcoat.2004.10.013>.
- (56) Trier, X.; Granby, K.; Christensen, J. H. Polyfluorinated Surfactants (PFS) in Paper and Board Coatings for Food Packaging. *Environmental Science and Pollution Research* **2011**, *18* (7), 1108–1120. <https://doi.org/10.1007/s11356-010-0439-3>.
- (57) Glüge, J.; Scheringer, M.; Cousins, I. T.; Dewitt, J. C.; Goldenman, G.; Herzke, D.; Lohmann, R.; Ng, C. A.; Trier, X.; Wang, Z. An Overview of the Uses of Per- And Polyfluoroalkyl Substances (PFAS). *Environ Sci Process Impacts* **2020**, *22* (12), 2345–2373. <https://doi.org/10.1039/d0em00291g>.
- (58) Kjellgren, H.; Gällstedt, M.; Engström, G.; Järnström, L. Barrier and Surface Properties of Chitosan-Coated Greaseproof Paper. *Carbohydr Polym* **2006**, *65* (4), 453–460. <https://doi.org/10.1016/j.carbpol.2006.02.005>.
- (59) Rhim, J. W.; Lee, J. H.; Hong, S. I. Water Resistance and Mechanical Properties of Biopolymer (Alginate and Soy Protein) Coated Paperboards. *LWT* **2006**, *39* (7), 806–813. <https://doi.org/10.1016/j.lwt.2005.05.008>.
- (60) Matsui, K. N.; Larotonda, F. D. S.; Paes, S. S.; Luiz, D. B.; Pires, A. T. N.; Laurindo, J. B.



- Cassava Bagasse-Kraft Paper Composites: Analysis of Influence of Impregnation with Starch Acetate on Tensile Strength and Water Absorption Properties. *Carbohydr Polym* **2004**, 55 (3), 237–243. <https://doi.org/10.1016/j.carbpol.2003.07.007>.
- (61) Li, Z.; Rabnawaz, M. Oil- And Water-Resistant Coatings for Porous Cellulosic Substrates. *ACS Appl Polym Mater* **2019**, 1 (1), 103–111. <https://doi.org/10.1021/acsapm.8b00106>.
  - (62) Nair, A.; Kansal, D.; Khan, A.; Rabnawaz, M. Oil-and Water-Resistant Paper Substrate Using Blends of Chitosan-Graft-Polydimethylsiloxane and Poly (Vinyl Alcohol). *J. Appl. Polym. Sci.* **2021**, 138 (21), 50494.
  - (63) Nair, A.; Kansal, D.; Khan, A.; Rabnawaz, M. New Alternatives to Single-Use Plastics: Starch and Chitosan-Graft-Polydimethylsiloxane-Coated Paper for Water-and Oil-Resistant Applications. *Nano Sel.* **2022**, 3 (2), 459.
  - (64) Hamdani, S. S.; Li, Z.; Sirinakbumrung, N.; Rabnawaz, M. Zein and PVOH-Based Bilayer Approach for Plastic-Free, Repulpable and Biodegradable Oil-and Water-Resistant Paper as a Replacement for Single-Use Plastics. *Ind. Eng. Chem. Res.* **2020**, 59 (40), 17856.
  - (65) Alam, M.; Akram, D.; Sharmin, E.; Zafar, F.; Ahmad, S. Vegetable Oil Based Eco-Friendly Coating Materials: A Review Article. *Arabian Journal of Chemistry*. Elsevier **2014**, pp 469–479. <https://doi.org/10.1016/j.arabjc.2013.12.023>.
  - (66) Khan, A.; Huang, K.; Sarwar, M. G.; Cheng, K.; Li, Z.; Tuhin, M. O.; Rabnawaz, M. Self-Healing and Self-Cleaning Clear Coating. *J Colloid Interface Sci* **2020**, 577, 311–318. <https://doi.org/10.1016/j.jcis.2020.05.073>.
  - (67) Geyer, R.; Jambeck, J. R.; Law, K. L. Production, Use, and Fate of All Plastics Ever Made. *Sci. Adv.* **2017**, 3 (7), e1700782.
  - (68) Garcia, J. M.; Robertson, M. L. The Future of Plastics Recycling. *Science (1979)* **2017**, 358 (6365), 870–872. <https://doi.org/10.1126/science.aag0324>.
  - (69) Kumar, V.; Khan, A.; Rabnawaz, M. Efficient Depolymerization of Polystyrene with Table Salt and Oxidized Copper. *ACS Sustain Chem Eng* **2022**, 10 (19), 6493–6502. <https://doi.org/10.1021/acssuschemeng.1c08400>.
  - (70) Shaker, M.; Kumar, V.; Saffron, C. M.; Rabnawaz, M. Revolutionizing Plastics Chemical Recycling with Table Salt. *Adv Sustain Syst* **2024**, 8 (1), 2300306. <https://doi.org/10.1002/adsu.202300306>.
  - (71) Kunam, P. K.; Ramakanth, D.; Akhila, K.; Gaikwad, K. K. Bio-Based Materials for

Barrier Coatings on Paper Packaging. *Biomass Convers. Biorefinery* **2022**.

- (72) Khan, A.; Naveed, M.; Rabnawaz, M. Melt-Reprocessing of Mixed Polyurethane Thermosets. *Green Chem.* **2021**, *23*, 4771.
- (73) Chamas, A.; Moon, H.; Zheng, J.; Qiu, Y.; Tabassum, T.; Jang, J. H.; Abu-Omar, M.; Scott, S. L.; Suh, S. Degradation Rates of Plastics in the Environment. *ACS Sustain. Chem. Eng.* **2020**, *8* (9), 3494.
- (74) Khan, A.; Naveed, M.; Aayanifard, Z.; Rabnawaz, M. Efficient Chemical Recycling of Waste Polyethylene Terephthalate. *Resour Conserv Recycl* **2022**, *187*, 106639. <https://doi.org/https://doi.org/10.1016/j.resconrec.2022.106639>.
- (75) dos Santos, J. W. S.; Garcia, V. A. d. S.; Venturini, A. C.; Carvalho, R. A. d.; da Silva, C. F.; Yoshida, C. M. P. Sustainable Coating Paperboard Packaging Material Based on Chitosan, Palmitic Acid, and Activated Carbon: Water Vapor and Fat Barrier Performance. *Foods* **2022**, *11* (24), 4037.
- (76) Mahalik, N. P.; Nambiar, A. N. Trends in Food Packaging and Manufacturing Systems and Technology. *Trends Food Sci Technol* **2010**, *21* (3), 117–128. <https://doi.org/https://doi.org/10.1016/j.tifs.2009.12.006>.
- (77) Zhang, Y.; Duan, C.; Bokka, S. K.; He, Z.; Ni, Y. Molded Fiber and Pulp Products as Green and Sustainable Alternatives to Plastics: A Mini Review. *J. Bioresour. Bioprod.* **2022**, *7* (1), 14.
- (78) Yook, S.; Park, H.; Park, H.; Lee, S. Y.; Kwon, J.; Youn, H. J. Barrier Coatings with Various Types of Cellulose Nanofibrils and Their Barrier Properties. *Cellulose* **2020**, *27* (8), 4509–4523. <https://doi.org/10.1007/s10570-020-03061-5>.
- (79) Tyagi, P.; Salem, K. S.; Hubbe, M. A.; Pal, L. Advances in Barrier Coatings and Film Technologies for Achieving Sustainable Packaging of Food Products-a Review. *Trends Food Sci. Technol.* **2021**, *115*, 461.
- (80) Herrmann, C.; Rhein, S.; Sträter, K. F. Consumers' Sustainability-Related Perception of and Willingness-to-Pay for Food Packaging Alternatives. *Resour. Conserv. Recycl.* **2022**, *181*, 106219.
- (81) Kwak, H.; Kim, H.; Park, S. A.; Lee, M.; Jang, M.; Park, S. B.; Hwang, S. Y.; Kim, H. J.; Jeon, H.; Koo, J. M.; Park, J.; Oh, D. X. Biodegradable, Water-Resistant, Anti-Fizzing, Polyester Nanocellulose Composite Paper Straws. *Advanced Science* **2023**, *10* (1). <https://doi.org/10.1002/advs.202205554>.

- (82) Lim, X. Microplastics Are Everywhere—but Are They Harmful. *Nature* **2021**, 593 (7857), 22.
- (83) Hamdani, S. S.; Emch, H.; Isherwood, J.; Khan, A.; Kumar, V.; Alford, A.; Wyman, I.; Sharma, R.; Mayekar, P.; Bher, A. Waterborne Poly (Butylene Succinate)-Coated Paper for Sustainable Packaging Applications. *ACS Appl. Polym. Mater.* **2023**, 5 (10), 7705.
- (84) Rendon, R.; Ortiz, A.; Tovar-Sánchez, E.; Flores Huicochea, E. The Role of Biopolymers in Obtaining Environmentally Friendly Materials. In *Composites from Renewable and Sustainable Materials*; Poletto, M., Ed.; IntechOpen: Rijeka, **2016**. <https://doi.org/10.5772/65265>.
- (85) Samyn, P. Active Coating for Packaging Papers with Controlled Thermal Release of Encapsulated Plant Oils. *Surfaces and Interfaces* **2022**, 32, 102106.
- (86) Wang, X.; Zhang, Y.; Liang, H.; Zhou, X.; Fang, C.; Zhang, C.; Luo, Y. Synthesis and Properties of Castor Oil-Based Waterborne Polyurethane/Sodium Alginate Composites with Tunable Properties. *Carbohydr. Polym.* **2019**, 208, 391.
- (87) Biermann, U.; Bornscheuer, U.; Meier, M. A. R.; Metzger, J. O.; Schäfer, H. J. Oils and Fats as Renewable Raw Materials in Chemistry. *Angewandte Chemie International Edition* **2011**, 50 (17), 3854–3871. <https://doi.org/https://doi.org/10.1002/anie.201002767>.
- (88) Wang, Q.; Chen, G.; Cui, Y.; Tian, J.; He, M.; Yang, J. W. Castor Oil Based Biothiol as a Highly Stable and Self-Initiated Oligomer for Photoinitiator-Free UV Coatings. *ACS Sustain Chem Eng* **2017**, 5 (1), 376–381. <https://doi.org/10.1021/acssuschemeng.6b01756>.
- (89) Bher, A.; Cho, Y.; Auras, R. Boosting Degradation of Biodegradable Polymers. *Macromol. Rapid Commun.* **2023**, 44 (5), 2200769.
- (90) Kijchavengkul, T.; Auras, R.; Rubino, M.; Ngouajio, M.; Fernandez, R. T. Development of an Automatic Laboratory-Scale Respirometric System to Measure Polymer Biodegradability. *Polym. Test.* **2006**, 25 (8), 1006.
- (91) Wu, F.; Misra, M.; Mohanty, A. K. Challenges and New Opportunities on Barrier Performance of Biodegradable Polymers for Sustainable Packaging. *Progress in Polymer Science*. Elsevier Ltd June 1, **2021**. <https://doi.org/10.1016/j.progpolymsci.2021.101395>.
- (92) Trinh, B. M.; Chang, B. P.; Mekonnen, T. H. The Barrier Properties of Sustainable Multiphase and Multicomponent Packaging Materials: A Review. *Progress in Materials Science*. Elsevier Ltd March 1, **2023**. <https://doi.org/10.1016/j.pmatsci.2023.101071>.
- (93) Rachtanapun, P.; Boonyawan, D.; Auras, R. A.; Kasi, G. Effect of Water-Resistant

Properties of Kraft Paper (KP) Using Sulfur Hexafluoride (SF<sub>6</sub>) Plasma Coating. *Polymers (Basel)* **2022**, *14* (18). <https://doi.org/10.3390/polym14183796>.

- (94) El Bourakadi, K.; Hassani, F.-Z. S. A.; Qaiss, A. E. K.; Bouhfid, R. Antimicrobial Coated Food Packaging Paper from Agricultural Biomass. In *Biopolymers and Biocomposites from Agro-Waste for Packaging Applications*; Elsevier, **2021**; pp 35–63. <https://doi.org/10.1016/b978-0-12-819953-4.00013-6>.
- (95) Lai, T. T.; Pham, T. T. H.; van Lingen, M.; Desaulniers, G.; Njamen, G.; Tolnai, B.; Jabrane, T.; Moineau, S.; Barnabé, S. Development of Antimicrobial Paper Coatings Containing Bacteriophages and Silver Nanoparticles for Control of Foodborne Pathogens. *Viruses* **2022**, *14* (11). <https://doi.org/10.3390/v14112478>.
- (96) Papadochristopoulos, A.; Kerry, J. P.; Fegan, N.; Burgess, C. M.; Duffy, G. Natural Antimicrobials for Enhanced Microbial Safety and Shelf-life of Processed Packaged Meat. *Foods* **2021**, *10* (7). <https://doi.org/10.3390/foods10071598>.
- (97) Khan, M. H.; Yadav, H. Sanitization During and After COVID-19 Pandemic: A Short Review. *Transactions of the Indian National Academy of Engineering* **2020**, *5* (4), 617–627. <https://doi.org/10.1007/s41403-020-00177-9>.
- (98) Das, K. P.; Sharma, D.; Saha, S.; Satapathy, B. K. From Outbreak of COVID-19 to Launching of Vaccination Drive: Invigorating Single-Use Plastics, Mitigation Strategies, and Way Forward. <https://doi.org/10.1007/s11356-021-16025-4>/Published.
- (99) Kramer, A.; Assadian, O. Survival of Microorganisms on Inanimate Surfaces. In *Use of Biocidal Surfaces for Reduction of Healthcare Acquired Infections*; Springer International Publishing, **2014**; Vol. 9783319080574, pp 7–26. [https://doi.org/10.1007/978-3-319-08057-4\\_2](https://doi.org/10.1007/978-3-319-08057-4_2).
- (100) Kramer, A.; Schwebke, I.; Kampf, G. How Long Do Nosocomial Pathogens Persist on Inanimate Surfaces? A Systematic Review. *BMC Infectious Diseases*. August 16, **2006**. <https://doi.org/10.1186/1471-2334-6-130>.
- (101) Nechita, P.; Iana-Roman, M. R. Review on Polysaccharides Used in Coatings for Food Packaging Papers. *Coatings*. MDPI AG June 1, **2020**. <https://doi.org/10.3390/COATINGS10060566>.
- (102) Abinaya, S.; Kavitha, H. P. Magnesium Oxide Nanoparticles: Effective Antilarvicidal and Antibacterial Agents. *ACS Omega* **2023**, *8* (6), 5225–5233. <https://doi.org/10.1021/acsomega.2c01450>.
- (103) Chokboribal, J.; Amornkitbamrung, L.; Somchit, W.; Suchaiya, V.; Khamweera, P.;

- Pankaew, P. Effects of ZnO/Trimethylsilyl Cellulose Nano-Composite Coating on Anti-UV and Anti-Fungal Properties of Papers. *Sci Rep* **2023**, *13* (1). <https://doi.org/10.1038/s41598-023-45853-2>.
- (104) Pan, X.; Wang, Y.; Chen, Z.; Pan, D.; Cheng, Y.; Liu, Z.; Lin, Z.; Guan, X. Investigation of Antibacterial Activity and Related Mechanism of a Series of Nano-Mg(OH)<sub>2</sub>. *ACS Appl Mater Interfaces* **2013**, *5* (3), 1137–1142. <https://doi.org/10.1021/am302910q>.
- (105) Halbus, A. F.; Horozov, T. S.; Paunov, V. N. Controlling the Antimicrobial Action of Surface Modified Magnesium Hydroxide Nanoparticles. *Biomimetics* **2019**, *4* (2). <https://doi.org/10.3390/biomimetics4020041>.
- (106) Zhu, Y.; Tang, Y.; Ruan, Z.; Dai, Y.; Li, Z.; Lin, Z.; Zhao, S.; Cheng, L.; Sun, B.; Zeng, M.; Zhu, J.; Zhao, R.; Lu, B.; Long, H. Mg(OH)<sub>2</sub> Nanoparticles Enhance the Antibacterial Activities of Macrophages by Activating the Reactive Oxygen Species. *J Biomed Mater Res A* **2021**, *109* (11), 2369–2380. <https://doi.org/https://doi.org/10.1002/jbm.a.37219>.
- (107) Nguyen, N. Y. T.; Grelling, N.; Wetteland, C. L.; Rosario, R.; Liu, H. Antimicrobial Activities and Mechanisms of Magnesium Oxide Nanoparticles (NMgO) against Pathogenic Bacteria, Yeasts, and Biofilms. *Sci Rep* **2018**, *8* (1). <https://doi.org/10.1038/s41598-018-34567-5>.
- (108) Wang, Y.; Liu, Y.; Li, X.; Wang, F.; Huang, Y.; Liu, Y.; Zhu, Y. Investigation of the Biosafety of Antibacterial Mg(OH)<sub>2</sub> Nanoparticles to a Normal Biological System. *J Funct Biomater* **2023**, *14* (4). <https://doi.org/10.3390/jfb14040229>.
- (109) Meng, Y.; Zhang, D.; Jia, X.; Xiao, K.; Lin, X.; Yang, Y.; Xu, D.; Wang, Q. Antimicrobial Activity of Nano-Magnesium Hydroxide against Oral Bacteria and Application in Root Canal Sealer. *Medical Science Monitor* **2020**, *26*. <https://doi.org/10.12659/MSM.922920>.
- (110) He, Y.; Ingudam, S.; Reed, S.; Gehring, A.; Strobaugh, T. P.; Irwin, P. Study on the Mechanism of Antibacterial Action of Magnesium Oxide Nanoparticles against Foodborne Pathogens. *J Nanobiotechnology* **2016**, *14* (1). <https://doi.org/10.1186/s12951-016-0202-0>.
- (111) Andrady, A. L.; Neal, M. A. Applications and Societal Benefits of Plastics. *Philosophical Transactions of the Royal Society B: Biological Sciences* **2009**, *364* (1526), 1977–1984. <https://doi.org/10.1098/rstb.2008.0304>.
- (112) Thompson, R. C.; Moore, C. J.; vom Saal, F. S.; Swan, S. H. Plastics, the Environment and Human Health: Current Consensus and Future Trends. *Philosophical Transactions of the Royal Society B: Biological Sciences* **2009**, *364* (1526), 2153–2166. <https://doi.org/10.1098/rstb.2009.0053>.

- (113) Rhodes, Christopher J. Solving the Plastic Problem: From Cradle to Grave, to Reincarnation. *Sci Prog* **2019**, *102* (3), 218–248.  
<https://doi.org/10.1177/0036850419867204>.
- (114) Wojnowska-Baryła, I.; Bernat, K.; Zaborowska, M. Plastic Waste Degradation in Landfill Conditions: The Problem with Microplastics, and Their Direct and Indirect Environmental Effects. *Int J Environ Res Public Health* **2022**, *19* (20).  
<https://doi.org/10.3390/ijerph192013223>.
- (115) Manikanda Bharath, K.; Muthulakshmi, A. L.; Natesan, U. Microplastic Contamination around the Landfills: Distribution, Characterization and Threats: A Review. *Curr Opin Environ Sci Health* **2023**, *31*, 100422.  
<https://doi.org/https://doi.org/10.1016/j.coesh.2022.100422>.
- (116) Sangkham, S. Global Perspective on the Impact of Plastic Waste as a Source of Microplastics and Per- and Polyfluoroalkyl Substances in the Environment. *ACS ES and T Water*. American Chemical Society January 12, **2024**, pp 1–4.  
<https://doi.org/10.1021/acsestwater.3c00607>.
- (117) Williams, A. T.; Rangel-Buitrago, N. The Past, Present, and Future of Plastic Pollution. *Mar Pollut Bull* **2022**, *176*, 113429.  
<https://doi.org/https://doi.org/10.1016/j.marpolbul.2022.113429>.
- (118) Khan, A.; Hamdani, S. S.; Duncan, E.; Rabnawaz, M. High-Performance Synthetic Waxes for a Sustainable Packaging Ecosystem. *ACS Sustain Chem Eng* **2024**, *12* (32), 12188–12199. <https://doi.org/10.1021/acssuschemeng.4c04229>.
- (119) Ghosh, K.; Jones, B. H. Roadmap to Biodegradable Plastics-Current State and Research Needs. *ACS Sustainable Chemistry and Engineering*. American Chemical Society May 10, **2021**, pp 6170–6187. <https://doi.org/10.1021/acssuschemeng.1c00801>.
- (120) Yadav, S.; Khan, A.; Hamdani, S. S.; Rabnawaz, M. Degradable Polymeric Waxes for Paper Coating Applications. *ACS Appl Polym Mater* **2024**, *6* (6), 3263–3272.  
<https://doi.org/10.1021/acsapm.3c03072>.
- (121) Shaker, M.; Muzata, T. S.; Hamdani, S. S.; Wyman, I.; Saffron, C. M.; Rabnawaz, M. Chemical Upcycling of High-Density Polyethylene into Upcycled Waxes as Rheology Modifiers and Paper Coating Materials. *J Clean Prod* **2024**, *467*, 142943.  
<https://doi.org/https://doi.org/10.1016/j.jclepro.2024.142943>.
- (122) Shaker, M.; Hamdani, S. S.; Muzata, T. S.; Rabnawaz, M. Driving Selective Upcycling of Mixed Polyethylene Waste with Table Salt. *Sci Rep* **2024**, *14* (1).  
<https://doi.org/10.1038/s41598-024-63482-1>.

- (123) Shankar, A.; A.K., A. M.; Narayan, R.; Chakrabarty, A. Emulsion Polymerized Styrene Acrylic/Nanocellulose Composite Coating to Improve the Strength and Hydrophobicity of Kraft Paper. *Prog Org Coat* **2023**, *182*, 107634. <https://doi.org/https://doi.org/10.1016/j.porgcoat.2023.107634>.
- (124) Naitzel, T. de C.; Garcia, V. A. dos S.; Lourenço, C. A. M.; Vanin, F. M.; Yoshida, C. M. P.; Carvalho, R. A. de. Properties of Paperboard Coated with Natural Polymers and Polymer Blends: Effect of the Number of Coating Layers. *Foods* **2023**, *12* (14). <https://doi.org/10.3390/foods12142745>.
- (125) Khan, A.; Kumar, V.; Anulare, J.; Dam, M.; Wyman, I.; Mayekar, P.; Rabnawaz, M. Sustainable Packaging with Waterborne Acrylated Epoxidized Soybean Oil. *ACS Sustainable Resource Management* **2024**, *1* (5), 879–889. <https://doi.org/10.1021/acssusresmg.3c00093>.
- (126) Yu, R.; Yuan, X. Rising of Boron Nitride: A Review on Boron Nitride Nanosheets Enhanced Anti-Corrosion Coatings. *Progress in Organic Coatings*. Elsevier B.V. January 1, **2024**. <https://doi.org/10.1016/j.porgcoat.2023.107990>.
- (127) Kim, H. M.; Kim, H. R.; Kim, B. S. Soybean Oil-Based Photo-Crosslinked Polymer Networks. *J Polym Environ* **2010**, *18* (3), 291–297. <https://doi.org/10.1007/s10924-010-0174-3>.
- (128) Gonzalez Ortiz, D.; Pochat-Bohatier, C.; Cambedouzou, J.; Balme, S.; Bechelany, M.; Miele, P. Inverse Pickering Emulsion Stabilized by Exfoliated Hexagonal-Boron Nitride (h-BN). *Langmuir* **2017**, *33* (46), 13394–13400. <https://doi.org/10.1021/acs.langmuir.7b03324>.
- (129) Su, Y.; Zhang, S.; Zhou, X.; Yang, Z.; Yuan, T. A Novel Multi-Functional Bio-Based Reactive Diluent Derived from Cardanol for High Bio-Content UV-Curable Coatings Application. *Prog Org Coat* **2020**, *148*. <https://doi.org/10.1016/j.porgcoat.2020.105880>.
- (130) Wu, Q.; Hu, Y.; Tang, J.; Zhang, J.; Wang, C.; Shang, Q.; Feng, G.; Liu, C.; Zhou, Y.; Lei, W. High-Performance Soybean-Oil-Based Epoxy Acrylate Resins: “Green” Synthesis and Application in UV-Curable Coatings. *ACS Sustain Chem Eng* **2018**, *6* (7), 8340–8349. <https://doi.org/10.1021/acssuschemeng.8b00388>.
- (131) Kim, S. K.; Guymon, C. A. Effects of Polymerizable Organoclays on Oxygen Inhibition of Acrylate and Thiol-Acrylate Photopolymerization. *Polymer (Guildf)* **2012**, *53* (8), 1640–1650. <https://doi.org/10.1016/j.polymer.2012.02.028>.
- (132) Basak, S.; Dangate, M. S.; Samy, S. Oil- and Water-Resistant Paper Coatings: A Review. *Progress in Organic Coatings*. Elsevier B.V. January 1, **2024**. <https://doi.org/10.1016/j.porgcoat.2023.107938>.

- (133) Ragoobur, D.; Huerta-Lwanga, E.; Somaroo, G. D. Reduction of Microplastics in Sewage Sludge by Vermicomposting. *Chemical Engineering Journal* **2022**, 450. <https://doi.org/10.1016/j.cej.2022.138231>.
- (134) Rupani, P. F.; Embrandiri, A.; Garg, V. K.; Abbaspour, M.; Dewil, R.; Appels, L. Vermicomposting of Green Organic Wastes Using *Eisenia Fetida* Under Field Conditions: A Case Study of a Green Campus. *Waste Biomass Valorization* **2023**, 14 (8), 2519–2530. <https://doi.org/10.1007/s12649-022-02004-4>.
- (135) Ding, W.; Li, Z.; Qi, R.; Jones, D. L.; Liu, Q.; Liu, Q.; Yan, C. Effect Thresholds for the Earthworm *Eisenia Fetida*: Toxicity Comparison between Conventional and Biodegradable Microplastics. *Science of the Total Environment* **2021**, 781. <https://doi.org/10.1016/j.scitotenv.2021.146884>.



## **APPENDIX A: SUPPLEMENTARY MATERIALS FOR CHAPTER - SUSTAINABLE PACKAGING WITH WATERBORNE ACRYLATED EPOXIDIZED SOYBEAN OIL**

### **A.1 Experimental**

#### **A.1.1 Materials**

The acrylated epoxidized soybean oil (AESO) used in this investigation contained almost 4,000 ppm of monomethyl ether hydroquinone as the inhibitor was obtained from Sigma Aldrich. 2-Hydroxy-2-methylpropiophenone from Genocure was used as photo initiator. Polyvinyl alcohol (PVOH), having molecular weights of 30000-70000 g/mol with 80-90% hydrolysis, was purchased from Sigma Aldrich. Starch powder was also obtained from Sigma Aldrich. Paper (35-liner kraft) was purchased from Uline.

#### **A.1.2 Methods**

##### **A.1.2.1 Preparation for the Starch Solution**

Starch (10 g) was dispersed in 90 mL of deionized water (DI), and the mixture was stirred for 35 min at 105 °C. Once the solution appeared to be transparent, it could then be used for coating.

##### **A.1.2.2 Preparation of Starch-coated Kraft Paper (KP/S)**

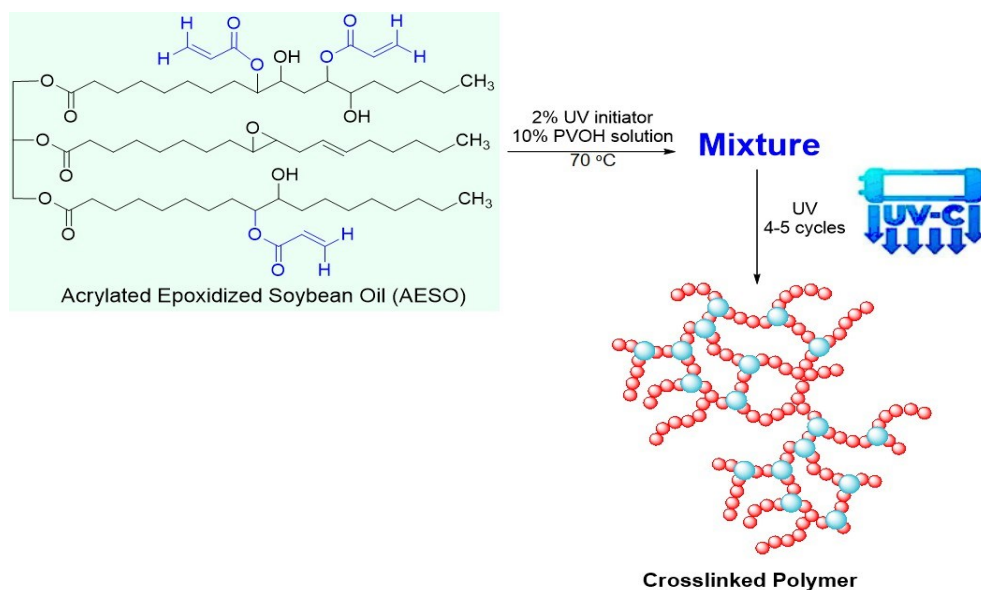
Kraft paper (KP) was cut into dimensions of  $\sim 30 \times 30 \text{ cm}^2$  and subsequently, the freshly prepared starch solution (approximately 12 mL) was applied to this paper. Once the starch solution had been applied to KP, the starch-coated paper (KP/S) was subsequently dried at room temperature for 24 hours for further use.

##### **A.1.2.3 Preparation of the PVOH Solution**

2.0 g of PVOH ( $M_w$ : 30000-70000 g/mol, 80-90% hydrolyzed) in 18 mL of deionized water were mixed and then the mixture was subsequently heated at 80 °C for 45 min once a clear solution was acquired.

#### A.1.2.4 Preparation of the emulsion of AESO/PVOH

Three final solutions have been prepared by the following procedure. 5.0 g of AESO along with 2 wt% (100 mg) of the photoinitiator (2-Hydroxy-2-methylpropiophenone) was mixed in a vial using stirrer, and the mixture was then allowed to stir for 2 min at 70 °C. To the above solution, 10% PVOH solution (0.5, 0.1 and 2.0 mL) was added in a dropwise manner, and the resultant solution was stirred for 2 min to ensure that it was well-mixed. A second batch of hot water (4.5 mL, 4.0 mL and 3.0 mL, respectively) was also added dropwise and stirred for an additional 10 min. The prepared three final solutions of AESO-emulsions (WSO-P0.5, WSO-P1.0, and WSO-P2.0) were next cast onto KP/S, where 0.5 mL, 1.0 mL, and 2.0 mL represent the amount of PVOH solution used for making emulsions.



**Scheme A.S1** Photo crosslinking of AESO-emulsion. Chemical structure of AESO and schematic depiction of the crosslinking procedure.

#### A.1.2.5 UV Curing of the Coated Samples

All the coated samples were dried for 5 min in open air and then passed under a UV Chamber (Heraeus Noblelight from Cambridge, UK) for five cycles (each cycle offers nearly 10 second

UV exposure). The light used for the UV curing of the coated samples had a radiation intensity of approximately 5.0 W/cm<sup>2</sup> and a wavelength of about 385 nm. The cycle time was around 10 seconds on the conveyor belt under the UV tunnel. In our initial study, we observed that after one or two cycles, the coated paper was soft and wet; thus, we allowed a maximum of five cycles for each sample to ensure that almost all acrylic double bonds underwent polymerization.

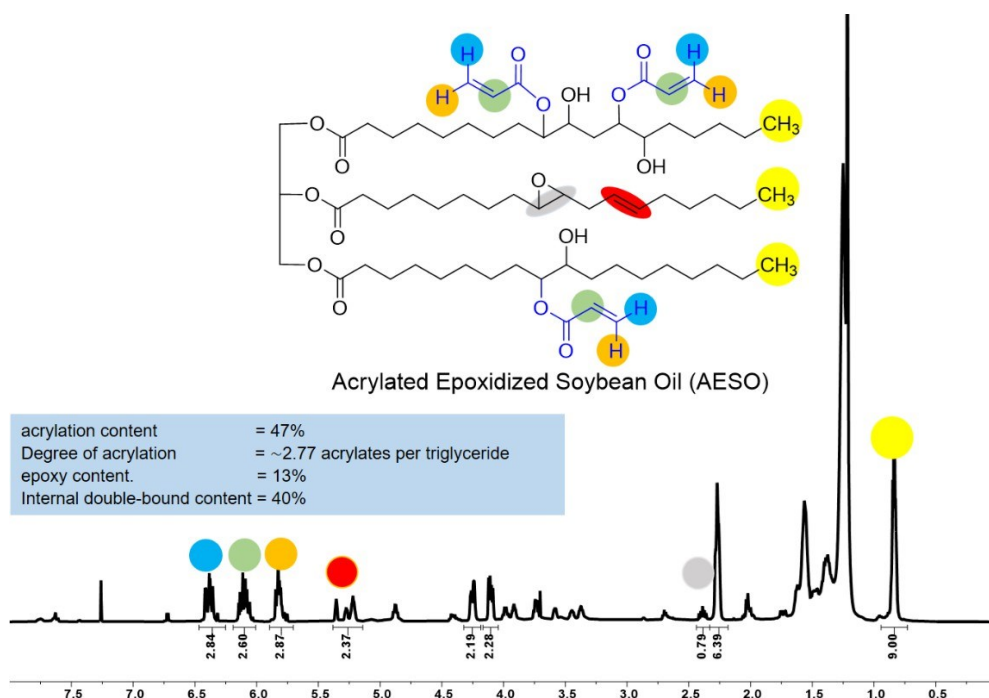


**Figure A.S1** <sup>1</sup>H-Nuclear magnetic resonance (NMR) spectrum (CDCl<sub>3</sub> is used as solvent, frequency- 500 MHz) of AESO denoting the percent content of acrylic bonds, epoxy groups as well as internal double bond.

### A.1.3 Characterization

#### A.1.3.1 Fourier-transform Infrared (FTIR) Analysis

FTIR spectroscopy (model FT/IR-6600 type A FTIR spectrometer) was used to determine the functional group present in AESO and cured AESO at ATR (attenuated total reflectance) mode. A total of 32 scans were recorded having a resolution of 4 cm<sup>-1</sup>. The spectral range was kept

between 500-4000 cm<sup>-1</sup>.

#### **A.1.3.2 Basis Weight and Thickness Measurements**

The basis weight of all our coated samples was calculated via the following formula:

$$\text{Coating Load} = \text{basis weight (coated paper} - \text{uncoated paper)}$$

$$\text{Where basis weight} = \text{weight (g)/area (m}^2\text{)}.$$

Each sample was cut down as a circular disc (diameter of ~13 cm) (see **Figure A.S8**). The thickness was recorded in  $\mu\text{m}$ , using a micrometer (Testing Machine Inc., New Castle, DE) at five different locations on each sample. All the basis weights and thickness measured for these samples are listed in **Table A.S5**.

#### **A.1.3.3 Water-Resistance Tests**

Cobb-600 and Cobb-1800 tests were performed according to TAPPI 441 and ISO 535 protocols to measure the amount of water absorbed by the KP, KP/S, and AESO-emulsion coated papers (KP/S/WSO-P0.5, KP/S/WSO-P1.0, and KP/S/WSO-P2.0). The circular discs prepared of all samples were subsequently exposed to 100 mL of deionized water for 600 s (10 mins) and 1800 s (30 mins) to measure the Cobb-600 and Cobb-1800 values, respectively. The exposed area is equal to ~100cm<sup>2</sup>.

The reported Cobb-600 and Cobb-1800 values in **Figure A.4A** are the amount of water absorbed (in gm) by the paper (per m<sup>2</sup>) during 10 and 30-minute time frames, respectively.

#### **A.1.3.4 Kit Rating or Oil/Grease Resistance**

The oil/grease repellency of the KP, KP/S, and AESO-emulsion coated papers was also measured by following the TAPPI UM 557 criteria. The test involved placing a droplet of different kit solutions on the coated paper surface and observing the degree of penetration over a 15 s period. The penetration was then rated on a scale of 1 to 12, with higher values indicating greater resistance

to oil or grease. The appearance of any dark color indicated that the sample had failed if these different kit solutions were applied; no visible spots meant the sample had passed the test.

#### **A.1.3.5 Tensile Measurements**

The tensile properties of all the samples were measured using a universal testing machine (Instron Series 556, MA, USA) according to the TAPPI standard T494 procedure. All measurements were performed in the machine direction (MD) and cross-machine direction (CD) of the coated papers (KP/S/WSO-P0.5, KP/S/WSO-P1.0, and KP/S/WSO-P2.0). The samples were prepared according to the ASTM D-882-10 standard. The test was performed by clamping the ends of the sample into the machine (gap separation = 7.1 in) and applying a load until the sample breaks. The paper dimensions (10.23"x1") were used consistently for all samples. The stretching rate was kept at 12.75 mm/min. The load and elongation were recorded, and subsequently, the tensile strength, elongation at break, and Young's modulus were calculated from these data. The results of the tensile tests can provide information about the strength and flexibility of the coated paper samples, which is important for packaging applications where the paper must withstand stress and strain during handling and transportation.

#### **A.1.3.6 Ring Crush Test (RCT)**

The ring crush test (RCT) is used to determine the ring crush resistance of paper. The tests were performed according to the standard method TAPPI - T882 protocol by using a TMI crush tester (Model1210, Instron, MA, USA). For all measurements, the sample dimension was kept at 0.5" x 6".

#### **A.1.3.7 Bending Stiffness (BS)**

The bending stiffness of the coated paper was determined with a Taber stiffness tester (model 150-D, Teledyne Taber, NY, USA). The TAPPI standard T489 procedure was followed for

measurement. The samples were cut in dimensions of 1.5” x 2.75” and subsequently bent at 15° with a total force of 1000 Taber stiffness units using the Taber stiffness tester. The raw data collected was further converted by the following equation:

$$\text{Bending Moment} = (\text{Average of right and left reading}) \times P$$

where  $P = 10$  when the weight is marked as 1000 Taber stiffness units.

#### **A.1.3.8 Internal Tearing Resistance (ITR)**

ITR is an important property of paper samples as it determines their ability to resist tearing when subjected to stress or tension. All our measurements for the coated papers were performed via the TAPPI standard T414 protocol by using an instrument (ME-1600 Manual Elmendorf-type tearing tester). Two piles were kept together for the measurement.

To measure ITR, samples were prepared with a rectangular shape from coated paper and a cut was made at the center of each specimen. The specimens/samples were then clamped in the tensile tester, and a load was applied on the samples to tear it apart from the center cut. The force required to tear the specimens were recorded as the ITR. The recorded value was calculated via the equation given below:

$$\text{Average tearing force, grams} = (16 \times \text{scale reading}) / \text{number of plies}$$

#### **A.1.3.9 Thermogravimetric Analysis (TGA)**

To study the thermal stability and decomposition of our coated materials, TGA measurements were carried out for the coated materials by using a thermographic analyzer (TA Instruments, Q50). A total of 10-15 mg of the sample was heated at a ramping rate of 10°C per min and the data was collected in the range of 0 to 600 °C.

#### **A.1.3.10 Dynamic Scanning Calorimetry (DSC)**

The glass transition temperature ( $T_g$ ) and the melting temperature ( $T_m$ ) of the coating materials

were evaluated using DSC analysis (TA Instruments Q100 system). The data was collected from 0 to 300 °C. The DSC thermograms were recorded during the second heating cycle.

#### **A.1.3.11 Scanning Electron Microscopy (SEM) analysis**

SEM is a technique used to obtain high-resolution images of the surface morphology of samples. In this case, SEM images were captured to investigate the surface morphologies of KP, KP/S and AESO-emulsion coated (KP/S-WSO-P2.0) via a SEM microscope (JEOL 6610 SEM system). The samples were prepared by sputter-coating a thin layer of gold (15 nm) onto their surfaces to enhance their conductivity prior to SEM analysis.

#### **A.1.3.12 Nuclear Magnet resonance (NMR) analysis**

NMR analysis of the AESO sample was performed using 500/54 Premium Shielded NMR instrument of Agilent Technologies. The NMR was run in CDCl<sub>3</sub> solvent at frequency 500 MHz.

#### **A.1.3.13 Leica Stellaris Confocal Microscope**

Brightfield-transmitted light images were collected for emulsions on a Nikon Eclipse Ni upright microscope using a 10 x Plan Apo objective (NA 0.3) and a Nikon DS-Fi2 color camera. Emulsion droplet size was analyzed using the Nikon NIS-Elements AR Imaging Software (version 5.42.03).

### **A.1.4 Biodegradability**

#### **A.1.4.1 Conditioning of compost**

The compost was acquired by the Composting Facility from Michigan State University (MSU) for the biodegradability test. Screening (using a 10 mm screen) was performed to remove the larger particles. Subsequently, the compost was pretreated and maintained at ~50% relative humidity (RH) using deionized water and kept at a temperature of 58 °C before use.<sup>1</sup> The compost's carbon analysis and total nutrients analysis were analyzed and presented in **Tables A.S1** and **A.S2**.

#### **A.1.4.2 Preparation of samples and bioreactors**

The bioreactor was filled with 400 g of already conditioned compost followed by addition of 8 g of kraft paper and coated paper for testing. Paper samples were cut down into 1 cm<sup>2</sup> size before placing them in the bioreactors. The background CO<sub>2</sub> evolution signal was detected by using three bioreactors having compost in the absence of samples (blank bioreactors). For the positive control, cellulose was chosen for biodegradation. Three sets of experiments have been performed for all the samples.

#### **A.1.4.3 Biodegradation test**

The aerobic biodegradation has been performed and was evaluated in compost under following conditions ( $58 \pm 2$  °C and  $50 \pm 5\%$  RH) by measuring the amount of evolved CO<sub>2</sub> using a direct measurement respirometer (DMR) equipped with a non-dispersive infrared gas analyzer (NDIR). The setup was in-house built, and these measurements were performed via ASTM and ISO standard protocols.<sup>2-4</sup> The carbon content of the different test materials was determined by elemental analysis (**Table A.S1**) using a PerkinElmer 2400 Series II CHNS/O Elemental Analyzer (Shelton, CT, USA). The test was conducted using ~ 2 mg of each sample weighed in small capsules. A blank, and standard values to establish the k-factors, were measured prior to assessing the samples. Additionally, compost was sent to the Soil and Plant Nutrient Laboratory at Michigan State University (MSU) for the determination of the physicochemical parameters (**Table A.S2**). DI water was regularly poured two times a week and reactors were agitated properly to maintain uniform distribution; these steps were essential to maintain the optimized condition. Air at  $50 \pm 5\%$  RH and CO<sub>2</sub> below 30 ppm were maintained in each reactor throughout the test, and the CO<sub>2</sub> evolved was measured using the near-infrared sensor at regular periods.<sup>1</sup>



**Table A.S1.** Carbon analysis of samples.

<b>Sample</b>	<b>Carbon</b>
Cellulose	$0.426 \pm 0.000$
Kraft paper	$0.427 \pm 0.001$
AESO	$0.452 \pm 0.003$

**Table A.S2.** Total nutrient analysis of compost.

<b>Parameter</b>	<b>Value</b>
Nitrogen %	2.46
Phosphorus %	1.52
Potassium %	3.03
Calcium %	6.09
Magnesium %	3.74
Sodium %	0.60
Sulfur %	0.66
Iron ppm	11390
Zinc ppm	508
Manganese ppm	454
Copper ppm	118
Boron ppm	44
Aluminum ppm	5198
% Moisture	50.8
% OM	44.6
Carbon %	25.9
C:N	10:1
pH	7.8
Total Dry Solids %	49.2
Total Volatile Solids %	44.6

The CO<sub>2</sub> that had evolved from the blank bioreactor was considered as the background signal, and this value was subtracted from the amount of CO<sub>2</sub> produced by each sample bioreactor to calculate the mineralization of each sample where the % mineralization is the total amount of carbon molecules converted to CO<sub>2</sub>, and it is calculated according to the equation below:<sup>5</sup>

The following equation has been used to deduce the % mineralization-

$$\% \text{Mineralization} = \frac{(CO_2)_t - (CO_2)_b}{M_t \times C_t \times \frac{44}{12}} \times 100$$

where  $(CO_2)_t$  represents amount of  $CO_2$  evolved from samples  $(CO_2)_b$  represents  $CO_2$  from blank reactor and  $M_t$  is the total mass of the sample,  $C_t$  denotes the proportion of carbon present in that sample (measured by CHN analysis), and 44 and 12 are the molecular mass of  $CO_2$  and the atomic mass of carbon.

### A.1.5 Optimization of the coating

In our initial study, different concentrations (i.e., different volumes of 10 wt% PVOH solution) were added dropwise followed by 2<sup>nd</sup> batch of water, keeping the total amount of water at 50% to AESO. The obtained emulsions were subsequently cast onto starch-coated Kraft paper (KP/S) before drying at room temperature for 24 h. Once dried, the coated samples subsequently underwent UV curing treatment. The preliminary water resistance data obtained by Cobb values indicated that there was not a significant change when the volume of 10 wt% PVOH used in the formulation was in the range of 0.5 – 2.0 mL (entries 1-4, **Table A.S3**). However, the Cobb values increased when the total concentration of PVOH in the emulsion was increased (entries 5-7, **Table A.S3**). The amount of coating was ~1 mL cast on ~13x13 cm<sup>2</sup> of paper for the optimization purpose. The amount of water in the emulsion is probably an important factor in the coating industry. Thus, our next study was to determine the dispersibility as well as the water resistance of our developed coatings. To adjust these two parameters, 0.5 mL of 10 wt% PVOH solution was added to all AESO mixtures while the amount of water gradually increased from 5.0 to 8.5 mL in the second batch. The results are summarized in **Table A.S4** and a larger amount of water in the emulsion led to poor water resistance (high Cobb-1800 values) or unsuccessful emulsion formation.

**Table A.S3.** PVOH concentration and their effect on water resistivity.

Entry	AESO	Hot solution of 10 wt% PVOH	Second batch of hot water	Cobb-1800 values on AESO-emulsion coated KP/S
1	5 g	0.5 mL	4.5 mL	~ 22
2	5 g	1.0 mL	4.0 mL	~ 27
3	5 g	1.5 mL	3.5 mL	~ 23
4	5 g	2.0 mL	3.0 mL	~ 22
5	5g	2.5 mL	2.5 mL	~ 37
6	5 g	3.0 mL	2.0 mL	~ 41
7	5 g	3.5 mL	1.5 mL	~ 54

**Table A.S4.** The amount of water added to the emulsion.

Entry	AESO	10 wt% PVOH dissolved in hot water	Second batch of hot water	Cobb-1800 values on AESO-emulsion coated KP/S
1	5 g	0.5 mL	5.0 mL	~ 9
2	5 g	0.5 mL	6.0 mL	~ 13
3	5 g	0.5 mL	6.5 mL	~ 33
4	5 g	0.5 mL	7.0 mL	~ 41
5	5g	0.5 mL	7.5 mL	Poor dispersibility
5	5 g	0.5 mL	8.0 mL	Poor dispersibility
6	5 g	0.5 mL	8.5 mL	Poor dispersibility

**A.1.6 Thickness, basis weight, and loading of the coated samples.**

The thickness, basis weight, and loading estimation are obviously the most fundamental properties in the paper industry. The mean thickness of the kraft paper employed in our study was ~175  $\mu\text{m}$ , yet this was increased to ~199  $\mu\text{m}$  after applying the starch coating. The paper gradually increased in thickness as the starch-coated kraft papers were further coated with different volumes of the AESO-emulsion, reaching a maximum average thickness of ~230  $\mu\text{m}$ . Similarly, the highest basis weight was ~152  $\text{g}/\text{m}^2$ , while the maximum loading was ~20  $\text{g}/\text{m}^2$ , which greatly enhances the viability of AESO as a coating material for kraft paper with numerous packaging applications. The basis weight of the paper is a vital parameter to consider when evaluating the performance of the paper for packaging applications. Hence the basis weight of all samples was

evaluated and we then compared them to the basis weight of KP ( $\sim 125 \text{ g/m}^2$ ). The highest basis weight was  $\sim 152 \text{ g/m}^2$ , which was obtained for KP/S/WSO-P2.0. The basis weight analysis allowed us to calculate the amount of AESO-emulsion loaded onto KP/S. We first calculated the total loading (starch + AESO-emulsion) listed in column 3 of **Table A.S5** and then excluded the starch loading (column 4, **Table A.S5**) to determine the AESO-emulsion loading for all coated samples. The loading on coated samples refers to the measurement of the amount of coating material that had been applied onto the paper substrate. This is an important parameter to consider when evaluating the performance of the coated paper, as the amount of coating can impact on the paper's properties and performance. The loading assessment of the coated samples (column 4, **Table A.S5**) indicates that the maximum amount of the AESO-emulsion applied onto the KP in this study was  $\sim 20 \text{ g/m}^2$ . This loading value can be considered reasonable and can provide sufficient coating coverage for most packaging applications. This loading is much lower than that described in our previous report,<sup>6</sup> where the minimum loading of AESO required to reach the desired properties was  $\sim 31 \text{ g/m}^2$  and the maximum loading reached  $\sim 114 \text{ g/m}^2$ . Thus, a steep decline in loading of AESO by  $\sim 50\%$  (w.r.t.  $\sim 31 \text{ g/m}^2$ ) and  $\sim 82\%$  (w.r.t.  $\sim 114 \text{ g/m}^2$ ) has been achieved, which greatly enhances the feasibility of AESO as a coating material for KP with numerous packaging applications. The ring crush test (RCT) measures the ability of the paper to tolerate crushing forces on edges. RCT measurements were performed to further evaluate the mechanical performance of the coated paper in comparison to uncoated paper, as shown in **Figure A.S2**. The RCT values reported in the MD refer to samples that were cut down in the MD direction but crushed perpendicularly in the CD, and vice versa. **Figure A.S2** represents all the RCT values in the MD and CD for different samples.

**Table A.S5.** Sample codes, thickness, basis weight, and loading estimation for the controls (Kraft paper and starch Kraft coated paper) as well as the AESO-emulsion coated samples.

Sample Code	Thickness ( $\mu\text{m}$ )	Basis Weight ( $\text{g/m}^2$ )	Loading ( $\text{g/m}^2$ ) w.r.t Kraft Paper	Loading ( $\text{g/m}^2$ ) w.r.t Kraft Paper/Starch
Kraft Paper (KP)	$175.00 \pm 0.19$	$124.47 \pm 1.56$	----	----
Kraft Paper/Starch (KP/S)	$199.00 \pm 6.08$	$131.31 \pm 2.67$	$6.93 \pm 2.67$	----
KP/S/WSO-P0.5	$230.33 \pm 10.01$	$147.74 \pm 2.71$	$23.36 \pm 2.71$	$16.58 \pm 2.71$
KP/S/WSO-P1.0	$222.00 \pm 10.81$	$151.76 \pm 2.42$	$27.38 \pm 2.42$	$20.60 \pm 2.42$
KP/S/WSO-P2.0	$229.66 \pm 5.50$	$152.01 \pm 2.17$	$27.63 \pm 2.17$	$20.85 \pm 2.17$

The RCT value for the uncoated sample measured in the MD and crushed in the CD is  $24.93 \pm 1.58$  lbs and the corresponding value for KP/S/WSO-P2.0 is  $22.76 \pm 2.00$  lbs. It is noteworthy that the difference between these two average values lies within the deviation range and that over 90% of the RCT performance exhibited by the uncoated paper was retained by the coated samples.

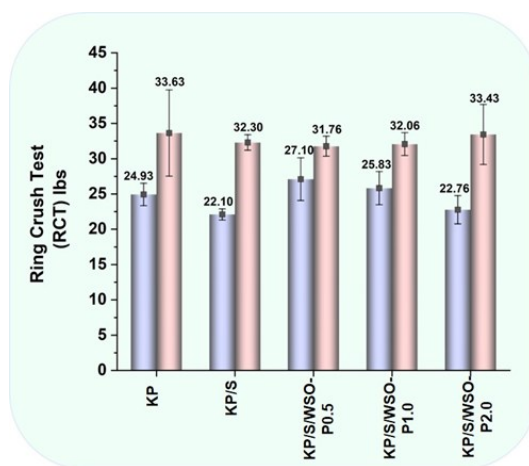


**Figure A.S2.** Ring crush test (RCT) measurements performed for the coated samples and uncoated paper samples in both the machine direction (MD) (light violet color) and the cross direction (CD) (light brown color).

Young's modulus is a measure of a material's stiffness and its resistance to deformation under

stress. It is an important property for materials used in packaging, as it affects how the packaging will perform under stress during transportation and storage. The Young's modulus value recorded for the KP was approximately  $\sim 4613 \pm 177$  MPa in the MD. However, a  $\sim 22\%$  decrease in this value was recorded for the KP/S/WSO-P2.0 sample, which exhibited a Young's modulus of  $\sim 3540$  MPa in the MD (**Figure A.S3**). Typically, the Young's modulus of coated paper used in packaging is within the range from 1000 to 5000 MPa.

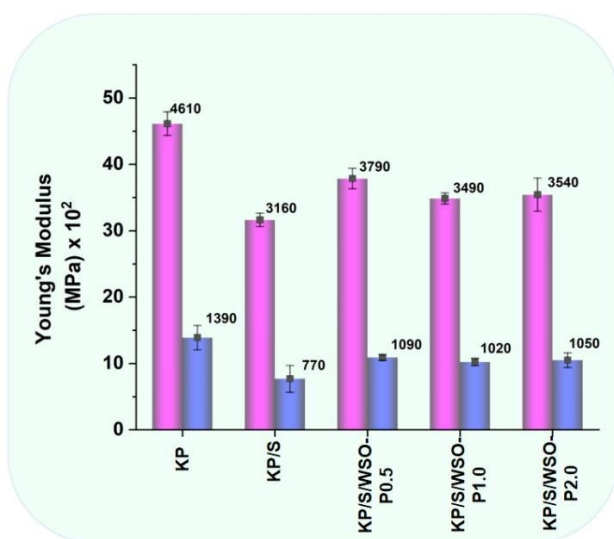


**Figure A.S3.** Young's modulus measurements performed for the coated and uncoated paper samples in both the machine direction (MD) (pink color) and the cross direction (CD) (violet color).

In packaging applications, it is important to balance the material's stiffness (Young's modulus) with its ability to stretch (elongation at break) to provide sufficient protection to the contents of the package during transportation and handling. Typically, the percentage elongation at break for coated paper used in packaging is between 2-5%. Here in this study the % elongation at break for the KP and KP/S were recorded to be  $\sim 2.14 \pm 0.02\%$  and  $3.10 \pm 0.09\%$  respectively. However, for the coated samples these values were approximately 2.55 (MD). Therefore, it can be estimated

that AESO-emulsion increased the % elongation at break by ~20% for the coated samples (**Figure A.S4**). We assumed that the increment in % elongation at break can be attributed to the polymeric nature of cross-linked AESO that was obtained upon UV curing.

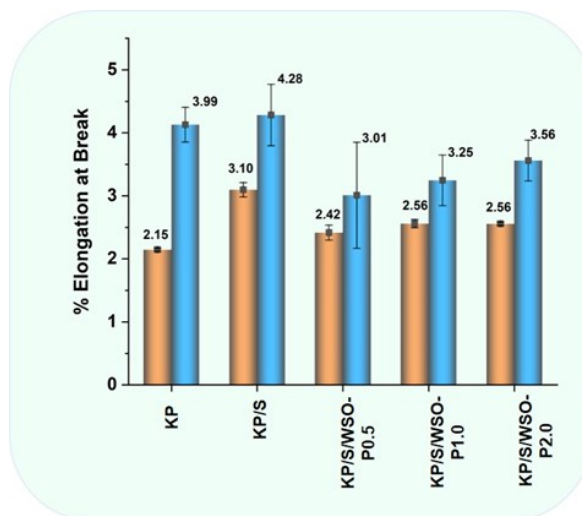


**Figure A.S4.** % Elongation at break for KP, KP/S, KP/S/WSO-P0.5, KP/S/WSO-P1.0, and KP/S/WSO-P2.0 in MD (dark yellow color) and CD (blue color).

Bending stiffness (BS) is another important mechanical property to consider when evaluating the performance of paper for packaging applications. It refers to the resistance of the coated sample to bending or deformation under an applied force. The bending stiffness of paper and paperboard is typically measured using a test method such as the Taber Stiffness test or the Gurley Stiffness test. The BS value for the KP was found to be  $49.50 \pm 1.73$  g·cm, while the corresponding value for KP/S/WSO-P2.0 had shifted slightly to  $48.66 \pm 5.96$  g·cm, thus indicating that most of the bending strength is retained upon coating (**Figure A.S5**). A material with higher bending stiffness will be more resistant to bending and deformation and therefore may provide better protection for the packaged product. However, a higher bending stiffness may also result in less flexible and less conformable material, which may not be suitable for all packaging applications.

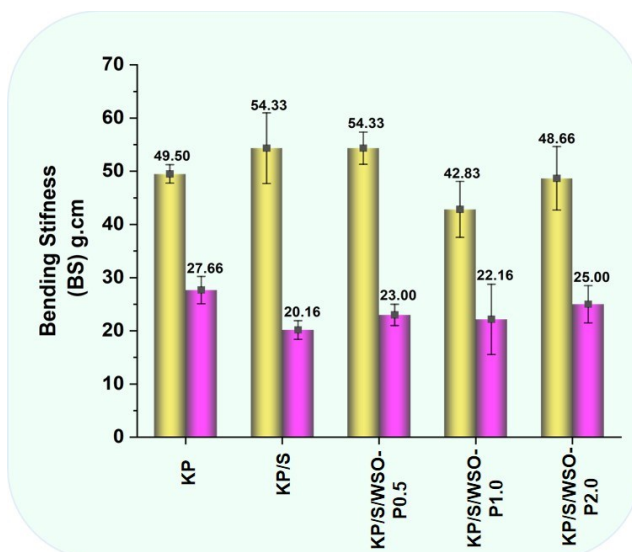


**Figure A.S5.** Bending Stiffness (BS) values obtained in the MD (yellow color) and CD (pink color) for KP, KP/S, KP/S/WSO-P0.5, KP/S/WSO-P1.0, and KP/S/WSO-P2.0.

In summary, it can be stated that the AESO-emulsion coated samples retained ~85% of the mechanical properties exhibited by their uncoated counterparts as observed via BS, RCT, and ITR measurements. Additionally, the high tensile strength retention (>80%) exhibited by the coated sample suggests that the overall performance of the coated paper was enhanced in comparison with the uncoated paper, as the coated paper exhibited significantly better water and grease resistance at only a small cost to the mechanical properties.

Thermogravimetric analysis (TGA) was used to study the thermal stability and decomposition behavior of our coated materials. Through this study we aimed to compare the composition, thermal stability, and degradation products of the UV-cured AESO (without using any solvent or water) and UV-cured waterborne AESO that had been blended with PVOH (WSO- P2.0). The thermograms recorded for UV-cured AESO and AESO-emulsion (WSO-P2.0) in **Figure A.S6** indicate that there was no significant change in decomposition. Nevertheless, the WSO-P2.0 sample showed some initial loss (~2%) in weight after the temperature had reached 120 °C, and



this could be attributed to the presence of moisture. The TGA curves obtained for both samples show that decomposition started around  $\sim 350$  °C and reached a maximum at around  $\sim 450$  °C, with almost complete loss observed at  $\sim 460$ °C. Comparing both curves, it appears that the amount of PVOH added to the AESO did not significantly alter the thermal properties of the material. Besides these, the TGA thermograms also demonstrate that the dispersion of AESO in water followed by UV-curing did not change the thermal properties of WSO-2.0, if it was applied onto a paper substrate. Weight loss graph at around 350 °C ( $T_{\text{onset}}$ ) indicates that AESO-emulsion coated papers can be used for numerous industrial or practical applications without becoming damaged. These results suggest that the WSO-P2.0 sample exhibits good thermal stability and could be a suitable material for use in packaging applications where high temperatures may be encountered.

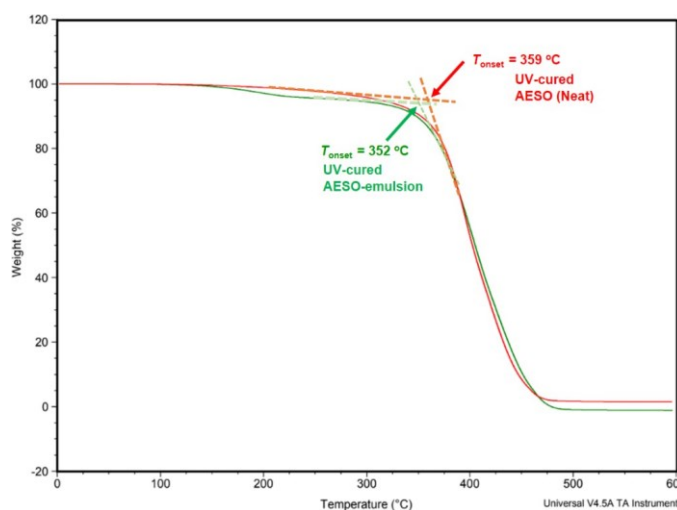


**Figure A.S6.** TGA thermograms of the UV-cured-AESO (without using any solvent or water) and UV-cured waterborne AESO-emulsion (WSO-P2.0).

Differential scanning calorimetry (DSC) analysis was also performed for the UV-cured AESO (without using any solvent or water) and UV-cured waterborne AESO-emulsion (WSO- P2.0) (**Figure A.S7**). The DSC curves recorded for UV-cured AESO and WSO-P2.0 demonstrated that

there was no significant effect in the thermograms for these thermosets. Here the DSC curves also reveal that both samples were fully crosslinked after they had passed through the UV chamber. This provides a very strong indication that almost all AESO monomers were polymerized, thus validating the suitability of our coated material for use in packaging applications.

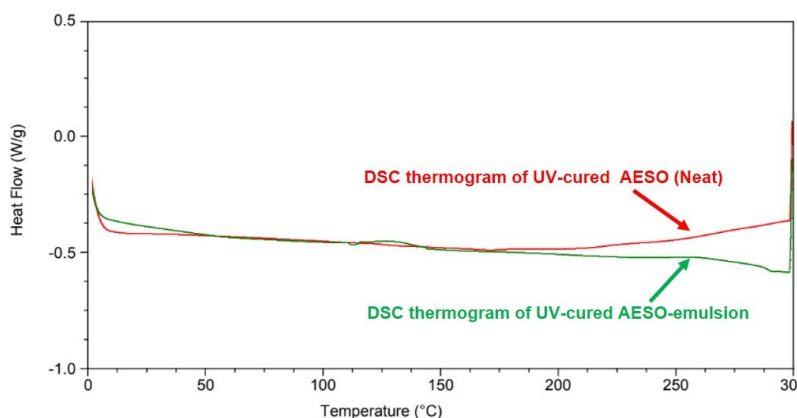


**Figure A.S7.** DSC analysis of the UV-cured AESO (without using any solvent or water) and UV-cured waterborne AESO-emulsion (WSO-P2.0).



**Figure A.S8.** The dimensions of the circular discs (coated papers) were used in this study for the Cobb-600 and Cobb-1800 measurements. Each sample has a diameter = ~13 cm.

SEM analysis examined the surface morphologies of coated and uncoated paper samples. The images revealed that the surfaces of the paper samples became smoother after applying waterborne AESO, indicating that the paper substrate was well-covered, and that its pores had been almost filled by the crosslinked AESO-emulsion. The SEM analysis was consistent with the

formulation of the latex used. Among the different coating formulations investigated, the best coverage was provided by KP/S/WSO-2.0 (**Figure A.S9**). It was expected that the range of these pores would also enhance the water and oil resistance of the paper. SEM images that were recorded at  $1K \times$  magnification is shown in **Figure A.S9** to provide a higher resolution of morphology.

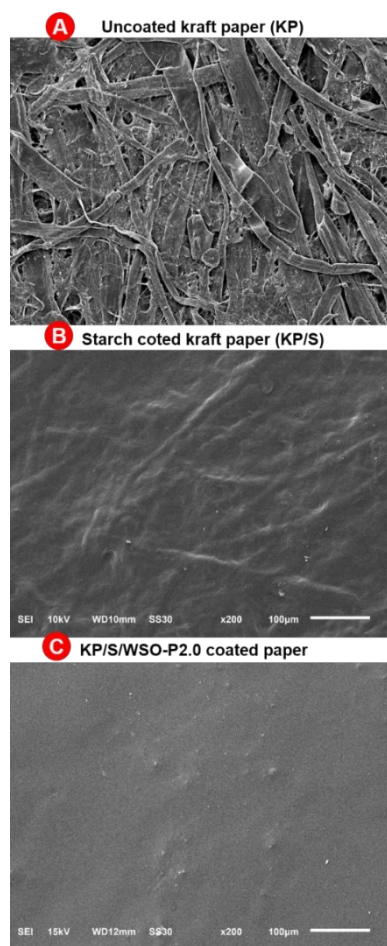


**Figure A.S9** SEM images of **A)** uncoated kraft paper (KP); **B)** Starch coated kraft paper (KP/S) and **C)** AESO-emulsion coated paper (KP/S/WSO-P2.0).

**Table A.S6** Cobb-600 and Cobb-1800 values for the lower loading (0.2, 0.3, 0.4, and 0.5 mL) of the latex (AESO-emulsion) cast on KP/S.

Sample Code	Volume Casted of AESO-emulsion (mL)	Cobb-600 (g/m <sup>2</sup> )	Cobb-1800 (g/m <sup>2</sup> )
KP	---	50.93 ± 1.93	80.96 ± 4.33
KP/S	---	63.40 ± 2.50	75.30 ± 7.20
KP/S/WSO-P0.5	0.2	37.40 ± 2.59	44.30 ± 5.37
KP/S/WSO-P0.5	0.3	25.10 ± 0.91	39.10 ± 0.84
KP/S/WSO-P0.5	0.4	21.43 ± 4.46	32.80 ± 1.69
KP/S/WSO-P0.5	0.5	16.16 ± 1.12	26.80 ± 3.67
KP/S/WSO-P1.0	0.2	27.73 ± 1.60	40.33 ± 6.18
KP/S/WSO-P1.0	0.3	21.83 ± 2.10	32.60 ± 6.43
KP/S/WSO-P1.0	0.4	20.43 ± 3.62	31.80 ± 1.74
KP/S/WSO-P1.0	0.5	13.70 ± 2.19	19.76 ± 1.50
KP/S/WSO-P2.0	0.2	20.30 ± 3.85	34.26 ± 3.35
KP/S/WSO-P2.0	0.3	11.20 ± 4.46	24.56 ± 1.71
KP/S/WSO-P2.0	0.4	11.06 ± 2.86	17.00 ± 2.74
KP/S/WSO-P2.0	0.5	9.43 ± 1.88	13.49 ± 0.84

**Table A.S7** Water resistance properties of our coated paper (KP/S/WSO-P2.0) of different products versus this work.

Sample	Methodology	Cobb 1800 (gsm)	Loading (gsm)	Reference
KP/S/WSO-P2.0	AESO blended in water using PVOH as an emulsifier and, casted on kraft paper, and cured via UV light	$13.49 \pm 0.84$	$20.85 \pm 2.17$	This Work
Crosslinked-AESO	AESO directly cast on kraft paper and cured via UV light	2.18	$114.4 \pm 5.0$	13
PBS-La 50/50-D	PBS blended with high/low molecular weight of PVOH using chloroform and water as solvent	$15.5 \pm 0.1$	$61.76 \pm 1.53$	83
PLA-F	Prepared using PLA film	2.60	NA	83
PLA-P	Prepared using PLA powder	2.35	NA	83
Dixie	Dixie ultra-brand paper plate	28.40	NA	83
LDPE-F	Prepared using LDPE film	0.55	NA	83
LDPE-P	Prepared using LDPE powder	1.15	NA	83
P-Sty	Polystyrene #6 commercial plates	5.00	NA	83
E-Shield	Eco-shield coated paper	4.95	NA	83
Chinet	Chinet classic brand paper plate	91.65	NA	83

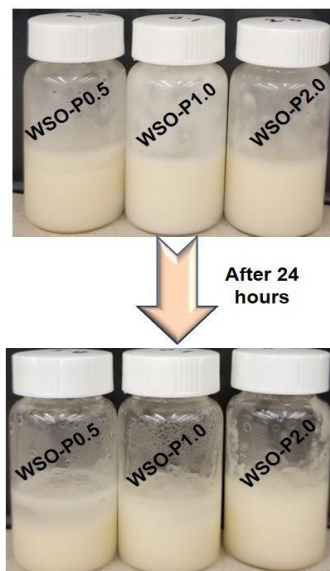


**Figure A.S10** Emulsion stability test. Photographs of WSO-P0.5, WSO-P1.0 and WSO-P2.0 emulsions after 5 min (top row) and after 24 hours (bottom row). The phase separation was lowest for WSO-P2.0. However, all these samples can be used for coating after stirring and heating at  $\sim 70$  °C for a few min.

## **APPENDIX B: SUPPLEMENTARY MATERIALS FOR CHAPTER - DESIGN OF COMPOSTABLE AND RECYCLABLE MODIFIED SOYBEAN OIL COATED PAPER WITH ENHANCED WATER AND OIL RESISTANCE**

### **B.1 Materials & Methods**

#### **B.1.1 Materials**

Acrylated epoxidized soybean oil (AESO), hexagonal boron nitride (H-BN) ( $\sim 1\mu\text{m}$ , 98%), isopropyl alcohol (IPA) is obtained from Sigma Aldrich. The photoinitiator 2,2-Dimethoxy-2-phenylacetophenone was also purchased from Sigma Aldrich. Kraft Paper was purchased from Uline.

Ethylene glycol, Tin(II) 2-ethylhexanoate, glycolic acid, triethyl amine, 4-Dimethylaminopyridine (DMAP) are purchased from Sigma Aldrich; lactide from (ASW MedChem), Acryloyl Chloride from (Alfa Aesar), glycolide from (TCI) and epoxidized soybean oil (ESO) from (Cargill).

#### **B.1.2 Methods**

##### **B.1.2.1 Synthesis of Acrylated Oligo Lactide (AOLA)**

In a dry condition and absence of solvent, a mixture of ethylene glycol (EG) (0.86 g, 0.014 mole), lactate (LA) (4.0 g, 0.028 mole) and Tin(II) 2-ethylhexanoate (20 mg, 0.5 wt% of lactide) were placed in dry 20 mL sized vial. The chemical mixture was heated at  $160^{\circ}\text{C}$  for 3 h in the oil bath. Cool down and obtained white viscous oil was used as it is for the next synthesis step (4.8 g, yield= 98%).  $^1\text{H}$  NMR ( $\text{CDCl}_3$ , ppm): 5.16 (m,  $-\text{CH}-\text{LA}$ ), 4.39 (m,  $-\text{OCH}_2\text{C}-\text{EG}$ ), 1.51 (m,  $-\text{CH}_3-\text{LA}$ ).

Under nitrogen atmosphere, in 100 mL sized two-neck round bottom flask, oligo lactate diol (0.014 mole = 4.8 g) was dissolved in 50 mL of chloroform. The flask was placed in the ice bath and the solution kept stirring for 10 min. The basic solution of Triethyl amine (3.61 g, 0.036

mole) was added portion wise, then the reaction mixture was again stirred for another 10 min. Acryloyl Chloride (2.85 g, 0.031 mole) was added drop wise very slowly via syringe. Finally, the reaction mixture kept for stirring in ice bath for 30 min followed by 6 h at room temperature. After completion of the reaction, the reaction mixture was thoroughly washed using DI water, and the excess chloroform removed using rotary evaporator to obtain viscous oil (7.0g, yield= 91%).  $^1\text{H}$  NMR ( $\text{CDCl}_3$ , ppm): 6.46 (m,  $\text{CH}_2=\text{CH}-$ ), 6.18 (m,  $\text{CH}_2=\text{CH}-$ ), 5.91 (d,  $\text{CH}_2=\text{CH}-$ ), 5.17 (m,  $-\text{CH}-\text{LA}$ ), 4.37 (m,  $-\text{CH}_2\text{CH}_2-\text{EG}$ ), 1.58 (m,  $-\text{CH}_3-\text{LA}$ ).

#### **B.1.2.2 Synthesis of Acrylated Oligo Glycolide (AOGL)**

In dry condition and absence of solvent, a mixture of ethylene glycol (1.0 g, 0.016 mole), glycolide (GL) (3.74 g, 0.032 mole) and Tin(II) 2-ethylhexanoate (30 mg, 0.5 wt% of glycolide) were placed in dry 20 mL sized vial. The chemical mixture was heated at  $160^\circ\text{C}$  for 3 h in an oil bath. Cool down and the obtained white viscous oil was used as it is for the next synthesis step (4.2 g, yield= 88%).  $^1\text{H}$  NMR ( $\text{CDCl}_3$ , ppm): 4.84 (m,  $-\text{OCH}_2\text{C}=\text{O}$ ), 4.74 (m,  $\text{HO}-\text{CH}_2\text{C}=\text{O}$ ), 4.40 (m,  $-\text{OCH}_2\text{C}-\text{EG}$ ), 4.3 (m,  $-\text{CH}_2\text{OH}-\text{EG}$ ).

Under nitrogen atmosphere, in 100 mL size two-neck round bottom flask. Oligo glycolate diol (0.014 mole = 4.2 g) was solublize in 50 mL of chloroform. The flask was placed in ice bath and the solution was then stirred for 10 min. Next, the basic solution triethyl amine (3.62 g, 0.036 mole) was added drop wise, and stirring was continued for next 10 min. Acryloyl Chloride (2.85 g, 0.031 mole) was added drop wise very slowly via syringe. After complete addition, the reaction mixture was stirred in ice bath for 30 min and 6 h at room temperature. Next, the end reaction mixture was washed using DI water thoroughly, and the excess chloroform removed using rotary evaporator to obtain viscous oil (4.5g, yield = 65%).  $^1\text{H}$  NMR ( $\text{CDCl}_3$ , ppm): 6.54 (m,  $\text{CH}_2=\text{CH}-$ ), 6.23 (m,  $\text{CH}_2=\text{CH}-$ ) 5.94 (d,  $\text{CH}_2=\text{CH}-$ ), 4.84 (m,  $-\text{OCH}_2\text{CO}-$ ), 4,74 (m,  $-\text{OCH}_2\text{CO}-$ ), 4.40 (m, -



OCH<sub>2</sub>CH<sub>2</sub>-EG).

### B.1.2.3 Synthesis of Metha Acrylate Glycolate Soybean Oil (MAGSO)

In dry conditions, a mixture of glycolic acid (GA) (1 g, 0.013 mole) and epoxidized soybean oil (ESO) (4.23 g, 0.0043 mole) was placed in a 10 mL vial. Under solvent free condition, the chemical mixture was heated at 100 °C for 1 h in an oil bath. Then cool down to room temperature, the organic product was extracted by chloroform from water. The organic layer washed several times with water. The excess of chloroform was evaporated by rotatory evaporation to obtain viscous oil in tan color (5 g, ~82% yield). <sup>1</sup>H NMR (CDCl<sub>3</sub>, ppm): 5.23 (m, CH-bear glycolate unit), 4.19 (CH<sub>2</sub> protons of -CH<sub>2</sub>-OH glycolic unit), 4.12 (CH proton of CH-OH oil backbone), 3.36 (m, CH-glycerol unit), 3.43-3.97 (CH proton of CH-O glycolic link), 2.27 (CH<sub>2</sub> of RCH<sub>2</sub>COO-fatty acid link), 1.27 (CH<sub>2</sub> protons of fatty acid chain), 0.85 ppm (CH<sub>3</sub> protons at the end of fatty acid chain). The product was termed GA-SO and used further for the next step of reaction.

5 g of GA-SO (0.0039 mole) and (4w% equivalents based on oil) of 4- Dimethylaminopyridine (DMAP) were introduced to a 100 mL flask, 100 mL of chloroform was added. and the system was sealed and purged with Nitrogen then dipped in ice bath. After that, methyl acrylic anhydride (0.9 g, 0.0058 mole) was added drop wise. The final mixture stirred for 48 h, and then allowed to wash with water several times, and extracted with chloroform to remove the unreacted methacrylic anhydride and methacrylic acid.

Finally, a pale-yellow viscous oil product (4 g, 57% yield) was obtained after drying over MgSO<sub>4</sub>, filtering, concentrating under reduced pressure. <sup>1</sup>H NMR (CDCl<sub>3</sub>, ppm): 6.21 (1H of CH<sub>2</sub>=CMe, acryl unit), 5.65 (1H of CH<sub>2</sub>=CMe, acryl unit), 5.25 (m, CH-bear glycolate unit), 4.71 (CH<sub>2</sub> protons of -COCH<sub>2</sub>O acryl glycolic unit), 4.29 ppm (CH proton adjacent to -O-CO-R),

4.27 (CH<sub>2</sub> protons of OCH<sub>2</sub>CHCH<sub>2</sub>O glycerin backbone), 4.12 (CH proton of CH–OH oil backbone), 3.36–3.97 (CH proton of CH–O- acryl glycolic link), 3.18 (m, CH-glycerol unit), 2.30 (CH<sub>2</sub> of RCH<sub>2</sub>COO-fatty acid link), 1.94 (CH<sub>3</sub>, methyl of acryl unit), 1.29 (CH<sub>2</sub> protons of fatty acid chain), 0.87 ppm (CH<sub>3</sub> protons belonging to the end of fatty acid chain). The sample was termed as metha acryl glycolate soybean oil (MAGSO).

#### **B.1.2.4 Preparation of starch solution (5wt%) coated on Kraft Paper**

5 gm of starch (Corn) was dispersed in 95 mL deionized (DI) water and heated at 105 °C for 35 mins. The prepared solution (~12mL) then was cast on kraft paper (~30x30 cm<sup>2</sup>) using coating machine (using rod no. 8) and then left for air dry for 24 hr. The Kraft/starch coated paper was labelled as KP/S.

#### **B.1.2.5 Preparation of H-BN dispersion in IPA/DI water**

80 mL of IPA:DI Water (1:1) was taken in a conical flask and then H-BN (240 mg) was added to the solution to yield a dispersion of H-BN in IPA:DI water solution. Then the mixture was sonicated for 4.5 h followed by centrifugation at 4000 rpm to settle down the multilayer H- BN. Finally, the supernatant solution was collected and utilized as dispersing agent for soybean oil in water.

#### **B.1.2.6 AESO blended acrylated oligo lactide (AOLA)/ acrylated oligo glycolide (AOGL) coated kraft paper (Extrinsic Approach)**

1 g of AESO and 1 g of AOLA/AOGL were taken in a vial along with 2 wt% (40 mg) of photoinitiator (2,2-Dimethoxy-2-phenylacetophenone) and heated at 65°C for 5 mins. 2 mL of H-BN dispersion prepared in water and IPA was used as an emulsifier. H-BN dispersion was added dropwise manner to the system with continuous stirring at high rpm, and the addition resulted in stable emulsion at 65°C within 5 mins. The two samples prepared were called AOLA-AESO and

AOGL-AESO. Freshly prepared AOLA-AESO and AOGL-AESO were then cast ~1 mL on kraft paper/starch (~13 cm x 13 cm) and then cured via UV light for one cycle. The starch coated kraft paper with AOLA-AESO and AOGL-AESO named as KP/S/AOLA-AESO and KP/S/AOGL-AESO.

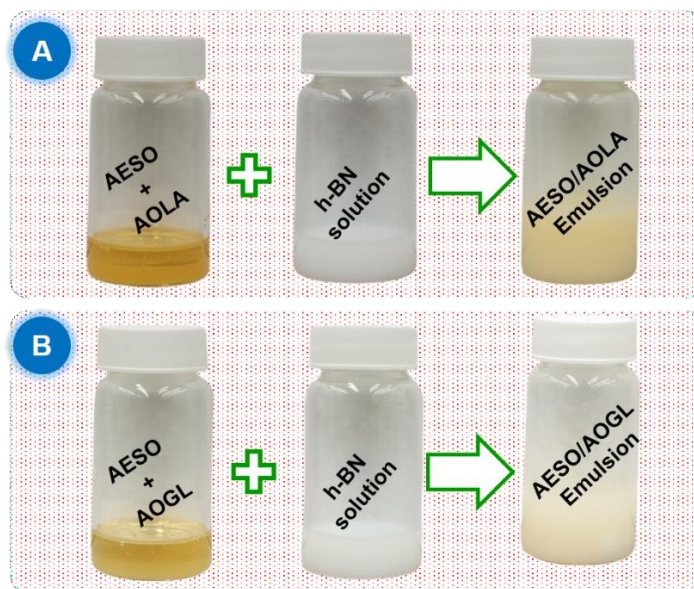


**Figure B.S1.** Photographs of AESO mixed with oligo lactide and AESO mixed with oligo glycolide in H- BN solution to form AOLA-AESO and AOGL-AESO emulsion.

#### **B.1.2.7 MAGSO coated kraft paper (Intrinsic Approach)**

2 gm of MAGSO was taken in a vial along with 2wt% (40 mg) of photoinitiator (2,2-Dimethoxy-2-phenylacetophenone) and heated at 65°C for 5 mins. 2mL of H-BN dispersion prepared in water and IPA was used as an emulsifier. H-BN dispersion was added dropwise manner to the system with continuous stirring at high rpm, and the addition resulted in stable emulsion at 65°C within 5 mins. Freshly prepared MAGSO was then cast 1 mL on kraft paper/starch (~13 cm x13 cm) and then cured via UV light for one cycle. The starch coated kraft paper with MAGSO is named KP/S/MAGSO.

## **B.2 Characterization**

### **B.2.1 Basis Weight and Thickness Measurement**

The basis weight of the kraft paper (KP), Kraft paper/Starch (KP/S), and KP/S coated with AOLA-AESO, AOGL-AESO and MAGSO emulsion were calculated using the ASTM D646 protocol. The paper was trimmed into a circular shape with a radius = ~6.5 cm; area = ~132 cm<sup>2</sup>.

The coating material weight was determined by using Equations (1) and (2):

Coating Load = basis weight (coated paper–uncoated paper) (1) Where

basis weight = weight (g)/area (m<sup>2</sup>) (2)

The thickness was measured in a micrometer (μm) based on measurements at three different spots.

The final values are given in **Table 1**.

### **B.2.2 Water-Resistance Tests**

In accordance with the TAPPI 441 and ISO 535 protocols, the Cobb test was implemented to calculate the water absorption in each of the three samples. A circular disc sample paper with a radius of ~6.5 cm and an area of 100 cm<sup>2</sup> was subjected to deionized (DI) water (100 mL) for a duration of a total of 1800 seconds (30 minutes). The recorded Cobb1800 values signify the amount of water absorbed per square meter during these 30-minutes.

### **B.2.3 Oil/Grease Resistance (Kit Rating)**

Oil/grease repellency was measured in accordance with the TAPPI UM 557 standards. The solutions designed to measure resistance for the samples, assigned kit numbers (0 (the least resistance) to 12 (the most resistance), were directly exposed to the sample surfaces for 15 seconds, followed by cleaning with tissue paper. The regions that were exposed to the kit solutions underwent investigation. The stains signified area or the presence of darkened spots on the sample

had not passed to that specific kit solution are considered to fail. The key with the highest number that did not result in staining on the coated surface is recorded as the "kit rating".

#### **B.2.4 Water vapor transmission rate (WVTR)**

The water resistance against water vapors was tested by measuring WVTR. A Permatran- W (Model 3/34, Mocon Inc. MN, United States) was deployed for this analysis, and samples were preconditioned for one hour at 37°C with relative humidity (RH) of 90%. The paper specimen with specific dimensions of  $2 \times 2 \text{ cm}^2$  was trimmed and positioned on an aluminum mask (with area  $\sim 0.5 \text{ cm}^2$ ) to prepare test samples. The flow rate of water vapors was maintained at  $100 \text{ cm}^3/\text{min}$ . The SI unit of  $\text{g}/\text{m}^2\cdot\text{day}$  was used to represent the WVTR value.

#### **B.2.5 Leica Stellaris Confocal Microscope**

Emulsion images were collected by using confocal microscope with 10 x Plan Apo having objective (Numerical Aperture- 0.3) and color camera (Nikon DS-Fi2).

#### **B.2.6 Contact Angles (CAs) Measurements**

Automated goniometer (590-U1, Ramé-Hart Instrument Co., USA) was used to check the contact angles for the coated and uncoated paper. The CA of water droplets has been collected after a time interval of 5 min.

#### **B.2.7 Burst Test Measurements**

Mullen burst tester-Auto-TMI-paperboard corrugated Mullen was used to measure the impact of force applied on the paper and the value is reported in psi.

### **B.3 Repulping and Recycling Testing Methods**

#### **B.3.1 Repulping Method**

FBA Voluntary Standard method was adopted for Repulping and Recycling procedure.

## Description

Modified Waring Blender and British Disintegrator are two equipment used for repulping process.

The coated paper is repulped in DI water and the temperature is kept 125°F (±10°F). After completing the process, the pulped paper is poured on a screen (with 0.010-inch slots), this helps to separate pulp from unwanted impurities.

This method helps to calculate the amount of recovered fiber compared to the original fiber. 85% repulping yield is required to pass this test. The yield of repulping is calculated as:

$$\text{Yield \%} = \frac{\text{Net Accepts}}{\text{Net Accepts} + \text{Net Rejects}} \times 100\%$$

### B.3.2 Recyclability of Coated Paper Samples AESO-Lactide: Testing methods:

TAPPI T205 Making Hand sheets.

TAPPI T815 Coefficient of Static Friction (Slide Angle). TAPPI T831 Water Drop Penetration Test.

TAPPI T826 Short Span Compression Strength (STFI).

TAPPI T403 Burst Strength.

TAPPI T277 Stickies Count.

### B.3.3 Evaluation criteria

The hand sheets composed using recycled samples should show no difference in appearance as compared to control sheet and the stickies count is less than 15, else should not exceed 30% compared to the control sheets.

1. Drop in the value of slide angle of the hand sheets made from test sample shall not exceed 15%.

2. STFI as well as burst strength calculated for the hand sheets composed using recycled paper, must show no more than a 10% decrease for the respective values compared to the control.
3. Penetration of water droplets through the hand sheets made using the recycled sample should not cross the water droplets penetration time from the control sheet by 200 seconds or more.

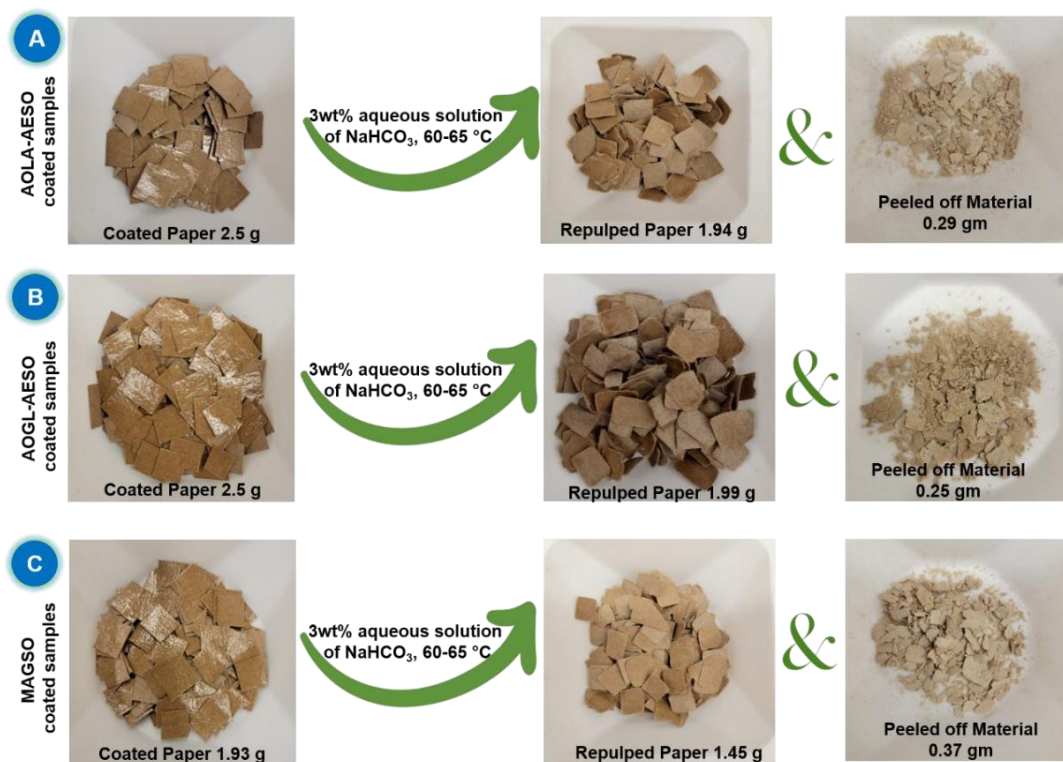


**Figure B.S2.** Lab scale repulpability of the coating on Kraft paper, A) AOLA-AESO coating; B) AOGL- AESO coating; C) MAGSO coating.

### B.3.4 Cobb1800 evaluation of pure AOLA and AOGL

**Table B.S1.** Cobb 1800 value of KP/S/AOLA & KP/S/AOGL.

KP/S/AOLA	KP/S/AOGL
30	31
30	32
31	32
30.3 ± 0.2	31.6 ± 0.2

### B.3.5 Emulsion stability of MAGSO

Emulsion stability for the MAGSO sample was tested after 24 h and the coating material was found with a small phase separation, however by gentle shaking it came to the one phase (**Figure B.S3**). The optical microscope image was also collected and found to have emulsion size mostly in the range of 10-30  $\mu\text{m}$  (**Figure B.S4**).



**Figure B.S3.** Photograph of the MAGSO emulsion before and after 24 h.

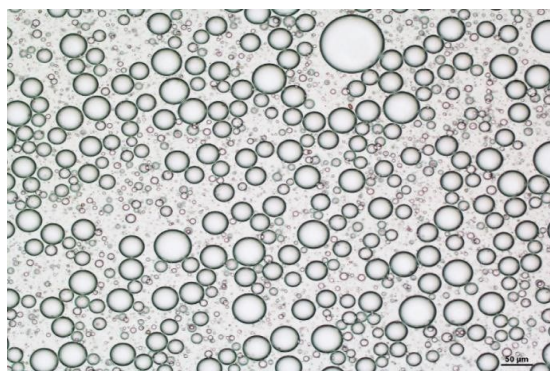


**Figure B.S4.** Optical microscope image of the MAGSO emulsion.

### B.3.6 Water resistance test at extreme temperatures

#### B.3.6.1 Cold water resistance test of the coated sample (MAGSO)

To analyze the coating behavior at extreme temperature, cold water ( $\sim 4$  to  $5^{\circ}\text{C}$ ) was added to the cobb tester and  $8.10 \pm 1.68$  gsm for Cobb-1800 value was reported for the cold-water resistance test (**Table S2**).



### B.3.6.2 Hot water resistance test of the coated sample (MAGSO)

Similarly, to investigate the coating performance at extreme temperature, boiled water ( $\sim 90$  to  $95^{\circ}\text{C}$ ) was added to the cobb tester and  $22.13 \pm 1.60$  gsm for Cobb-1800 value was reported for the hot water resistance test.

**Table B.S2** Water resistance test at extreme temperatures.

	<b>MAGSO sample</b>	<b>Values</b>
1	Cobb-1800 at $\sim 25^{\circ}\text{C}$	$5.63 \pm 0.32$
2	Cobb-1800 at $\sim 5^{\circ}\text{C}$	$8.10 \pm 1.68$
3	Cobb-1800 at $\sim 95^{\circ}\text{C}$	$22.13 \pm 1.60$

### B.3.7 Burst test of paper

The burst test was conducted for the coated sample (MAGSO) and the obtained data was compared with that obtained for the control samples (KP and KP/S). The coated paper performs better than the control samples and shows a burst strength value of  $\sim 89.4$  psi, where those for the KP and KP/S samples were 74.6 and 84.9 psi, respectively (**Figure B.S3**). This finding demonstrates that the load bearing capacity of the coated sample is more than those of the control samples.

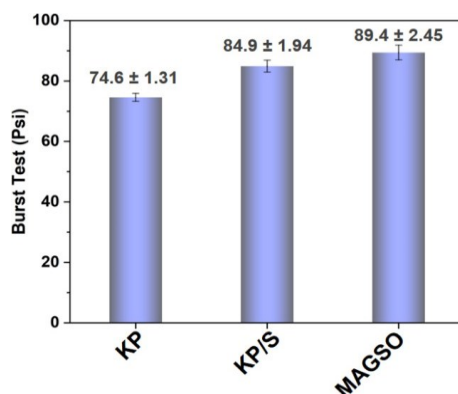


**Figure B.S3.** Burst test for the uncoated (controls) and coated sample (MAGSO).

### B.3.8 Contact angle measurement

**Table B.S3.** Contact angle measurement after 5 min for the uncoated and coated samples.

Sample name	Contact angle measurement after 5 min
KP	NA
KP/S	NA
MAGSO	$95 \pm 1.6$
AOLA-AESO	$92 \pm 2$
AOGL-AESO	$94 \pm 1.5$

**Table B.S4.** Water- and oil-resistant (Cobb-1800 and Kit rating) of our coated samples that are compared with previously reported literature as well as benchmarked products in the market.

Sample	Methodology	Cobb 1800 (gsm)	KIT Rating	Reference
MAGSO	Modified ESO cured via UV light	5.03 ± 2.17	12/12	<b>This Work</b>
AOLA-AESO	AESO cross-linked using AOLA cured via UV light	6.83 ± 0.76	12/12	
AOGL-AESO	AESO cross-linked using AOGL cured via UV light	11.46 ± 1.46	12/12	
KP/S/WSO-P2.0	AESO blended in water using PVOH	13.49 ± 0.84	7/12	125
KP/S-carnauba	Carnauba wax coated paper	45.6 ± 1.4	12/12	118
KP/S-paraffin	Paraffin wax coated paper	22.0 ± 1.2	12/12	118
KP/S-W-L7	PLA-stearate-based wax samples (1.0 g) was further dissolved in 2 mL of ethylacetate or hexane	3.3 ± 1.2	12/12	118
P-W-LA3	Degradable Polymeric Waxes coated on kraft paper using CHCl <sub>3</sub> solvent.	4.10 ± 1.41	12/12	118
Crosslinked-AESO	Neat AESO cured via UV light	2.18	12/12	13
PBS-La 50/50-D	PBS blended with high/low molecular weight of PVOH using chloroform and water as solvent	15.5 ± 0.1	12/12	83
PLA-F	PLA film Coated paper	2.60	12/12	83
PLA-P	PLA powder coated paper	2.35	12/12	83
Dixie	paper plate from Dixie company	28.40	12/12	83
LDPE-F	LDPE film coated paper	0.55	12/12	83
LDPE-P	LDPE powder coated paper	1.15	12/12	83
P-Sty	Commercial plates of Polystyrene	5.00	5/12	83
E-Shield	coated paper from Eco-shield	4.95	12/12	83
Chinet	Paper plate from Chinet classic	91.65	3/12	83

### B.3.9 Vermicomposting of KP/S/MAGSO sample

We have performed vermicomposting of coated kraft (KP/S/MAGSO). Vermicomposting is a very simple technique in which worms along with shredded leaves, waste food mixed and then sprinkled with water. The prepared mixture is then mixed with our coated paper and then left for two months.



**Figure B.S6.** KP/S/MAGSO coated paper shredded into four different dimensions.



**Figure B.S7.** Shredded coated KP/S/MAGSO paper in four different dimensions added mixed with the prepared compost.



**Figure B.S8.** (1.5 cm x 15 cm) and (15 cm x 15 cm) Shredded paper is not fully decomposed after two months of vermicomposting.

### B.3.10 $^1\text{H}$ -NMR spectra

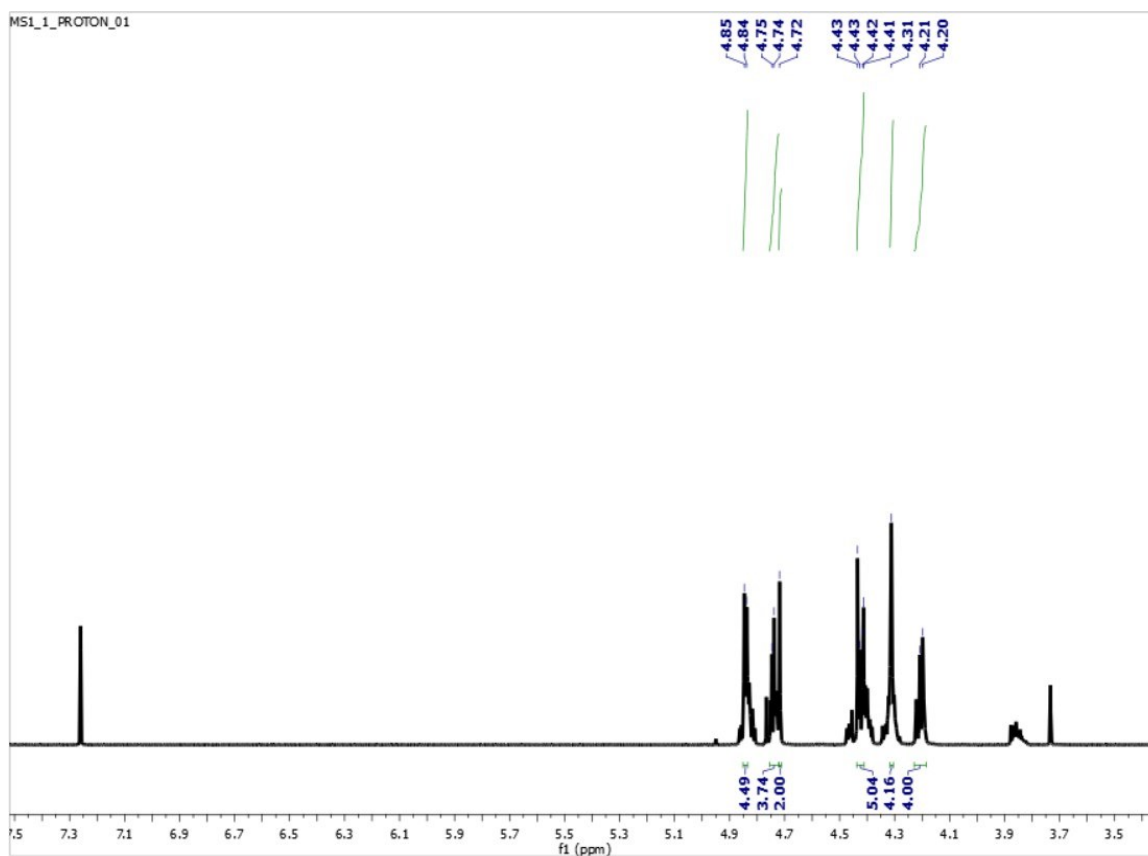


**Figure B.S9.**  $^1\text{H}$ -NMR spectrum ( $\text{CDCl}_3$  is used as solvent, frequency- 500 MHz) of oligoglycolate diol.

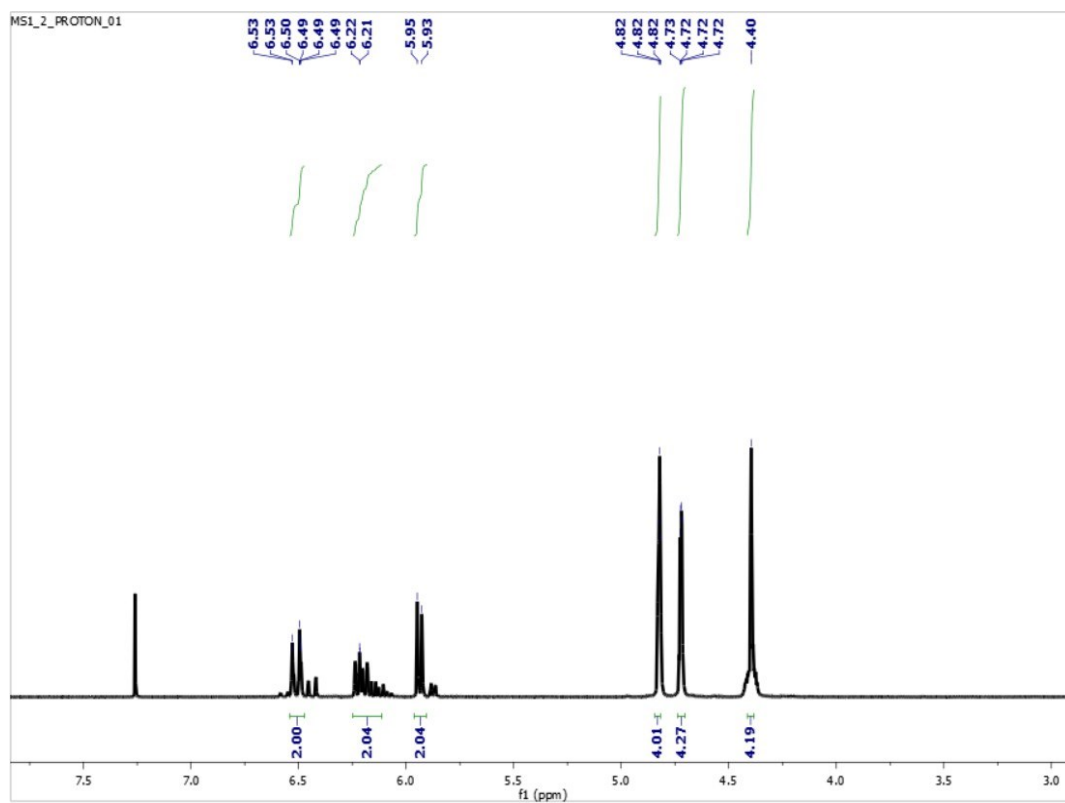


**Figure B.S10.**  $^1\text{H}$ -NMR spectrum ( $\text{CDCl}_3$  is used as solvent, frequency- 500 MHz) of acrylated oligo glycolate (AOGL).

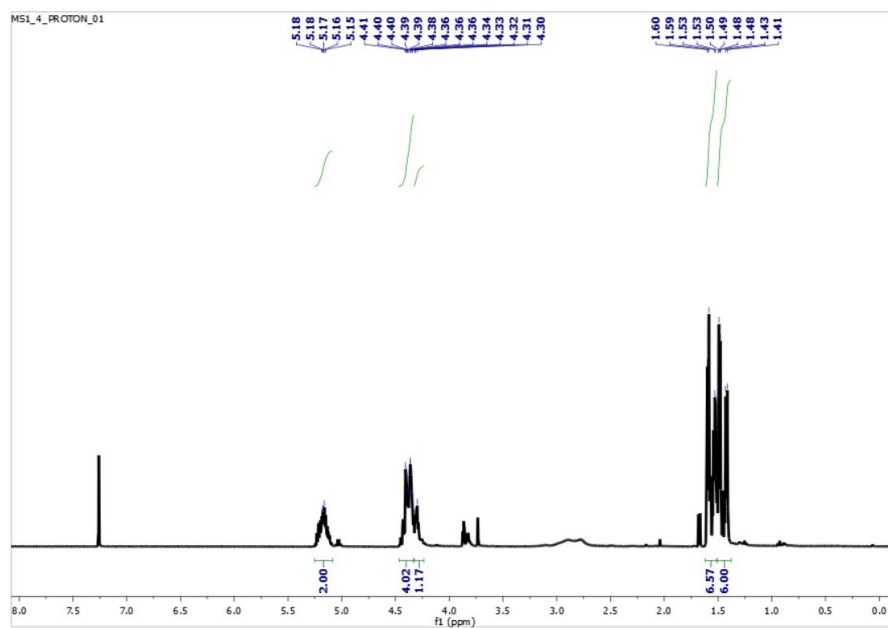


**Figure B.S11.**  $^1\text{H}$ -NMR spectrum ( $\text{CDCl}_3$  is used as solvent, frequency- 500 MHz) of oligo lactide diol.

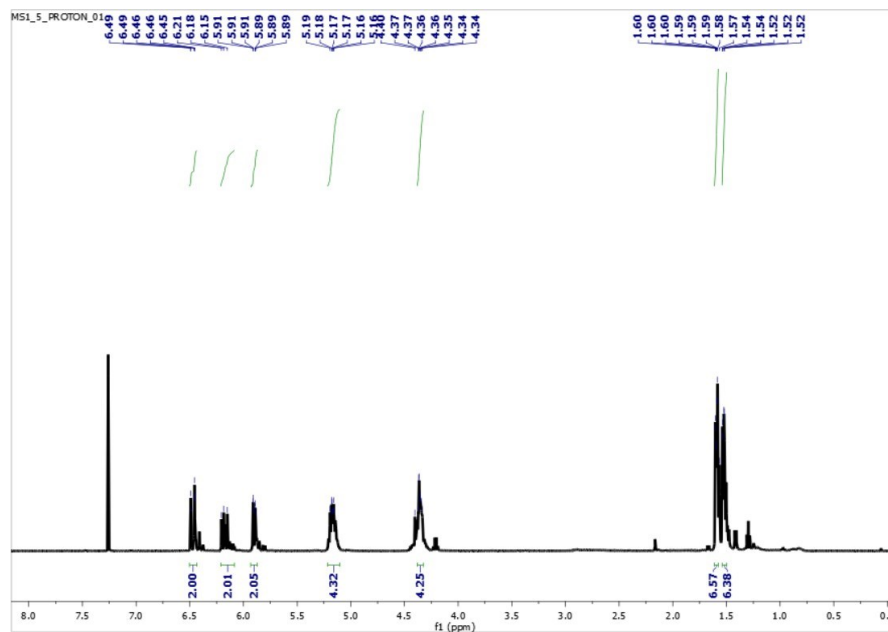


**Figure B.S12.**  $^1\text{H}$ -NMR spectrum ( $\text{CDCl}_3$  is used as a solvent, frequency- 500 MHz) of acrylated oligo lactide (AOLA).

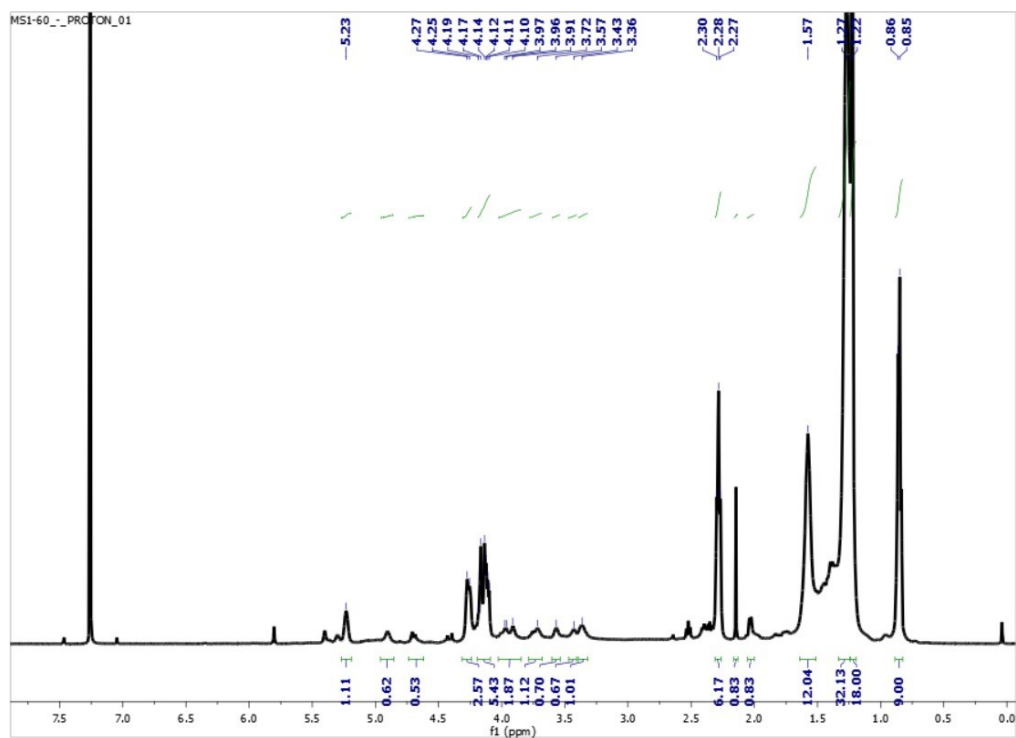


**Figure B.S13.**  $^1\text{H}$ -NMR spectrum ( $\text{CDCl}_3$  is used as solvent, frequency- 500 MHz) of glycolate epoxy soybean oil.



## Elemental Analysis

**Table B.S5.** Elemental analysis of vermicompost of KP/S/MAGSO paper. The C/N ratio for the composted sample is 18.4:1.

Analysis	Unit	Analysis Result	Dry Basis Result	Analysis Method
Moisture @ 70 C	%	71.62		TMECC 03.09-A
Solids	%	28.38		TMECC 03.09-A
Total Nitrogen (N)	%	0.62	2.18	TMECC 04.02-D
Phosphorus (P)	%	0.06	0.22	TMECC 04.03-A
Phosphate (P <sub>2</sub> O <sub>5</sub> )	%	0.14	0.50	TMECC 04.03-A
Potassium (K)	%	0.20	0.69	TMECC 04.04-A
Potash (K <sub>2</sub> O)	%	0.23	0.83	TMECC 04.04-A
Sulfur (S)	%	0.08	0.27	TMECC 04.05-S
Magnesium (Mg)	%	0.16	0.56	TMECC 04.05-MG
Calcium (Ca)	%	1.16	4.09	TMECC 04.05-CA
Sodium (Na)	%	0.03	0.09	TMECC 04.05-NA
Iron (Fe)	%	0.08	0.28	TMECC 04.05-FE
Aluminum (Al)	%	0.06	0.20	TMECC 04.07-AL
Copper (Cu)	mg/kg	5	18	TMECC 04.05-CU
Manganese (Mn)	mg/kg	39	137	TMECC 04.05-MN

TMECC - Test Methods for the Examination of Composting and Compost (TMECC), The U.S. Composting Council.

-COMPOST

Analysis	Unit	Analysis Result	Dry Basis Result	Analysis Method
Zinc (Zn)	mg/kg	21	73	TMECC 04.05-ZN
pH	-	7.4		TMECC 04.11-A
Soluble Salts	dS/m	3.32		TMECC 04.10-A
Ash @ 550 C	%	5.56	19.58	TMECC 03.02-B
Organic Matter (LOI @ 550 C)	%	22.82	80.42	TMECC 05.07-A
Total Organic Carbon (C)	%	11.41	40.21	TMECC 04.01-A
Carbon:Nitrogen Ratio (C:N)	-	18.4:1	18.4:1	TMECC 05.02-A

**Table B.S6.** Elemental analysis of standard vermicompost sample prepared without the coated paper. The C/N ratio for the composted sample is 10.4:1.

Analysis	Unit	Analysis Result	Dry Basis Result	Analysis Method
Moisture @ 70 C	%	65.08		TMECC 03.09-A
Solids	%	34.92		TMECC 03.09-A
Total Nitrogen (N)	%	1.16	3.31	TMECC 04.02-D
Phosphorus (P)	%	0.13	0.37	TMECC 04.03-A
Phosphate (P <sub>2</sub> O <sub>5</sub> )	%	0.30	0.85	TMECC 04.03-A
Potassium (K)	%	0.47	1.36	TMECC 04.04-A
Potash (K <sub>2</sub> O)	%	0.57	1.63	TMECC 04.04-A
Sulfur (S)	%	0.13	0.37	TMECC 04.05-S
Magnesium (Mg)	%	0.23	0.66	TMECC 04.05-MG
Calcium (Ca)	%	1.51	4.31	TMECC 04.05-CA
Sodium (Na)	%	0.09	0.27	TMECC 04.05-NA
Iron (Fe)	%	0.13	0.36	TMECC 04.05-FE
Aluminum (Al)	%	0.07	0.20	TMECC 04.07-AL
Copper (Cu)	mg/kg	14	39	TMECC 04.05-CU
Manganese (Mn)	mg/kg	74	211	TMECC 04.05-MN

TMECC - Test Methods for the Examination of Composting and Compost (TMECC), The U.S. Composting Council.

-COMPOST

Analysis	Unit	Analysis Result	Dry Basis Result	Analysis Method
Zinc (Zn)	mg/kg	26	75	TMECC 04.05-ZN
pH	-	7.3		TMECC 04.11-A
Soluble Salts	dS/m	5.34		TMECC 04.10-A
Ash @ 550 C	%	10.87	31.12	TMECC 03.02-B
Organic Matter (LOI @ 550 C)	%	24.05	68.88	TMECC 05.07-A
Total Organic Carbon (C)	%	12.03	34.44	TMECC 04.01-A
Carbon:Nitrogen Ratio (C:N)	-	10.4:1	10.4:1	TMECC 05.02-A

TMECC - Test Methods for the Examination of Composting and Compost (TMECC), The U.S. Composting Council.

-COMPOST